AMERICAN UNIVERSITY OF BEIRUT

ISOINDIGO AND NDI DERIVATIVES: PROMISING BUILDING BLOCKS FOR ORGANIC ELECTRONICS

by
CHRISTA ABDULLAH SHARABATI

A thesis
submitted in partial fulfillment of the requirements
for the degree of Master of Science
to the Department of Chemistry
of the Faculty of Arts and Sciences
at the American University of Beirut

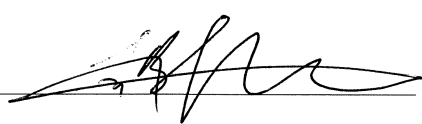Beirut, Lebanon
April 2019

AMERICAN UNIVERSITY OF BEIRUT

ISOINDIGO AND NDI DERIVATIVES: PROMISING BUILDING BLOCKS FOR ORGANIC ELECTRONICS

by
Christa Abdullah Sharabati

Approved by:

_____

Dr. Bilal Kaafarani, Professor   Advisor

Chemistry

_____

Dr. Makhlouf Haddadin, Professor   Member of Committee

Chemistry

_____

Dr. Digambara Patra, Associate Professor   Member of Committee

Chemistry

Date of thesis defense: April 18, 2019

AMERICAN UNIVERSITY OF BEIRUT

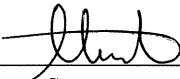# THESIS, DISSERTATION, PROJECT RELEASE FORM

Student Name: <u>Sharabati</u>   <u>Christa</u>   <u>Abdullah</u>
               Last   First   Middle

☑ Master's Thesis   ◯ Master's Project   ◯ Doctoral Dissertation

☐   I authorize the American University of Beirut to: (a) reproduce hard or electronic copies of my thesis, dissertation, or project; (b) include such copies in the archives and digital repositories of the University; and (c) make freely available such copies to third parties for research or educational purposes.

☑   I authorize the American University of Beirut, to: (a) reproduce hard or electronic copies of it; (b) include such copies in the archives and digital repositories of the University; and (c) make freely available such copies to third parties for research or educational purposes after: **One ___ year from the date of submission of my thesis, dissertation or project.**
    Two ___ years from the date of submission of my thesis , dissertation or project.
    Three ☑ years from the date of submission of my thesis , dissertation or project.

_____   April 19, 2019
    Signature   Date

This form is signed when submitting the thesis, dissertation, or project to the University Libraries

ACKNOWLEDGMENTS

AN ABSTRACT OF THE THESIS OF

Christa Abdullah Sharabati   for   Master of Science

Major: Chemistry

Title: Isoindigo and NDI derivatives: Promising building blocks for organic electronics.

We report the synthesis and characterization of a series of isoindigo-based and naphtalene diimide (NDI)-based organic materials as promising building blocks for different fields of organic electronics including organic photovoltaics (OPVs) and organic field effect transistors (OFETs). The synthesis of these compounds was carried out through three steps via condensation, nucleophilic aromatic substitution and Suzuki coupling reactions.

In Chapter 2, we present the synthesis of six new isoindigo-based small molecules as potential molecules for OPVs and OFETs. We report the effect of altering the substituent on the photophysical and thermal properties.

In Chapter 3, we report DFT calculations and electrochemistry of isoindigo-based molecules in effort to provide a better understanding of the substituent effects on the energy levels. This chapter was done in collaboration with Prof. Brigitte Wex from the Lebanese American University and aims to offer better insight to the design of small molecules for electronic applications.

In Chapter 4, we report the synthesis of two new isoindigo-based small molecules as precursors for covalent organic framework (COF) materials. The synthesis of isoindigo dialdehydes were prepared in our laboratory whereas the COF materials were done by the work of Prof. Ali Trabolsi from the New York University in Abu Dhabi.

Finally, Chapter 5 discusses the synthesis of three NDI-based molecules for electronic applications. It provides understanding of the effect of the substituent through photophysical, thermal and computational studies.

CONTENTS

Appendix

ILLUSTRATIONS

TABLES AND SCHEMES

Scheme

ABBREVIATIONS

A: Area under the curve

abs: Absorption

AcOH or CH3COOH: Acetic acid

Anal. Calcd.: Analytically calculated

Ar: Aryl substituent

BDP: benzodipyrrolidone

BHJ: bulk heterojunction

Blue shift: Hypsochromic shift

BTD: benzothiaziazole

°C: Degree Celsius

CDCl3 or chloroform-d: Deuterated chloroform

CHCl3: Chloroform

cm: centimeter

cNDI: core-substituted naphtalene diimide

COF: covalent organic framework

2D COF: two-dimensional covalent organic framework

3D COF: three-dimensional covalent organic framework

CT: Charge Transfer

CV: cyclic voltammetry

d: doublet

dd: doublet of doublets

D-A: Donor-Acceptor

D-A-D: Donor-Acceptor-Donor

DCM or CH2Cl2: Dichloromethane

DFT: Density Functional Theory

DLC: Discotic Liquid Crystal

DMF: *N,N'*-Dimethylformamide

DMSO: Dimethylsulfoxide

DMSO-d6: Deuterated dimethylsulfoxide

DNA: deoxyribonucleic acid

DSC: Differential Scanning Calorimetry

DTA: Differential Thermal Analysis

DPP: Pdiketopyrrolopyrrole

DPV: Differential Pulse Voltammetry

E: applied electric filed in V/m or potential

E_{ox}: oxidation potential

EA: Electron Affinity

$e/bohr^3$: electron per bohr cubed

EDG: electron donating group

E_g: Energy bandgap

eq: Equation

eqv: Molar equivalent

E_{red}: reduction potential

et al.: and others

EWG: electron withdrawing group

EtOAc: Ethyl acetate

EtOH or C_2H_5OH: Ethanol

eV: electron Volt

f: Oscillator strength

f_{exp}: experimental oscillator strength

FET: Field-Effect Transistor

g: Gram

GOF: Goodness-Of-Fit (X-ray)

H_2O: Water

H_2SO_4: Sulfuric acid

H-bond: Hydrogen bond

HBr: Hydrogen bromide

HCl: Hydrogen chloride

Hex: Hexane

HNO_3: Nitric acid

HOMO: Highest Occupied Molecular Orbital

hr(s): Hour(s)

Hz: Hertz

I or *i*: Intensity of current

IC: Internal Conversion

ICT: Intramolecular Charge Transfer

i.e.: illustrative example

Ii: Isoindigo

IP: Ionization Potential

IUPAC: International Union of Pure and Applied Chemistry

J: Coupling constant (NMR) or current density parameter (OLED)

J/g: Joule per gram

Kcal/mol: kilocalorie per mole

kJ/mol: kilojoule per mole

K: Kelvin

K: calorimetric constant

K_2CO_3: Potassium carbonate

L: Liter

LAU: Lebanese American University

LC: Liquid Crystal

LED: Light-Emitting Diode

Lit.: Literature value

LUMO: Lowest Unoccupied Molecular Orbital

M: mol/Liter

m: Meter

Mol. Wt.: molecular weight

NDI: Naphtalene diimides

NIR: near infra-red

NMR: Nuclear Magnetic Resonnance

NPV: Normal pulse voltammetry

OFET: Organic Field Effect Transistor

OLED: Organic Light-Emitting Diode

OPV: Organic Photovoltaic

OSC: Organic Solar Cell

PHJ: planar heterojunction

PDI: Perylene diimides

$Pd(PPh_3)_4$: Tetrakis(triphenylphosphine)palladium(0)

q: quartet

RDI: rylene diimide

Red shift: Bathochromic shift

RT: Room temperature (25 °C)

s: singlet (NMR) or second (time)

SWV: Square-wave voltammetry

t: triplet

t: time

TBABr: Tetrabutylammonium bromide

TBAP: Tetrabutylammonium hexafluorophosphate

t-butyl or $tert$-butyl: Tertiary butyl

T_d: Decomposition temperature

(TD) DFT: Time-dependent differential functional theory

T_g: Glass transition temperature

TGA: Thermogravimetric analysis

THF: tetrahydrofuran

TLC: Thin-layer chromatography

UV: Ultraviolet

UV-vis: Ultraviolet-visible absorption spectroscopy

V: Volt

V_{on}: Turn-on voltage (threshold voltage)

W: Watt

%wt: Weight percent

XRD: X-ray diffraction

v_d: drift velocity in m/s

δ: chemical shift

ΔH: enthalpy of transition

ΔE_{opt}: optical gap calculated from the lowest energy band in the UV−vis absorption spectrum

ΔE_{th}: optical gap calculated from a level of theory

ε: dielectric constant of solvent or molar absorptivity of compound

λ: wavelength

λ_{max}: wavelength at maximum absorption

μ: absorption coefficient

μ: charge carrier mobility in $m^2/V.s$

μ_{ge}: Transition dipole moment in Debyes

$\mu_{ge\ expt}$: experimental transition dipole moment in Debyes

π: pi bonding orbital

π^*: pi antibonding orbital

ρ: density

σ: sigma bonding orbital

σ^*: sigma antibonding orbital

CHAPTER 1

INTRODUCTION

1.1. Organic Electronics

With today's rapidly advancing technology and rising global environmental issues, scientists are challenged to find greener, better performing, and more cost-effective devices. To meet this need, organic electronics has been an emerging field in the recent years.[1,2] Great effort has been made to develop new organic materials for their advantageous characteristics such as light-weight, low-cost, large scale fabrication, flexibility, and tunability.[1,3,4] Such materials have been studied extensively in many applications such as organic light emitting diodes (OLEDs),[5] organic photovoltaics (OPVs),[6] Organic Field-Effect Transistors (OFETs),[7] organic sensors,[8] organic optical data storage,[9] organic switches[10] and others. Generally, organic semiconductors offer key device performance features since the charge transport efficiency between their layers is crucial for better performance.[11] Therefore, it is important to understand the structure-property relationship of organic semiconductors to tailor specific outcomes for any desired application.[12]

1.1.1 Organic semiconductors

The introduction of organic semiconductors was a great revolution in the last century.[13] After the recent advances in manufacturing techniques such as thin film drop casting, spin coating, and inkjet printing, organic semiconductors were seen as good candidates to replace conventional silicon-based semiconductors which require high heat and expensive processing.[14] Chemically, organic semiconductors consist of conjugated organic

small molecules or polymers that possess an electronic conductivity between that of isolators and metals. Organic small molecules have many advantages to be used in organic electronics. To list few: 1. they can be easily synthesized on a large scale, purified, and isolated. 2. They have no batch-to-batch variation compared to polymers.[15] 3. The energies of their Highest Occupied Molecular Orbital (HOMO) and Lowest Unoccupied Molecular Orbital (LUMO) can be tuned.[16] 4. They can be easily processed under room temperature whether under dry or wet conditions.[17] 5. Their structural flexibility make them suitable for use in flexible display technology.[18]

The most important characteristic of semiconductors is charge transport, i.e. their ability to transport electrons (n-type) or holes (p-type) from one molecule to another through π orbitals upon photoexcitation (solar cell) or an applied voltage to an active layer between two electrodes (field-effect transistor).[19] Efficient charge-carrier transport is crucial in order to achieve high device performance.[19] This is measured by the mobility (μ) which is calculated from the following equation:

$$v_d = \mu E$$

where v_d is the drift velocity in m/s, E is the applied electric filed in V/m and μ is the mobility in m^2/V.s. Furthermore, the structural packing of the material has shown dependence on the charge-transport.[11] The level of solid state chain ordering and amount of chemical and structural defects can also play important roles.[20] For instance, one way to achieve high mobility is through discotic liquid crystals (DLCs),[21] a class of liquid crystals (LCs), that have the properties of both solid crystals and liquids. Their solid crystal character allows them to achieve high molecular order through self-assembly. Whereas, their liquid-like dynamics allows them to self-heal structural defects.[22] Yet, achieving high mobilities comparable to those of conventional silicone semiconductors in order to make their use

sufficiently profitable for market remains a challenge. Moreover, attaining thermal and mechanical stability accompanied with high levels of purity is still difficult.[23] Therefore, there is a need to further improve and investigate new organic semiconductor structures and to tailor them to each desired application. To that end, scientist have explored many promising building blocks for efficient conjugated small molecules and polymer organic semiconductors such as diketopyrrolopyrrole (DPP),[24] benzodipyrrolidone (BDP),[25] perylene diimides (PDI),[26] naphtalene diimides (NDI),[27] and Isoindigo (Ii).
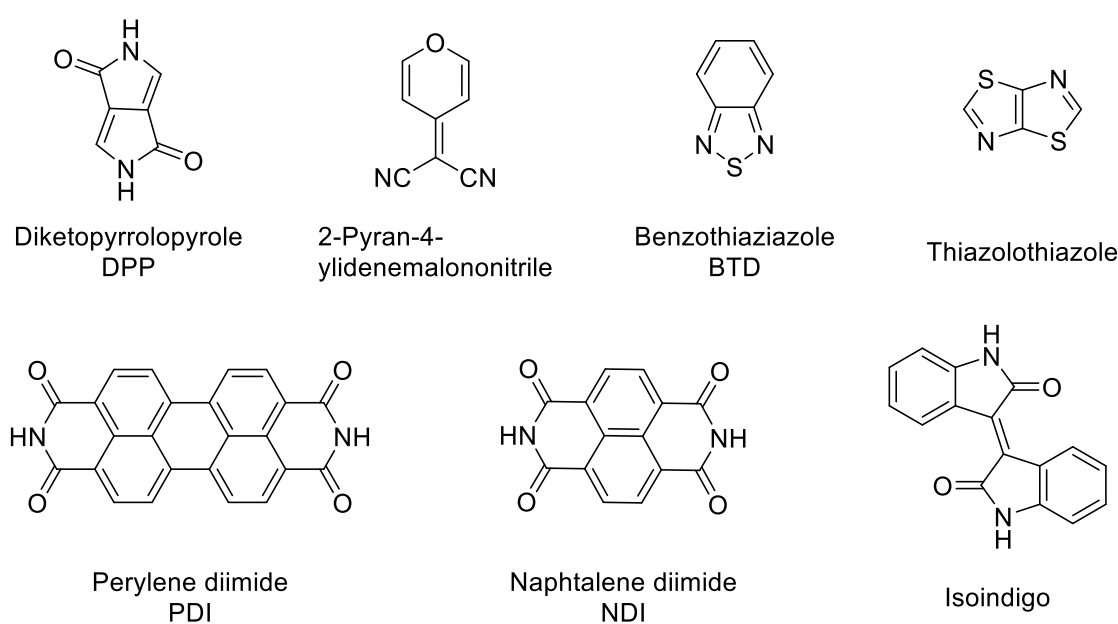
Figure 1.1. The chemical structures of some explored organic building blocks.

Isoindigo, a naturally occurring dye, is an electron-deficient core that gained significant attention in the recent years. Owing to its delocalized aromatic π-system as well as to its remarkable absorption properties, isoindigo was introduced to develop low band gap polymers and small molecules solar cells[28]. Furthermore, it has been introduced in organic field effect transistors,[29] and other applications. The electronic properties of isoindigo can be readily tuned by extension of conjugation.

Naphthalenetetracarboxylic diimde (NDI) is another important class of organic species. NDI is characterized by a large, robust, planar, electron deficient aromatic core. Studies showed that core substituted NDIs (cNDIs) can manifest a great variety of optical properties and colors[30], as well as diverse ranges of frontiers molecular orbital levels.[31] Therefore, core substituted NDIs have become very attractive and have rapidly emerged in the areas of solar cells, artificial photosynthesis, and supramolecular chemistry.[32,33] Furthermore, core substituting NDI at carbons 2,3,6,7 allows extended conjugation to their planar aromatic core, this permits π - π stacking, which makes them perfect candidates for achieving high electron mobility, ambient stable n-channel organic thin film transistorsOTFTs[34] and organic field effect transistors OFETs.[35]

1.1.2 Organic Photovoltaics (OPVs)

The importance of finding clean and renewable energy necessitates the development of organic photovoltaics. The gain in OPVs power-conversion efficiencies from about 1% to over 8%[36] over the past decade offers great hope for their use in this capacity. However, most OPVs have not achieved the efficiency of 10-15% needed for commercialization compared to silicon-based solar cells that have already have efficiencies of 45%. Many scientists pursue the development of novel materials, device architectures, and fabrication technologies to shorten this difference.[36]

Donor (p-type semiconductors) and acceptor (n-type semiconductors) make up the active layers of many organic semiconductors. Donor to acceptor photoinduced charge transfer, at the donor–acceptor (D–A) interface leads to a useful current, so it is crucial to have high absorption coefficient and a suitable band gap for optimal absorption of the solar spectrum.[14] To accomplish this, investigators use one of two D-A interface architecture formation strategies, either depositing donors and acceptors to form two successively layers, making a planar heterojunction (PHJ) or forming a bulk heterojunction (BHJ) through co-

deposition, forming a blended D–A film structure with a much higher internal interface due to the larger p/n interfaces, a higher chance of exciton formation and separation is acheived.[36] Two organic solar cell (OSC) processing techniques were established to produce more efficient materials. Researchers thermally evaporate excess materials to form either planar heterojunction (PHJ) or bulk heterojunction (BHJ) solar cells in dry processing, or use a process involving spin coating, inkjet printing, dip coating, and spraying in solution processing which can only form BHJ-type solar cells.[36] Multilayer device structures can only be formed through vacuum evaporation, whereas solution processing offers more expedient processing at a lower cost. [36]

Many advances have been done on polymer solar cells.[37] However, organic small molecules, having monodisperse nature, offer geometrically infinite structural possibilities which may possibly ameliorate molecular functionality, rigidity, stacking, strong intermolecular (π–π) interactions, and most importantly well-defined structure, high purity, among other properties.[36]

1.1.3 Organic Field-Effect Transistors (OFETs)

In recent years, Organic Field-Effect Transistors (OFETs) have rapidly emerged to develop low-cost, flexible and efficient electronic devices.[38] They are highly attractive because they can be incorporated in many applications such as chemical and biological sensors,[39,40] simple circuits and e-paper displays.[41] In principle, Field-Effect Transistors (FETs), introduced in 1930,[42] are electronic devices where the current direction is altered as a voltage is applied. It consists of three electrodes; the gate, the source, and the drain.[43] Once a voltage is applied to the gate, charge carriers (electrons or holes) flow from the source to the drain.[44] The charge carriers flow through the active layer which is composed of either a p-type or an n-type semiconductor.[45] Generally, three main material characteristics play a major role in the performance of OFETs. First is the field effect mobility (μ) which expresses ease

of charge carrier movement through the active layer. This measurement, used in the field to communicate the quality of a material ranges from >1–10 cm 2 V^{-1} s^{-1} in older discoveries to (0.5–1 cm^2 V^{-1} s^{-1}) which exceeds those of amorphous thin-film silicon devices.[38] Second is the on/off ratio (I_{on}/I_{off}) calculated as the ratio of the current from source to drain when the device is on to when it is off. [46] Third is the threshold voltage (U$_t$,) the extrapolated voltage that switches the device on.[46]

Another attractive and promising research area for next generation optoelectronic devices is multifunctional OFETs.[47] One interesting example is the integration of OFETs with OLEDs. Initial research suggests that OLETs may have superior mechanical qualities to those of silicon or oxide based TFTs. Nonetheless, many researchers deem it doubtful that OFETs will achieve the uniformity, performance, and operational stability needed to create a backplane matching an oxide or poly-Si TFT display in durability and reliability.[38] While modern silicone-based FET have been used widely with high efficiencies, they are processed under very harsh conditions with temperatures above 350 °C, that OFET manufacture does not require[48] which makes them promising for further development.

1.2 Aims and Objectives

The exciting field of organic electronics and the need to further enhance our daily use of technological devices has motivated our research group to invest in the synthesis and characterization of potential isoindigo and NDI small molecules for different electronic applications, mainly OFETs and OPVs. In this thesis work, we describe the synthesis, purification, and characterization (NMR, elemental analysis, UV-vis, TGA and DSC) of novel conjugated small molecules. Computational modeling and electrochemistry were attained in collaboration with Prof. Brigitte Wex from the Lebanese American University.

In Chapter 2, we report the synthesis and characterization of a series of isoindigo derivative materials as potential building blocks for OFETs and OPVs. Suzuki coupling of arylbromides with specific boronic acids was carried out in the presence of a palladium catalyst Pd(PPh$_3$)$_4$.[49] The effect of coupling with an electron-withdrawing group (EWG) or electrondonating group (EDG) has been studied by comparing the absorption and thermal properties of compounds **2.4-2.9**, Figure 1.2.
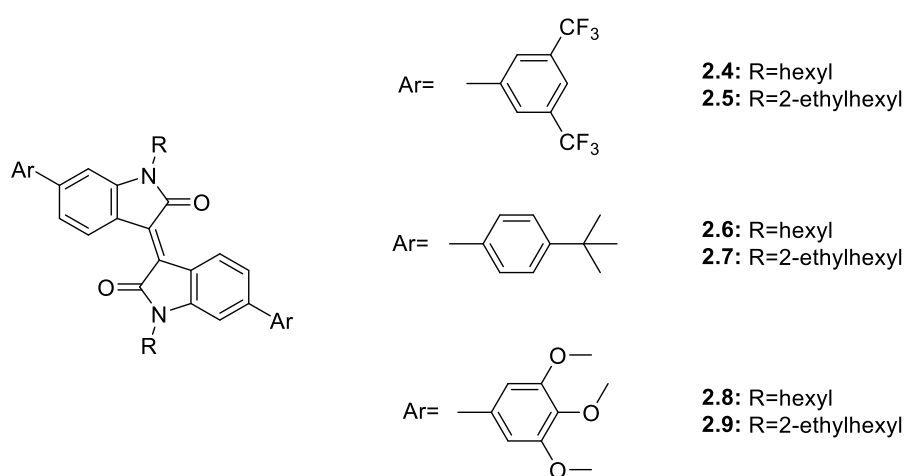
Figure 1.2. Synthesized isoindigo-based molecules.

In Chapter 3, we investigate isoindigo derivatives modulated on positions 6 and 6' with electron density-modulating groups for their electronic properties as explored by differential pulse voltammetry along with a comprehensive computational study of the ground and excited states by utilizing density functional theory both in gas phase and solution. This work was achieved by our collaborator Prof. Brigitte Wex and her student Peter Nasr from the Lebanese American University (LAU). The compounds included in this study are shown in Figure 2.3.
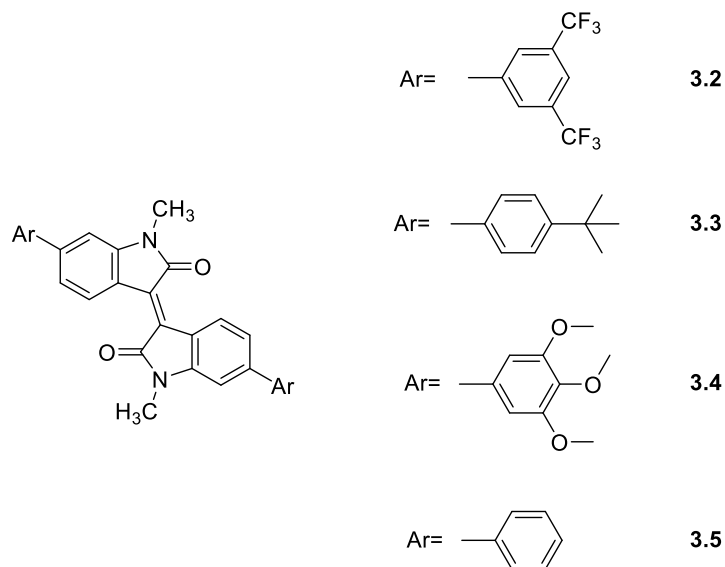
Figure 1.3. Isoindigo-based molecules used for computational modeling.

Chapter 4 includes the synthesis of two isoindigo dialdehydes derivatives as building blocks for COFs. The two compounds (**4.1-4.2**) were synthesized through Suzuki coupling reactions, purified and characterized by ^{1}H and ^{13}C NMR and elemental analysis. Our collaborator Prof. Ali Trabolsi from the New York University in Abu Dhabi is currently exploring these two isoindigo dialdehydes for the synthesis various COF materials. The condensation reaction of isoindigo dialdehydes (**4.1- 4.2**) and 1,3,5-tris(4-aminophenyl)benzene (TAPB) (**4.3**) successfully led to the formation of **COF 4.10** and **COF 4.11**. The properties of these two COFs are currently under investigation. The synthesis of other COFs using **4.7** and **4.8** is also ongoing.
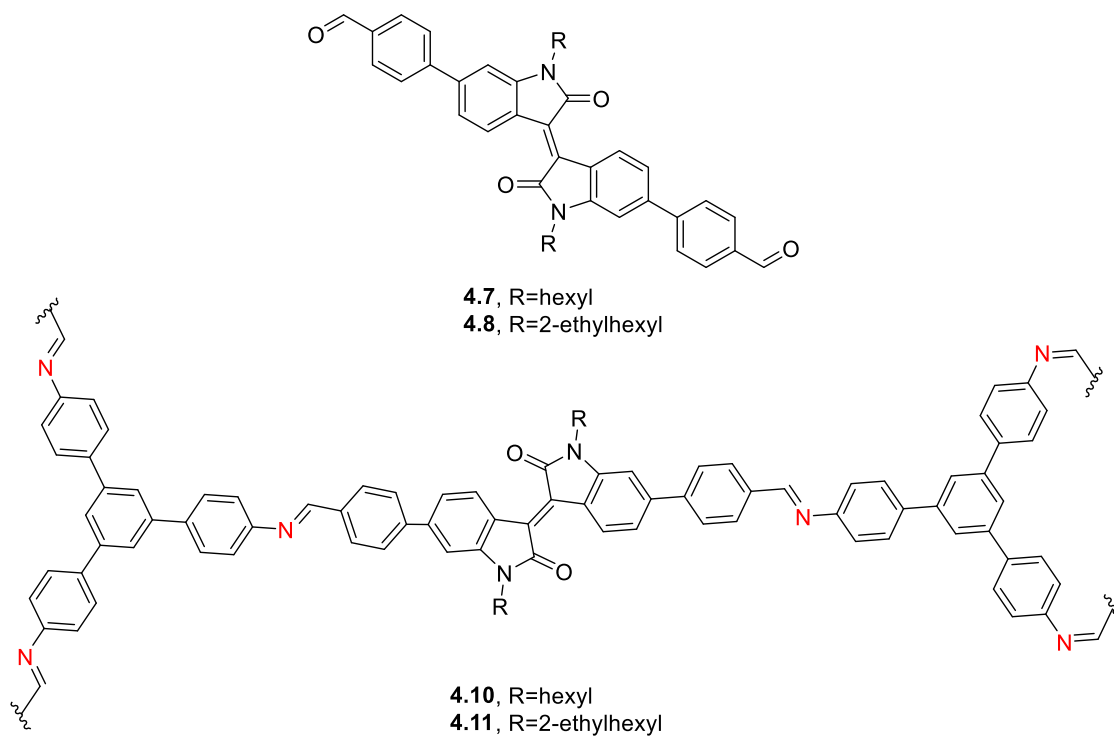
Figure 1.4. Synthesized isoindigo aldehydes and COF materials.

In Chapter 5, we report three core substituted NDI derivatives through a three-step synthetic pathway. The aim of the synthesis was to first add an alkyl group at the imide nitrogen atoms to enhance its solubility and stacking, and second, to core-functionalize it with three different aromatic substituents through Suzuki coupling in order to study and better understand the subsequent effect of different electron donating and withdrawing groups on the energy levels, photophysical properties, charge-carrier mobilities, stacking, and overall performance as potential materials for organic field effect transistors.
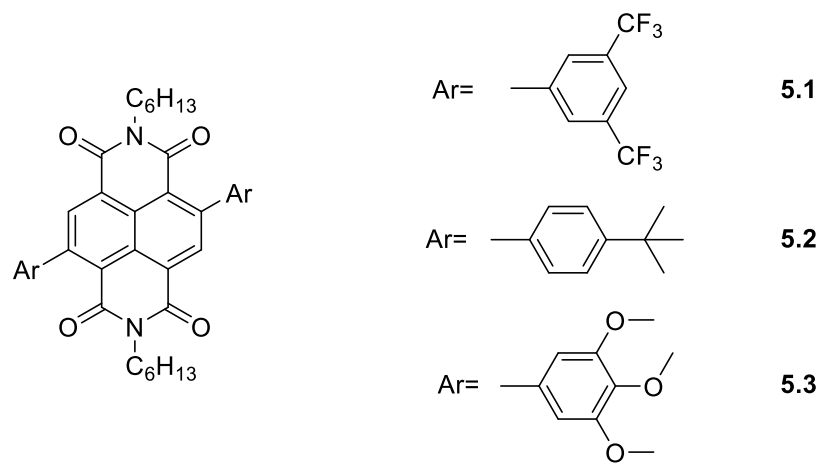
Figure 1.5. Synthesized NDI-based molecules.

CHAPTER 2

ISOINDIGO DERIVATIVES FOR ELECTRONIC APPLICATIONS

2.1 Introduction

In the scope of finding greener, recyclable and more efficient devices, and inspired form nature, significant focus has been directed towards bio-integration and bio-functionality of organic semiconducting materials intended for biomedical and electronic applications.[50] Many biocompatible organic electronic devices have aroused based on naturally derived dyes and pigments, Figure 2.1.[51]
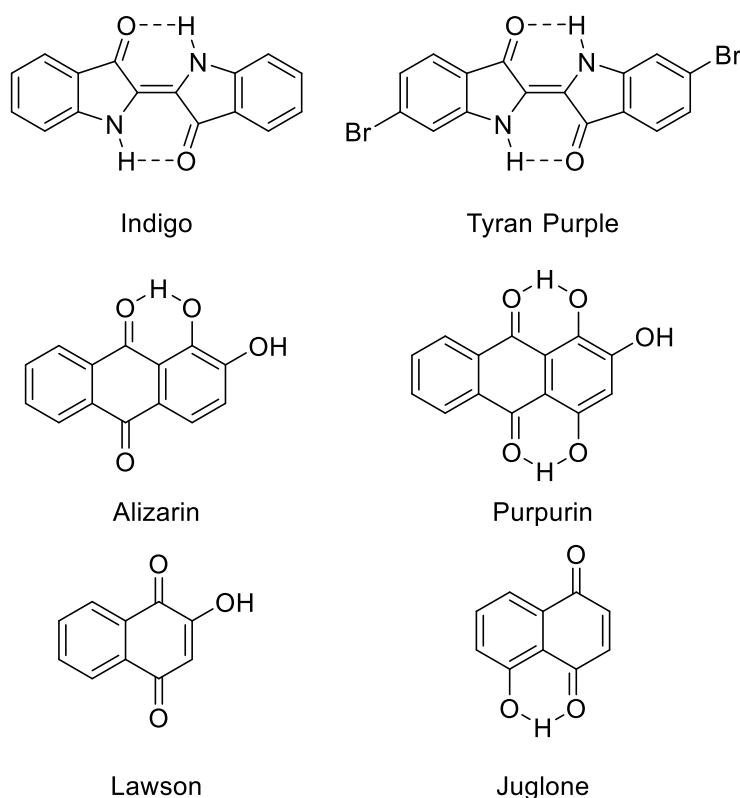
Figure 2.1. The chemical structures of some naturally-derived dyes and pigments.[51]

Generally, synthetic chemists have sought organic molecules with large fused aromatic rings to allow maximum π-conjugation when designing organic materials. However, the aggregation of small natural pigments is accompanied with large bathochromic shifts which suggests substantial electronic coupling. For instance, studies of the crystal structures of indigo dye show co-facial π-π stacking that favors charge transport.[51]

Indigo and tyran purple, are well-known ancient dyes throughout history.[52] Recently, they were reported to show potential in the field of organic electronics in the growing perspective of finding cheaper, more eco-friendly and nature-inspired semiconductors.[51] However, the excited state of H-bonded indigo molecules undergoes very rapid internal conversion, which suggests difficulty to generate reasonable efficiency of photocurrent.[51]

On the other hand, isoindigo, a structural isomer of indigo, has proven to be very successful in many fields. It was naturally found as a minor isomer of indigo in the plant *Isatis tinctoria*.[53] In 1988, the first synthesis of isoindigo was reported.[54] Pharmaceuticals and medicinal chemists developed different synthetic pathways to obtain isoindigo derivatives, mostly for their biological activity.[55-57] A well-known example is 1-methylisoindigo, which was proved to have cancer-reducing activity and was used in the treatment of leukemia.[58,59]

Isoindigo was first introduced to the organic electronics field in 2010 by Reynolds *et al.* as a promising conjugated building block for solar cells.[60] Soon afterwards, isoindigo gained significant popularity from researchers owing mainly to its ease of synthesis, availability, and suitability for large scale fabrication as well as the ability of fine tuning its properties for targeted electronic devices giving "state-of-the art" performances.[28]

The chemical structure of isoindigo is depicted in Figure 2.2. It is composed of two oxindole rings fused through a double bond in a *trans* configuration. The fully conjugated

system bearing the two electron-withdrawing lactam functions makes isoindigo an electron deficient molecule.
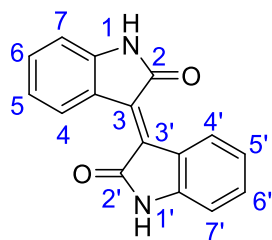
Figure 2.2. The chemical structure of isoindigo.

Isoindigo can exhibit π-π staking through hydrogen bonding on the hydrogen atoms of the lactam nitrogens. This makes the core almost insoluble in common organic solvents. In order to increase the solubility, different alkyl chains can be introduced. This is done by linking alkyl chains to the lactam nitrogens with considerably high yields.[60]

To incorporate isoindigo in polymers and small molecules for electronic applications, scientists have extended the core mainly through the well-known reactions: Suzuki coupling, Stille coupling, and direct arylation. These extensions can be done through two possible linkages: the 5,5' linkage and the 6,6' linkage as shown in Figure 2.3.

6,6'-linked isoindigo   5,5'-linked isoindigo
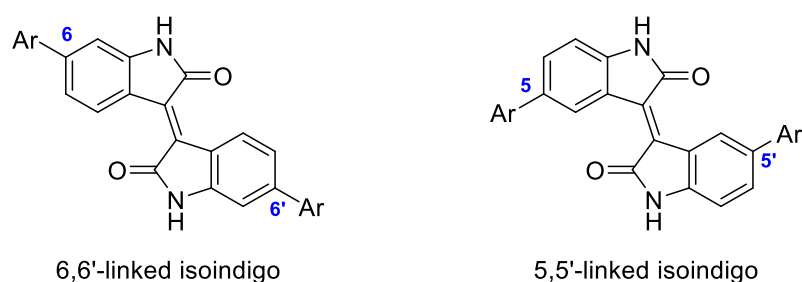
Figure 2.3. 6,6' and 5-5' linked isoindigo compounds.

Linking on the 6,6' positions is advantageous due to its ability to form the quinoid form allowing further extension of the conjugation of the different substituents compared to

13

the 5,5' linkage. Therefore, researchers have focused on developing new structures based on the 6,6' linkage where the molecules are fully conjugated.[28]

To better understand the electronic structure and optical properties of isoindigo, theoretical and experimental studies were exploited.[61] Reynolds *et al.* provided insightful understanding of the matter in conjugated systems, through the study of factionalized isoindigo with altered electronic nature substituents.[62] Through their combined theoretical and experimental studies, they arrived at the following conclusions about the effect of substituents on the frontier molecular orbitals: the HOMO is mainly affected by electron donating substituents whereas the LUMO is mainly governed by the isoindigo core and slightly affected by electron withdrawing groups. Concerning the pattern of substitution (5,5' vs. 6,6'), it was concluded that the pattern of substitution does not play a significant role in the electronic structure of isoindigo and that the substituent itself plays a bigger role. Yet, the significance of the patters comes into play when discussing oscillator strength, where it was found that 5,5' derivatives exhibited lower molar absorptivies in the visible spectrum. This gave researchers more interest in the 6,6' derivatives that are fully conjugated and provide higher molar absorptivities in the visible spectrum.
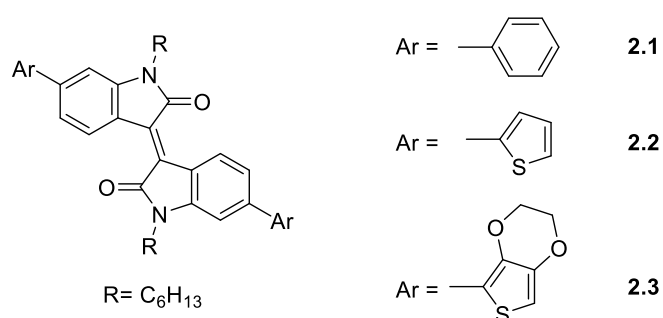
Figure 2.4. The structures of different isoindigo small molecules.

14

In the following sections of this chapter, we report the synthesis and characterization of a series of isoindigo derivative materials as potential building blocks for OFETs and OPVs. Suzuki coupling of arylbromides with specific boronic acids was carried out in the presence of a palladium catalyst such as Pd(PPh$_3$)$_4$.[49] The effect of coupling with an electron-withdrawing group (EWG) or electrondonating group (EDG) has been studied by comparing the absorption and thermal properties of compounds **2.4-2.9**, Figure 2.5.
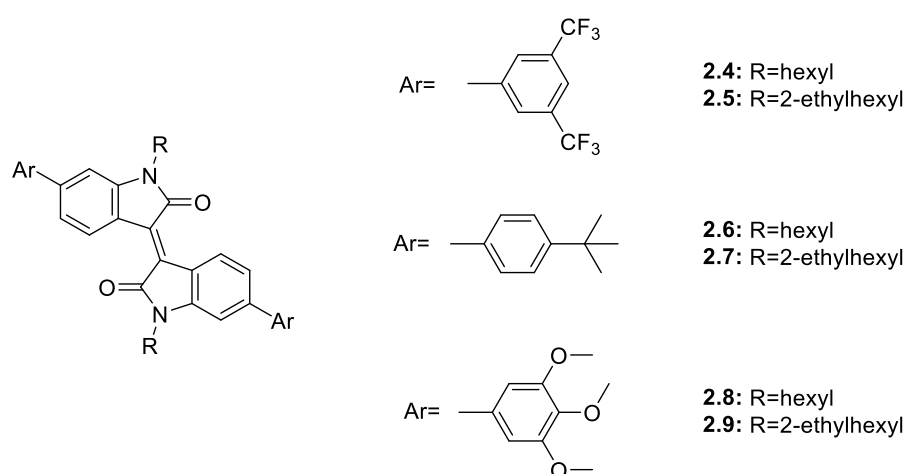
Figure 2.5. The structures of the synthesized isoindigo derivatives.

2.2. Results and Discussion

2.2.1. Synthesis

Six novel isoindigo derivatives were synthesized through a three-step synthesis. The synthesis is depicted in **Scheme 2.1**. The first step was done through the condensation of commercially available oxindole **2.10-2.11** and isatin **2.12-2.13** according to a modified procedure.[60] The reagents were refluxed in acetic acid with catalytic amounts of hydrochloric acid for 24 hours. The corresponding isoindigo compounds (**2.14-2.15**) were obtained in high yields (89%). Since isoindigos (**2.14-2.15**) are not soluble in most common organic solvents,

it is necessary to increase their solubility by *N,N'*-dialkylation.[60] Therefore, in the following step, compounds (**2.14-2.15**) were reacted with 1-hexylbromide or 2-ethylhexylbromide in DMF in the presence of dry potassium carbonate at 100 $^{\circ}$C for 16 hours under argon. In the third step, compounds (**2.18-2.19**) were reacted with three different boronic acids via Suzuki coupling reaction according to a modified literature procedure.[63] Many trials were carried out to obtain the products in good yields. Toluene turned out to be a better solvent than THF. All reactions were refluxed in toluene for 2 days to ensure the formation of the disubstituted coupling product. Traces of the mono-substituted product were obtained for the products bearing the *tert*-butyl (**2.6-2.67)** and the trimetoxy (**2.8-2.9)** substituents, whereas more of the mono substituted was formed when using the electron withdrawing bistrifluoromethyl substituent in compounds (**2.4-2.5**). Importantly, palladium zero catalyst Pd(PPh$_3$)$_4$ was synthesized and freshly used with a short period of storage (a week) in the dark under inert atmosphere due its instability and high sensitivity to oxygen, heat, and light.[49]
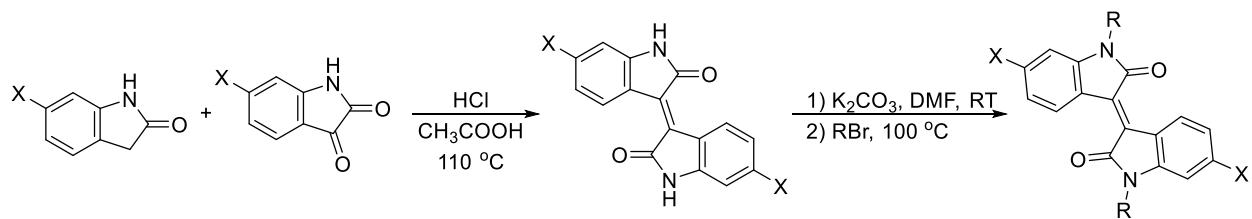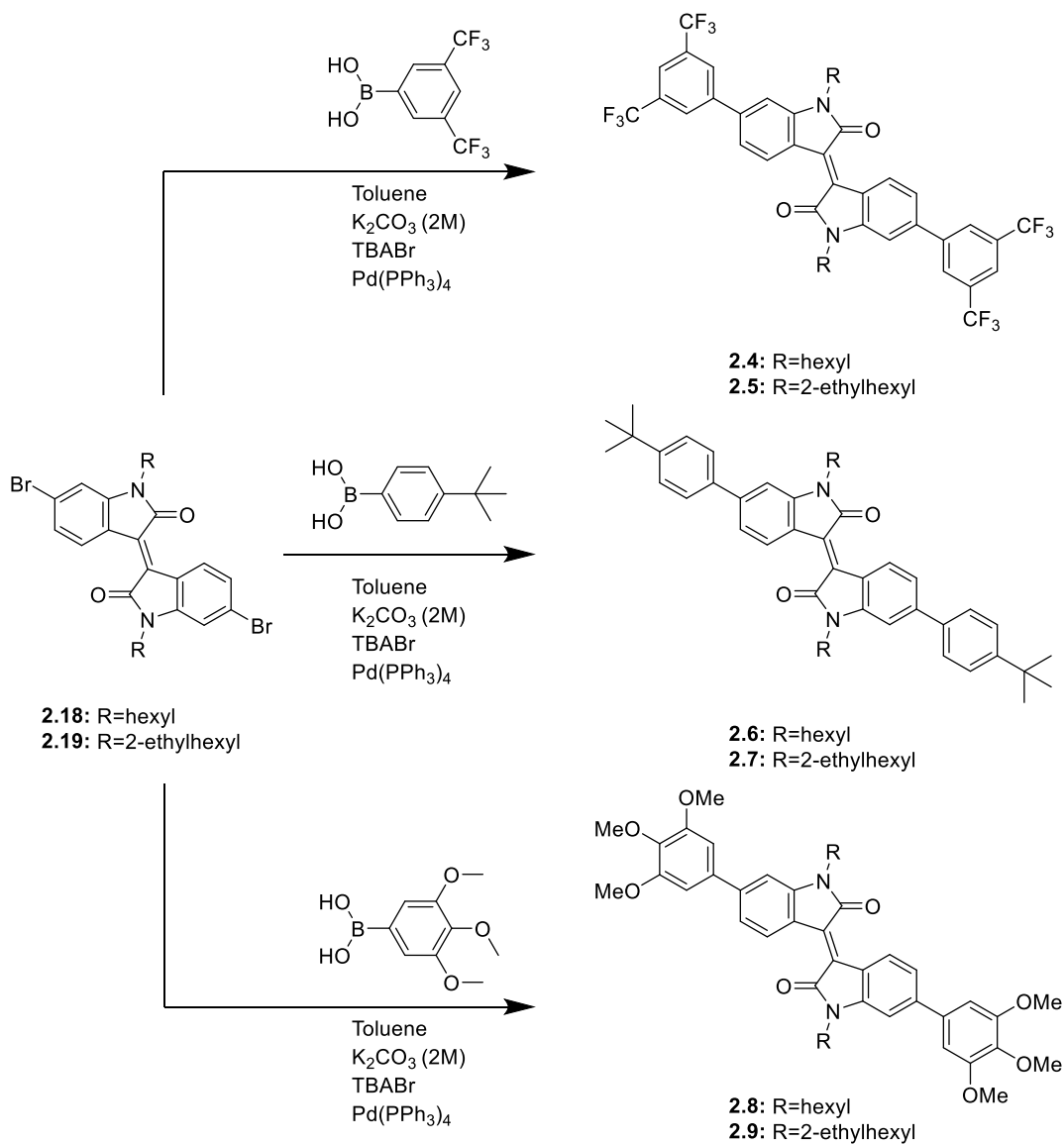
Scheme 2.1. Synthesis of isoindigo derivatives **2.4-2.9**.

2.2.2. Molecular Photophysics: Absorption

Figures 2.6-2.7 present the UV-vis absorption spectra of isoindigo compounds **2.4-2.9** and **2.17-2.18** in chloroform. The absorption spectra did not change while varying the alkyl chain from hexyl to 2-ethylhexyl since alkyl chains do not play a role in electronic transitions. Two main absorption bands were observed for all compounds, the higher energy band around 400 nm, and the lower energy band ranged around 500 nm. These two absorption bands were assigned to the π-π* transition and the intramolecular charge transfer (ICT), respectively.[64] It is noticeable that the absorption spectrum red-shifts going from unsubstituted isoindigo to substituted isoindigo. This is explained by the extended conjugation at the 6,6' position which promotes electron coupling, giving higher absorptivity.[61] Moreover, the absorption spectrum gradually red-shifts going from the most electron withdrawing substituent in compounds **2.4-2.5** to the most electron donating substituent in compounds **2.8-2.9**. This is mostly visualized at the higher energy band located at around 420 nm. The obtained trend is attributed to the enhancement of the ICT as the substituent group becomes more electron donating through the formation of an electron donor-acceptor-donor D-A-D system.[61] Compounds **2.8-2.9** bearing the electron donating group showed the highest molar absorptivity. The results of the absorption spectra for compounds **2.4-2.9** are summarized in Table 2.1**.**
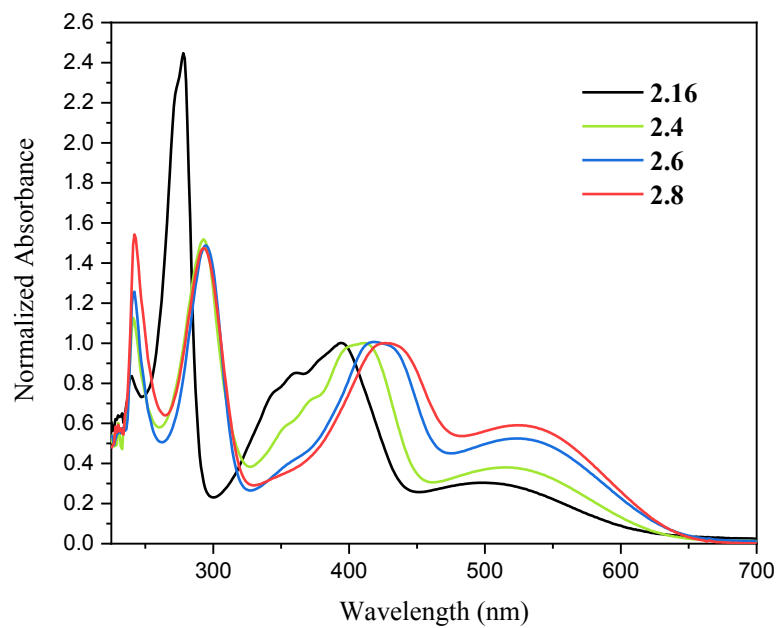
Figure 2.6. Normalized absorption of compounds **2.4**, **2.6**, **2.8** and **2.16** with (hexyl) in chloroform.
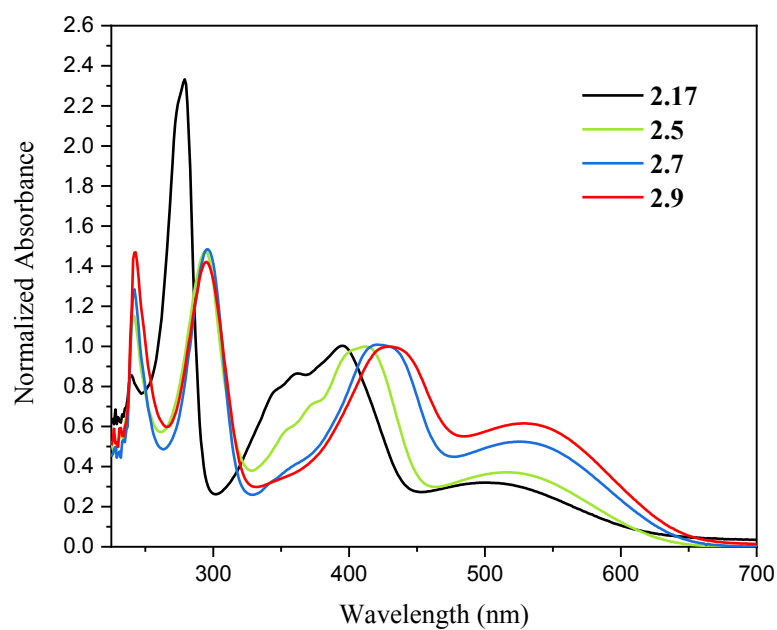
Figure 2.7. Normalized absorption of compounds **2.5**, **2.7**, **2.9** and **2.17** with (2-ethylhexyl) in chloroform.

Table 2.1. The absorption results of compounds **2.4-2.9** and **2.16-2.17** in chloroform.

Compound	λ_{max1} (nm)	ε (L.mol^{-1}.cm^{-1})	λ_{max2} (nm)	ε (L.mol^{-1}.cm^{-1})	λ_{max3} (nm)	ε (L.mol^{-1}.cm^{-1})
2.16	278	31865	396	12888	519	3406.2
2.17	361	9643.8	395	11354	496	3075
2.4	293	39451	411	25952	522	9495.7
2.5	295	37853	412	25665	516	9538.5
2.6	295	38006	420	25642	522	13114
2.7	296	37860	422	25673	530	13342
2.8	293	38168	426	25845	522	15250
2.9	294	39506	429	27767	532	16771

2.2.3. Thermal Analysis

Thermal methods of analysis have been used in a wide range of applications. These are generally used to characterize a system in order to provide insightful physical and chemical properties.[65] In this work, thermogravimetric analysis (TGA) and differential scanning calorimetry (DSC) are used to characterize and compare the synthesized isoindigo derivatives.

Thermogravimetric Analysis (TGA) is a technique that measures the change of weight as a function of temperature using a furnace and a high precision balance.[66] This method can give information on many physical and chemical phenomena such as thermal decomposition and gas reactions (i.e. oxidation and reduction).[66] Nevertheless, in the field of organic electronics, it is mainly used to investigate the thermal stability, where the decomposition temperature can be evaluated.[67] TGA experiments were performed on compounds **2.4-2.9** and **2.16-2.17** using a Bruker TGA-IR Tensor 27 at a scanning rate of 10 °C min^{-1} under nitrogen atmosphere. The decomposition temperature was determined from the first derivative of the TGA curve. The results showed increased thermal stability for all six compounds as compared to unsubstituted isoindigo **2.16-2.17**. In general, substituted compounds with branched alkyl chain (**2.5**, **2.7**, **2.9**, **2.17**) have higher decomposition temperatures than those of substituted compounds with hexyl alkyl chain (**2.4**, **2.6**, **2.8**, **2.16**). This could be due to branching. However, among substituted isoindigo compounds, fluorinated compounds **2.4-2.5** exhibited the lowest decomposition temperate even though they had the highest molecular weight.

Table 2.2. Decomposition temperatures of compounds **2.4-2.9** and **2.16-2.17**.

Compound	Empirical Formula	Molecular weight (g.mol^{-1})	T_d (°C)
2.16	$C_{28}H_{34}N_2O_2$	430.26	379
2.17	$C_{32}H_{42}N_2O_2$	486.7	337.3
2.4	$C_{44}H_{38}F_{12}N_2O_2$	854.77	388
2.5	$C_{48}H_{46}F_{12}N_2O_2$	910.87	393.1
2.6	$C_{48}H_{58}N_2O_2$	694.99	393.5
2.7	$C_{52}H_{66}N_2O_2$	751.09	402.4
2.8	$C_{46}H_{54}N_2O_8$	762.93	393.1
2.9	$C_{50}H_{62}N_2O_8$	819.04	393.9
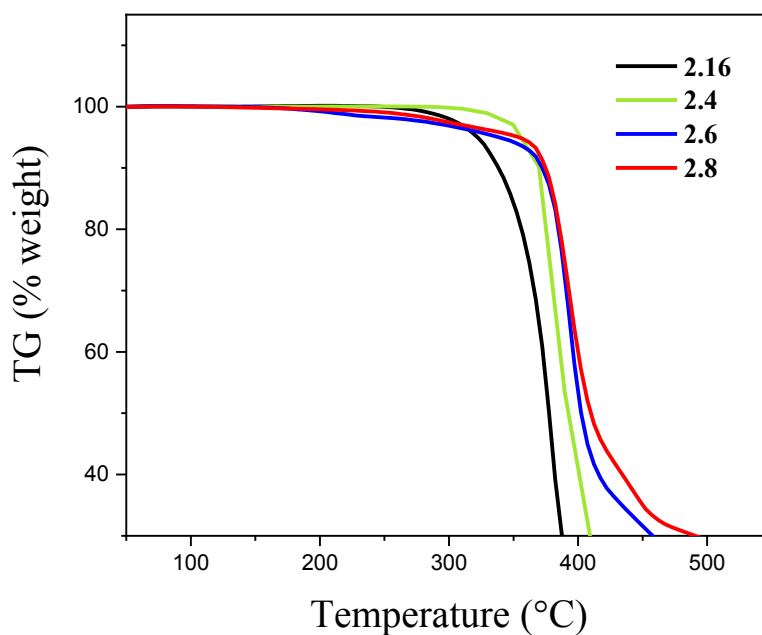
Figure 2.8. TGA results showing the thermal decomposition process of the hexyl-substituted series.
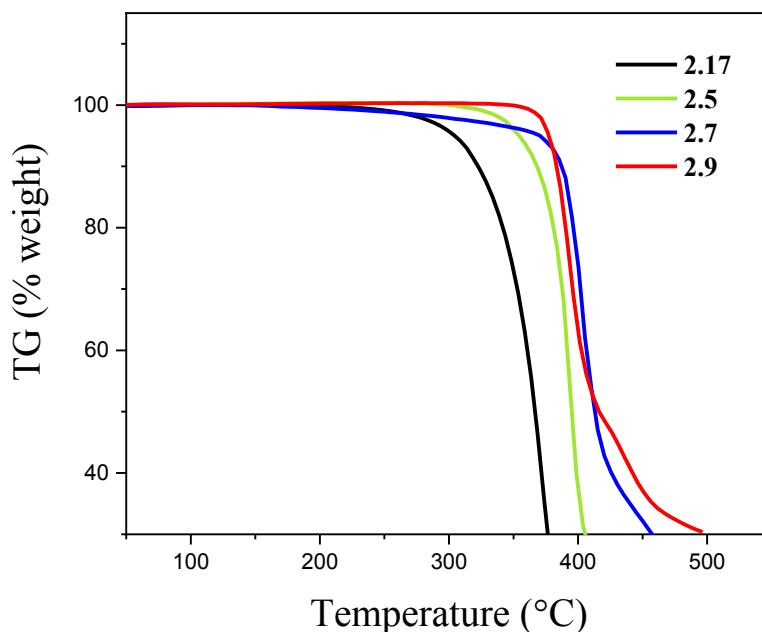
Figure 2.9. TGA results showing the thermal decomposition process of the 2-ethylhexyl-substituted series.

The phase transition of a compound can be detected by either differential thermal analysis (DTA) which measures the change of temperature as a function of time or temperature of by differential Scanning calorimetry (DSC). Nevertheless, DSC has been widely more used. DSC can be advantageous since it can study different types of reactions such as oxidation, and it can determine the glass transition temperature of amorphous solids.[68] Generally, DSC measures the change of the heat flow (energy) as a function of time or temperature, where the sample and the reference are maintained at the same temperature. Depending on the type of the phase transition (exothermic or endothermic), more or less heat flow is required to compensate the temperature of the sample to be equal to the reference. For instance, a crystallization is exothermic, thus it will give energy to the system and it requires less heat flow to have the same temperature of the empty reference. Such phase transitions are detected form the DSC curve. The integration of a peak on the curve corresponding to a certain transition can give the enthalpy of that transition according to the equation: $\Delta H = KA$

where ΔH is the enthalpy of the transition, K is the calorimetric constant (instrument dependent), and A is the area under the curve.[68]

DSC experiments were performed on compounds (**2.4-2.9**; **2.16-2.17**) using TA instrument. Heat/cool/heat cycles were carried out while maintaining a heating/cooling rate of 10 °C min^{-1} under nitrogen atmosphere. Heating cycles were set around 90 degrees below the corresponding decomposition temperatures determined by TGA. Figures 2.10-2.15 show the collected DSC curves of the 2nd heating and the 1st cooling cycles of the compounds (**2.4-2.9**). Noting that the 1st heating cycle was carried out to remove the thermal history of the compounds. Higher melting points were obtained for trifluoromethyl containing compounds **2.4-2.5**. All branched compounds exhibited a lower melting point than their unbranched derivatives except for compounds **2.8-2.9**. Moreover, only trifluoromethyl containing compounds **2.4-2.5** showed a crystallization temperature compared to the rest of the isoindigo derivatives. The results are summarized in Table 2.3.

Table 2.3. DSC results for compounds **2.4-2.9**.

	Mol wt, (g.mol^{-1})	Transition	Onset temp (ºC)	Maximum temp (ºC)	Area (J.g^{-1})	Molar enthalpy (kJ.mol^{-1})
2.4	854.77	crystallization	227.02	235.68	8.30	7.09
		melting	230.33	244.91	11.15	9.53
2.5	910.87	crystallization	129.58	141.92	8.59	7.83
		melting	167.42	179.75	8.67	7.90
2.6	694.99	crystallization	--	--	--	--
		melting	198.92	232.04	22.39	15.56
2.7	751.09	crystallization	--	--	--	--
		melting	142.02	172.34	20.36	15.29
2.8	762.93	crystallization	--	--	--	--
		melting	142.01	153.50	1.43	1.09
2.9	819.04	crystallization	--	--	--	--
		melting	160.49	173.00	8.60	7.05
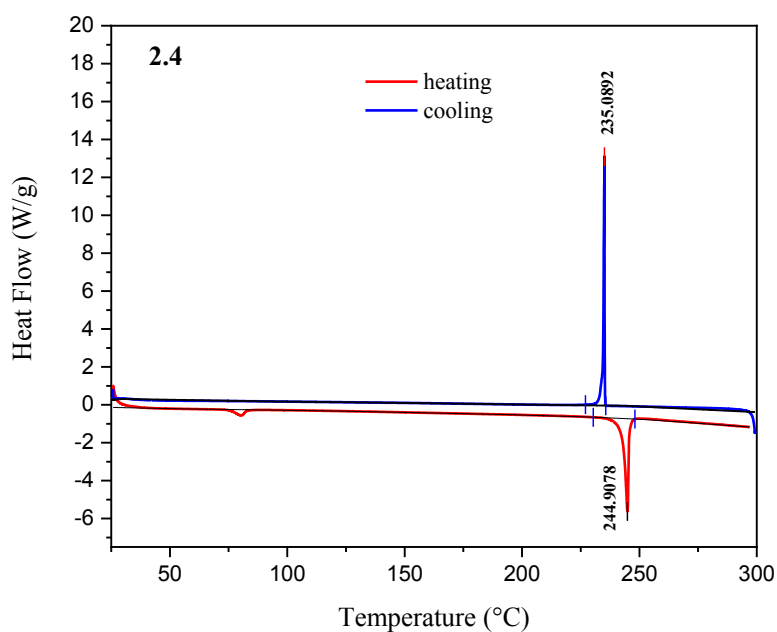
Figure 2.10. DSC analysis for compound **2.4**.
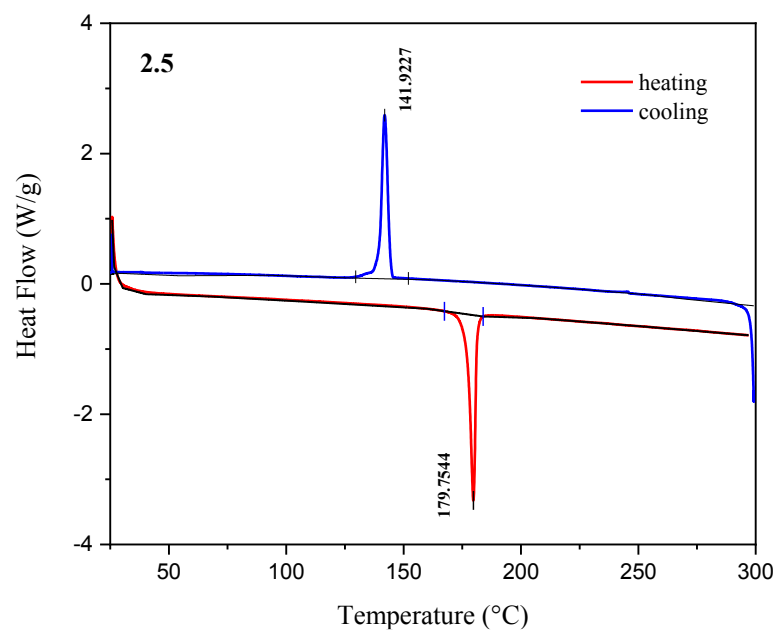
Figure 2.11. DSC analysis for compound **2.5**.
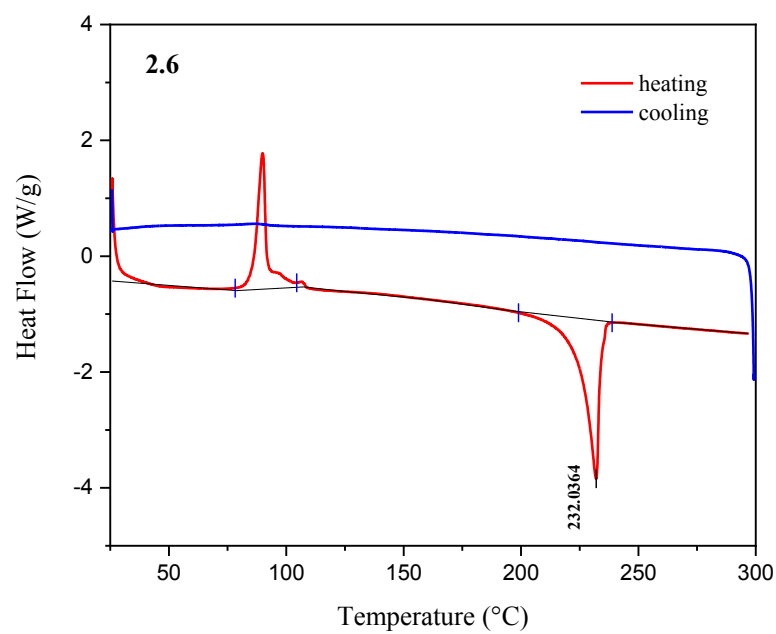
Figure 2.12. DSC analysis for compound **2.6**.

26
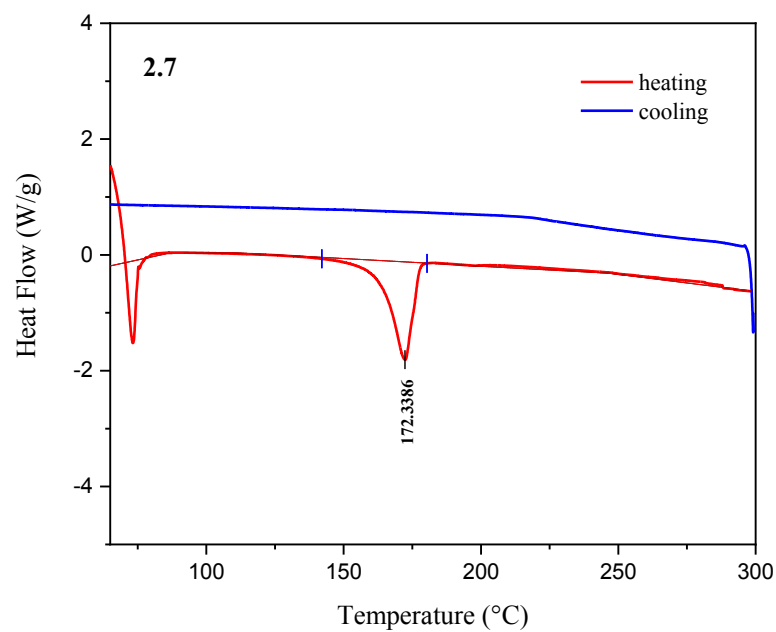
Figure 2.13. DSC analysis for compound **2.7**.
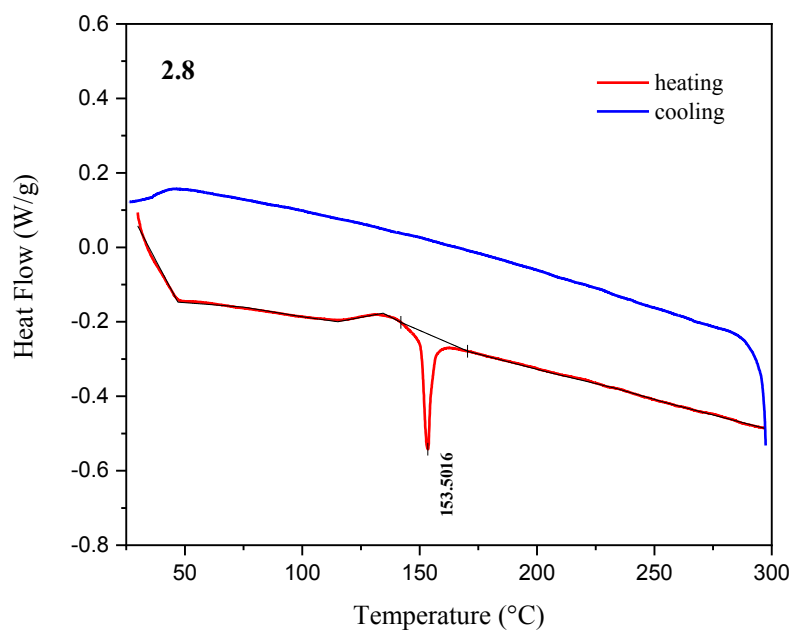
Figure 2.14. DSC analysis for compound **2.8**.
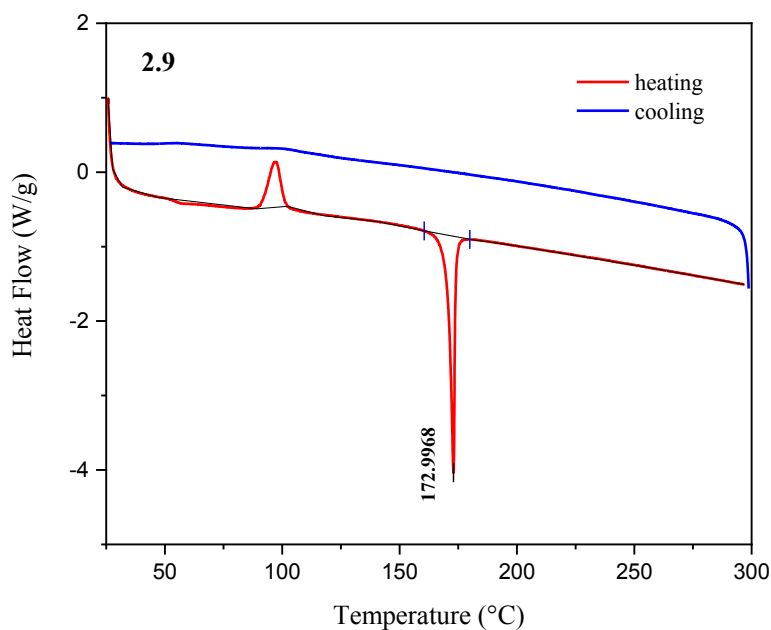
Figure 2.15. DSC analysis for compound **2.9**.

2.3. Experimental

2.3.1. Synthesis

All reactions were run using clean and oven dried glassware. Decomposition temperatures (T_d) were determined using a NETZSCH thermogravimetric analyzer and were defined to be as a loss of 5% of the initial sample mass upon heating at a 20 °C/min rate; under continuous flow of nitrogen gas in order to ensure a completely inert atmosphere inside the heating chamber during measurements. Melting temperatures were determined using a TA Instruments, Q2000 differential scanning calorimeter. NMR spectra were acquired using a 500 MHz Bruker NMR machine. Elemental analyses were performed at Atlantic Microlab, Inc., Norcross, USA.

(*E*)-[3,3'-biindolinylidene]-2,2'-dione (2.14)

The title compound was synthesized according to a literature procedure.[28] Compounds **2.10** (11.05 g, 75.10 mmol) and **2.12** (10.00 g, 75.10 mmol) were dissolved in 225 mL acetic

acid. 3 mL of concentrated HCl was then added, and the mixture was refluxed for 24 hours. The mixture was then cooled to room temperature and collected by vacuum filtration. The obtained dark brown solid was then washed with water, and methanol. Compound **2.14** (16.27 g, 83%) was obtained as a dark brown solid. ^{1}H NMR (500 MHz, DMSO-d$_6$): δ 10.91 (s, 2H), 9.05 (d, J = 7.5 Hz, 2H), 7.34 (dd, J_1 = 8 Hz, J_2 = 1.0 Hz, 2H), 6.98 (dd, J_1 = 8 Hz, J_2 = 1.0 Hz, 2H), 6.85 (dd, J = 7.5 Hz, J = 0.5 Hz, 2H). ^{13}C NMR (125 MHz, CDCl$_3$): δ 169.45, 144.54, 133.81, 133.11, 129.77, 122.15, 121.63, 110.01.

2.14
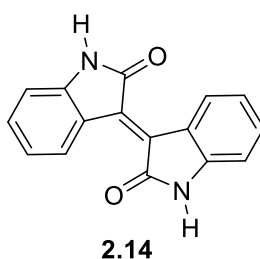
6,6'-Dibromo-[3,3'-biindolinylidene]-2,2'-dione (2.15)

The title compound was synthesized according to a modified literature procedure.[28] Compounds **2.11** (2.66 g, 11.79 mmol) and **2.13** (2.50 g, 11.79 mmol) were dissolved in 150 mL acetic acid. 1 mL of concentrated HCl was then added, and the mixture was stirred in a pressure vessel at 115 °C for 48 hours. The mixture was then cooled to room temperature and collected by vacuum filtration. The obtained dark brown solid was then washed with acetic acid, water (5×20 mL) and methanol, and then recrystallized from 1,2-dichlorobenzene. Compound **2.15** (4.20 g, 88%) was obtained as a dark brown solid. ^{1}H NMR (500 MHz, DMSO-d$_6$): δ 11.10 (s, 2H), 8.99 (d, J = 9.5 Hz, 2H), 7.19 (dd, J_1 = 10.5 Hz, J_2 = 7.0 Hz, 2H), 6.99 (d, J = 2.0 Hz, 2H). ^{13}C NMR (125 MHz, CDCl$_3$): δ 167.77, 145.80, 132.69, 131.20, 126.76, 125.16, 120.44, 111.34, 40.30, 31.46, 27.37, 26.67, 22.55, 14.02.

2.15
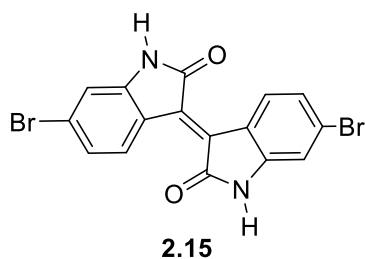
(*E*)-1,1'-dihexyl-[3,3'-biindolinylidene]-2,2'-dione (2.16)

The title compound was synthesized according to a modified literature procedure.[29] In a three-neck round bottom flask, compound **2.14** (1.0 g, 3.81 mmol) and potassium carbonate (2.63 g, 19.07 mmol, 5 eqv) were dissolved in 25 mL of DMF. The reaction mixture was then purged with argon for 30 minutes at room temperature. 1-Bromohexane (1.00 g, 6.04 mmol, 4 eqv) was added to the mixture drop wise, and without the interruption of the argon gas flow. The reaction mixture was then stirred at 200 °C, and refluxed for 1 hour. The reaction was cooled down to room temperature then filtered. The obtained red solid was washed with water and methanol and then purified by column chromatography over silica gel using hexane:dichlomethane (6:4) as eluent. Compound **2.16** (0.35 g, 22%) was obtained as a dark red solid. ^{1}H NMR (500 MHz, CDCl$_3$): δ 9.16 (dd, J_1= 8.0 Hz, J_2= 0.5 Hz, 2H), 7.34 (dt, J_1= 7.5 Hz, J_2= 1.0 Hz, 2H), 7.04 (dt, J_1= 8.0 Hz, J_2= 1.5 Hz, 2H), 6.78 (dd, J_1 = 8.0 Hz, J_2= 0.5 Hz, 2H), 3.76 (t, J = 7.5 Hz, 4H), 1.70 (p, J = 7.0 Hz, 4H), 1.37-1.29 (m overlapping, 12H), 0.87 (t, J = 7.0 Hz, 6H). ^{13}C NMR (125 MHz, CDCl$_3$): δ 167.87, 144.75, 133.58, 132.31, 129.93, 122.15, 121.73, 107.88, 40.11, 31.54, 27.46, 26.73, 22.54, 14.02.

2.16

(*E*)-1,1'-bis(2-ethylhexyl)-[3,3'-biindolinylidene]-2,2'-dione (2.17)

The title compound was synthesized according to a modified literature procedure.[29] In a three-neck round bottom flask, compound **2.14** (2.00 g, 7.63 mmol) and potassium carbonate (5.27 g, 30.50 mmol, 5 eqv) were dissolved in 30 mL of DMF. The reaction mixture was then purged with argon for 30 minutes at room temperature. 2-Ethylhexylbromide (5.83 g, 30.50 mmol, 4 eqv) was added to the mixture drop wise, and without the interruption of the argon gas flow. The reaction mixture was then stirred at 200 °C and refluxed for 1 hour. The reaction was cooled down to room temperature then poured into water. The mixture was extracted with dichloromethane. The organic layer was dried over $MgSO_4$ then filtered. The solvent was removed under reduced pressure. The obtained residue was washed with methanol, filtered and purified by column chromatography over silica gel using hexane: dichloromethane (9:1) as eluent to afford a dark purple red solid **2.17** (0.70 g, 43%). ^{1}H NMR (500 MHz, $CDCl_3$): δ 9.13 (d, $J = 8.0$ Hz, 2H), 7.31 (dt, $J = 8.5$ Hz, $J_2 = 1.0$ Hz, 2H), 7.03 (dt, $J = 8.5$ Hz, $J_2 = 1.0$ Hz, 2H), 6.75 (d, $J = 8.0$ Hz, 2H), 3.64 (m, 4H), 1.85 (p, $J = 6.0$ Hz, 2H), 1.36-1.28 (m overlapping, 14H), 0.90-0.86 (m overlapping, 12H). ^{13}C NMR (125 MHz, $CDCl_3$): δ 168.29, 145.13, 133.57, 132.32, 129.70, 122.17, 121.69, 108.18, 77.32, 77.06, 76.81, 44.21, 37.57, 30.72, 28.79, 24.07, 23.11, 14.14, 10.75. Anal. Calcd for $C_{32}H_{42}N_2O_2$: C, 78.97; H, 8.70; N, 5.76. Found: C, 79.18; H, 8.89; N, 5.51.
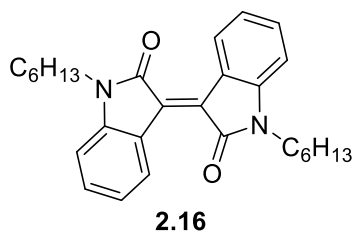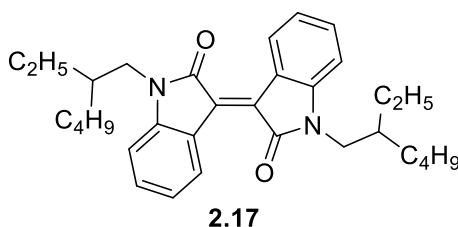

2.17

6,6'-Dibromo-1,1'-dihexyl-[3,3'-biindolinylidene]-2,2'-dione (2.18)

The title compound was synthesized according to a modified literature procedure. [29] In a three-neck round bottom flask, compound **2.15** (1.00 g, 2.30 mmol) and potassium bromide (1.60 g, 11.90 mmol, 5 eqv) were dissolved in 30 mL of DMF. The reaction mixture

was then purged with argon for 30 minutes at room temperature. 1-Bromohexane (1.59 g, 9.50 mmol, 4 eqv) was added to the mixture drop wise, and without the interruption of the argon gas flow. The reaction mixture was then stirred at 200 °C, and refluxed for 1 hour. The reaction was cooled down to room temperature and filtered. Compound **2.18** (1.06 g, 76 %) was obtained as a bright red solid and washed with minimal amount of DMF, (3 × 25 mL) water and (2 × 25 mL) methanol. ^{1}H NMR (500 MHz, CDCl$_3$): δ 9.08 (d, J = 8.5 Hz, 2H), 7.18 (dd, J_1 = 8.5 Hz, J_2 = 2.0 Hz, 2H), 6.93 (d, J = 2.0 Hz, 2H), 3.75 (t, J = 7.5 Hz, 4H), 1.71 (p, J = 7.5 Hz, 4H), 1.42-1.23 (m overlapping, 18H), 0.90 (t, J = 7 Hz, 7H). ^{13}C NMR (125 MHz, CDCl$_3$): δ 167.74, 145.77, 132.67, 131.17, 126.74, 125.14, 120.40, 111.32, 40.27, 31.45, 27.36, 26.66, 22.55, 14.03.

2.18

(*E*)-6,6'-dibromo-1,1'-bis(2-ethylhexa-3,5-diyn-1-yl)-[3,3'-biindolinylidene]-2,2'-dione compound with dihydrogen (1:6) (2.19)
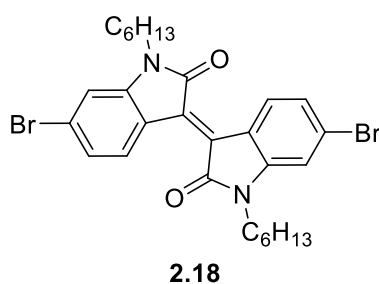
The title compound was synthesized according to a modified literature procedure.[29] In a three-neck round bottom flask, compound **2.15** (2.00 g, 4.80 mmol) and potassium carbonate (3.30 g, 23.80 mmol, 5 eqv) were dissolved in 30 mL of DMF. The reaction mixture was then purged with argon for 30 minutes at room temperature. 2-Ethylhexylbromide (3.64 g, 19.10 mmol, 4 eqv) was added to the mixture drop wise, and without the interruption of the argon gas flow. The reaction mixture was then stirred at 200 °C, and refluxed for 1 hour. The reaction was cooled down to room temperature and filtered. The brown solid was washed with minimal amount of DMF, (3×25 mL) water and (2×25 mL)

methanol, then purified by column chromatography on silica gel with hexane:dichloromethane (6:4) as eluent. Compound **2.19** (1.5 g, 50 %) was obtained as a brown solid.^{1}H NMR (500 MHz, CDCl$_3$): δ 8.98 (d, J = 8.5 Hz, 2H), 7.12 (dd, J_1 = 8.5 Hz, J_2 = 2.0 Hz, 2H), 6.82 (d, J = 1.5 Hz, 2H), 3.54 (m, 4H), 1.77 (t, J = 2.0 Hz, 2H), 1.32-1.127 (m overlapping, 14H), 0.88 (m overlapping, 12H).^{13}C NMR (125 MHz, CDCl$_3$): δ 168.02, 146.10, 130.99, 126.69, 125.10, 120.32, 111.51, 44.33, 37.41, 30.56, 28.58, 23.10, 14.13, 10.67.

2.19
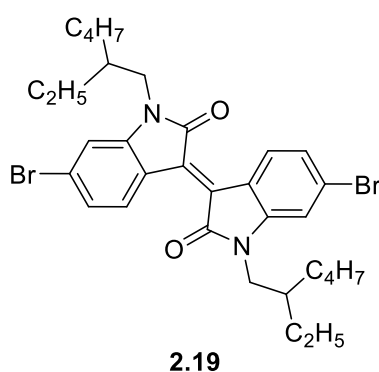
Tetrakis(triphenylphosphine)palladium(0)

The title compound was synthesized according to a literature procedure.[49] To a stirred solution of palladium(II) chloride (0.50 g, 2.82 mmol) in 30 mL DMSO, triphenylphosphine (3.70 g, 14.10 mmols, 5 eqv) was added. The mixture was purged with argon for 20 minutes, and stirred at 165 °C for 30 minutes under argon atmosphere. The reaction mixture turns from turbid to clear orange solution. Hydrazine monohydrate (550 μL) was then added dropwise, and the reaction was allowed to cool down gradually to room temperature over one hour under argon atmosphere and in the dark. Vacuum filtration was performed, a shiny yellow solid was obtained. The solid was washed with ethanol (3 x 10 mL), then with diethyl ether (3 x 10 mL), and dried under reduced pressure, in the dark, for 48 hrs. Tetrakis(triphenylphosphine)palladium(0) (3.00 g, 2.60 mmols, 92%) was immediately used for the next step without any further purification.

(*E*)-6,6'-bis(3,5-bis(trifluoromethyl)phenyl)-1,1'-dihexyl-[3,3'-biindolinylidene]-2,2'-dione (2.4)

The title compound was synthesized according to a modified literature procedure.[63] Compound **2.18** (0.30 g, 0.51 mmol), 3,5-bis(trifluoromethyl)phenylboronic acid (0.39 g, 1.53 mmol, 3 eqv), potassium carbonate 2M solution (3mL), and tetrabutylammonium bromide (10 mg) were added to 30 mL toluene. The mixture was purged with argon gas for 30 minutes. Freshly synthesized tetrakis(triphenylphosphine)palladium (0) (50 mg) was then added, and the reaction was refluxed at 110 °C for 48 hours under argon and in the dark. The reaction was then quenched with water and extracted with dichloromethane. The combined organic layer was dried over $MgSO_4$ and solvent was removed under reduced pressure. A dark brown residue was purified by silica gel column chromatography using hexane: dichloromethane (3:2) as mobile phase. The separated target compound was recrystallized from toluene-hexane. Compound **2.4** (0.36 g, 52%) was obtained as red purple small needles. ^{1}H NMR (500 MHz, CDCl$_3$): δ 9.34 (d, J = 8.5 Hz, 2H), 8.02 (s, 4H), 7.89 (s, 2H), 7.26 (dd, J_1 = 8.5 Hz, J_2 = 1.5 Hz, 2H), 6.93 (s, 2H), 3.87 (t, J = 7 Hz, 4H), 1.77 (p, J = 7 Hz, 4H), 1.43-1.23 (m overlapping, 12H), 0.87 (t, J = 7.0 Hz, 6H). ^{13}C NMR (125 MHz, CDCl$_3$): δ 167.91, 145.84, 142.69, 142.15, 133.12, 132.50, 132.233, 130.94, 127.17, 124.36, 122.15, 121.23, 106.35, 40.23, 31.46, 29.71, 29.37, 27.50, 26.70, 22.70, 22.53, 14.12, 13.97. Anal. Calcd for $C_{44}H_{38}F_{12}N_2O_2$: C, 61.83; H, 4.48; N, 3.28. Found: C, 61.94; H, 4.33; N, 3.27.

2.4
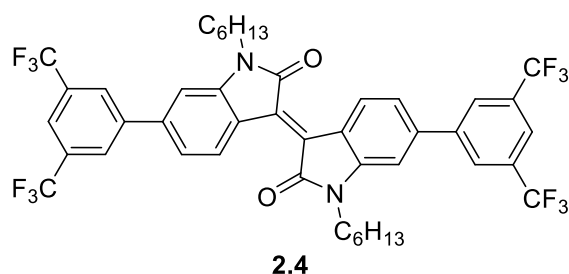
6,6'-Bis(4-(*tert*-butyl)phenyl)-1,1'-dihexyl-[3,3'-biindolinylidene]-2,2'-dione (2.6)

The title compound was synthesized according to a modified literature procedure.[63]

Compound **2.18** (0.25 g, 0.42 mmol), 4-*tert*-butylphenylboronic acid (0.23 g, 1.27 mmol, 3

eqv), potassium carbonate 2M solution (3mL), and tetrabutylammonium bromide (10 mg)

were added to 30 mL toluene. The mixture was purged with argon gas for 30 minutes.

Freshly synthesized tetrakis(triphenylphosphine)palladium (0) (50 mg) was then added, and

the reaction was refluxed at 110 °C for 48 hours under argon and in the dark. The reaction

was then quenched with distilled water, then extracted with dichloromethane. The combined

organic layer was dried over $MgSO_4$ and solvent was removed under reduced pressure. The

dark red brownish residue was obtained and purified by silica gel column chromatography

using hexane: dichloromethane (1:1) as mobile phase. **2.6** (0.20 g, 67%) was isolated as a

dark red brownish solid. ^{1}H NMR (500 MHz, CDCl$_3$): δ 9.26 (d, J = 8.0 Hz, 2H), 7.63 (d, J =

8.5 Hz, 4H), 7.54 (d, J = 8.5 Hz, 4H), 7.31 (dd, J_1 = 8.5 Hz, J_2 = 1.5 Hz, 2H), 7.01 (d, J = 1.5

Hz, 2H), 3.87 (t, J = 7.5 Hz, 4 H), 1.77(p, J = 7.5 Hz, 4H), 1.46 (p, J = 6.75 Hz, 4H), 1.40 (s,

18H), 1.37-1.27 (m overlapping, 8H), 0.92 (t, J = 7 Hz, 6H). ^{13}C NMR (125 MHz, CDCl$_3$): δ

168.30, 151.41, 145.26, 144.95, 137.73, 132.47, 130.23, 126.79, 125.88, 120.74, 106.28,

40.11, 34.67, 31.56, 31.33, 27.58, 26.78, 22.71, 22.58, 14.06. Anal. Calcd for $C_{48}H_{58}N_2O_2$: C,

82.95; H, 8.41; N, 4.03. Found: C, 82.66; H, 8.56; N, 3.88.

2.6

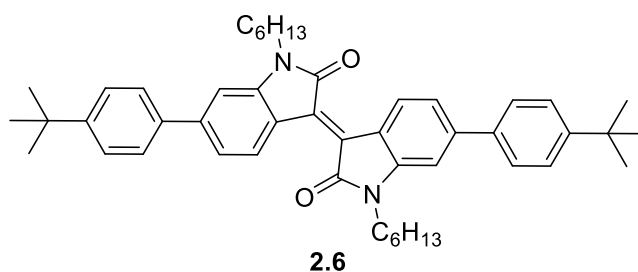**(*E*)-1,1'-dihexyl-6,6'-bis(3,4,5-trimethoxyphenyl)-[3,3'-biindolinylidene]-2,2'-dione (2.8)**

The title compound was synthesized according to a modified literature procedure.[63] Compound **2.18** (0.35 g, 0.59 mmol), 3,4,5-trimetoxyphenylboronic acid (0.38 g, 1.78 mmol, 3 eqv), potassium carbonate 2M solution (3mL), and tetrabutylammonium bromide (10 mg) were added to 30 mL toluene. The mixture was purged with argon gas for 30 minutes. Freshly synthesized tetrakis(triphenylphosphine)palladium (0) (50 mg) was then added, and the reaction was refluxed at 110 °C for 48 hours under argon and in the dark. The reaction was then quenched with distilled water, then extracted with dichloromethane. The combined organic layer was dried over Na_2SO_4 and solvent was removed under reduced pressure. The dark red brownish residue was obtained and purified by silica gel column chromatography using hexane:dichloromethane (1:9) as mobile phase. Compound **2.8** (0.36 g, 80%) was isolated as a dark maroon solid. ^{1}H NMR (500 MHz, CDCl$_3$): δ 9.25 (d, J = 8.0 Hz, 2H), 7.24 (dd, , J_1 = 8.5 Hz, J_2 = 1.5 Hz, 2H), 6.92 (d, J = 1.5 Hz, 2H), 6.82 (s, 4H), 3.96 (s, 12H), 3.91 (s, 6H), 3.87 (t, J = 7.5 Hz, 4 H), 1.78 (p, J = 7.5 Hz, 4H), 1.45 (p, J = 7 Hz, 4H), 1.40 (m, 8H), 0.89 (t, J = 7 Hz, 6H). ^{13}C NMR (125 MHz, CDCl$_3$): δ 168.29, 153.59, 145.41, 145.32, 138.59, 136.67, 132.54, 130.27, 120.95, 120.91, 106.40, 104.66, 61.03, 56.36, 40.13, 31.52, 27.57, 26.75, 22.55, 14.03. Anal. Calcld for $C_{46}H_{54}N_2O_8$: C, 72.42; H, 7.13; N, 3.67. Found: C, 72.71; H, 7.41; N, 3.49.

2.8

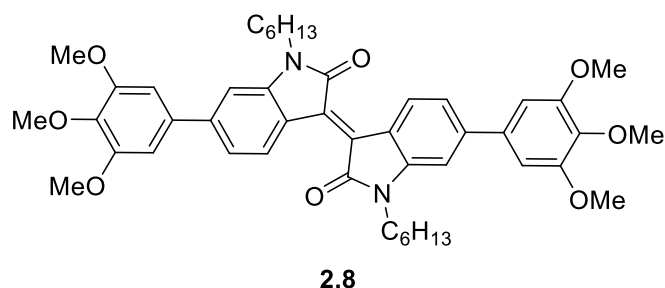**(E)-6,6'-bis(3,5-bis(trifluoromethyl)phenyl)-1,1'-bis(2-ethylhexyl)-[3,3'-biindolinylidene]-2,2'-dione (2.5)**

The title compound was synthesized according to a modified literature procedure.[63] Compound **2.19** (0.35 g, 0.54 mmol), 3,5-bis(trifluoromethyl)phenylboronic acid (0.42 g, 1.63 mmol, 3 eqv), potassium carbonate 2M solution (3.3 mL), and tetrabutylammonium bromide (10 mg) were added to 33 mL toluene. The mixture was purged with argon gas for 30 minutes. Freshly synthesized tetrakis(triphenylphosphine)palladium (0) (50 mg) was then added, and the reaction was refluxed at 110 ºC for 48 hours under argon and in the dark. The reaction was then quenched with distilled water, then extracted with dichloromethane. The combined organic layer was dried over Na_2SO_4 and solvent was removed under reduced pressure. The dark red brownish crude was purified by column chromatography using hexane:dichloromethane (7:3) as mobile phase and recrystallized from ethanol-hexane. Compound **2.5** (0.24 g, 70%) was isolated as a dark brown purple solid. ^1H NMR (500 MHz, CDCl$_3$): δ 9.34 (d, $J = 8.5$ Hz, 2H), 8.04 (s, 4H), 7.91 (s, 2H), 7.31 (dd, $J_1 = 8.5$ Hz, $J_2 = 1.5$ Hz, 2H), 6.97 (d, $J = 1.5$ Hz, 2H), 3.80 (m, 4 H), 1.91 (p, $J = 3$ Hz, 2H), 1.23-1.25 (m overlapping, 16H), 0.98 (t, $J = 7$ Hz, 6H), 0.91 (t, $J = 7$ Hz, 6H). ^{13}C NMR (125 MHz, CDCl$_3$): δ 168.29, 146.23, 142.58, 141.94, 133.10, 132.53, 132.26, 130.80, 127.06, 124.36, 122.18, 122.12, 121.74, 121.11, 106.60, 44.23, 37.79, 30.82, 29.72, 28.91, 24.27, 23.04, 14.00, 10.73. Anal. Calcd for $C_{48}H_{46}F_{12}N_2O_2$: C, 63.29; H, 5.09; N, 3.08. Found: C, 63.54; H, 5.12; N, 3.03.

2.5

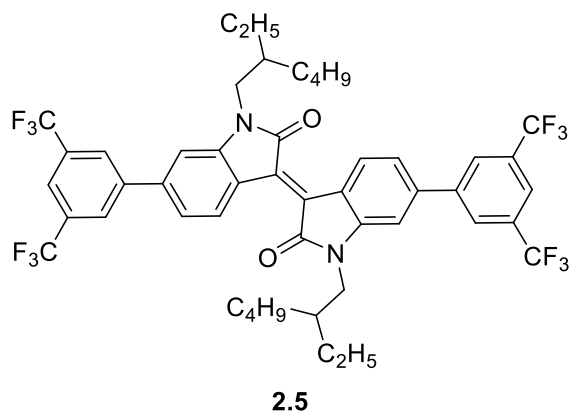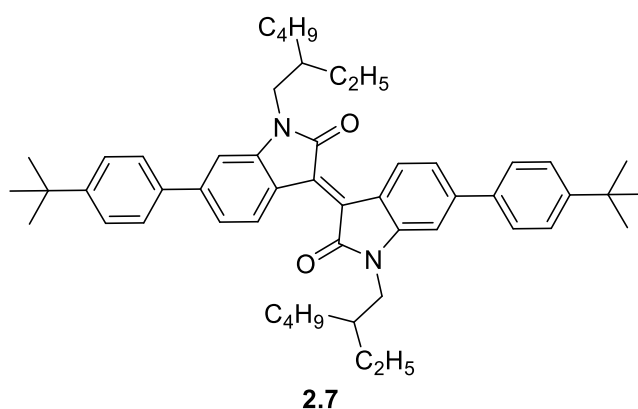**(*E*)-6,6'-bis(4-(*tert*-butyl)phenyl)-1,1'-bis(2-ethylhexyl)-[3,3'-biindolinylidene]-2,2'-dione (2.7)**

The title compound was synthesized according to a modified literature procedure.[63] Compound **2.19** (0.35 g, 0.54 mmol), 4-*tert*-butylphenylboronic acid (0.29 g, 1.63 mmol, 3 eqv), potassium carbonate 2M solution (3 mL), and tetrabutylammonium bromide (10 mg) were added to 30 mL toluene. The mixture was purged with argon gas for 30 minutes. Freshly synthesized tetrakis(triphenylphosphine)palladium (0) (50 mg) was then added, and the reaction was refluxed at 110 ºC for 48 hours under argon and in the dark. The reaction was then quenched with distilled water, then extracted with chloroform. The combined organic layer was dried over Na_2SO_4 and solvent was removed under reduced pressure. The dark red brownish residue was obtained and purified by column chromatography using hexane:chloroform (7:3) as mobile phase. Compound **2.7** (0.35 g, 86%) was isolated as a dark maroon solid. ^{1}H NMR (500 MHz, CDCl$_3$): δ 9.23 (dd, J_1 = 8.5 Hz, J_2 = 8.0 Hz, 2H), 7.61 (dd, J_1 = 8.0 Hz, J_2 = 5.5 Hz, 4H), 7.53 (dd, J_1 = 8.0 Hz, J_2 = 5.5 Hz, 4H), 7.31 (m, 2H), 7.00 (d, J = 4.0 Hz, 2H), 3.79 (m, 4 H), 1.93 (m, 2H), 1.39 (m overlapping, 16H), 1.34 (m overlapping, 12H), 0.97 (dd, J_1 = 6.0 Hz, J_2 = 12.0 Hz, 8H), 0.92 (dd, J_1 = 6.0 Hz, J_2 = 12.0 Hz, 8H). ^{13}C NMR (125 MHz, CDCl$_3$): δ 168.75, 151.42, 145.70, 144.82, 137.70, 132.46, 130.04, 126.69, 125.91, 120.68, 106.50, 44.24, 37.70, 34.67, 31.33, 30.78, 28.81, 24.15,

23.10, 14.09, 10.79. Anal. Calcd for $C_{52}H_{66}N_2O_2$: C, 83.15; H, 8.86; N, 3.73. Found: C, 83.28; H, 9.01; N, 3.60.

2.7

(E)-1,1'-bis(2-ethylhexyl)-6,6'-bis(3,4,5-trimethoxyphenyl)-[3,3'-biindolinylidene]-2,2'-dione (2.9)

The title compound was synthesized according to a modified literature procedure.[63] Compound **2.19** (0.30 g, 0.47 mmol), 3,4,5-trimetoxyphenylboronic acid (0.30 g, 1.40 mmol, 3 eqv), potassium carbonate 2M solution (3 mL), and tetrabutylammonium bromide (10 mg) were added to 30 mL toluene. The mixture was purged with argon gas for 30 minutes. Freshly synthesized tetrakis(triphenylphosphine)-palladium (0) (50 mg) was then added, and the reaction was refluxed at 110 ºC for 48 hours under argon and in the dark. The reaction was then quenched with distilled water, then extracted with dichloromethane. The combined organic layer was dried over Na_2SO_4 and solvent was removed under reduced pressure. The dark red brownish residue was purified by silica gel column chromatography using hexane:ethyl acetate (9:1) as mobile phase. The isolated product was recrystallized from toluene-hexane **2.9** (0.34 g, 89%) was isolated as a dark brown solid. ^{1}H NMR (500 MHz, CDCl$_3$): δ 9.24 (d, J = 8.5 Hz, 2H), 7.24 (d, J = 1.5 Hz, 2H), 6.95 (d, J = 1.5 Hz, 2H), 6.83 (s, 4H), 3.95 (d, J = 17 Hz, 18H), 3.81 (m, 4 H), 1.93 (p, J = 6.5 Hz, 2H), 1.42-1.25 (m overlapping, 18H), 0.98 (t, J = 7 Hz, 6H), 0.97 (t, J = 7 Hz, 6H). ^{13}C NMR (125 MHz, CDCl$_3$): δ 168.69, 153.59, 145.71, 145.12, 138.54, 136.51, 132.49, 130.11, 120.94, 120.74,

106.59, 104.42, 61.02, 56.27, 44.13, 37.88, 30.95, 29.70, 28.98, 24.24, 23.08, 22.70, 14.08, 10.83. Anal. Calcd for $C_{50}H_{62}N_2O_8$: C, 73.32; H, 7.63; N, 3.42. Found: C, 73.28; H, 7.68; N, 3.45.

2.9

2.3.2. Photophysical Studies

Absorption spectra were measured using a Thermo scientific Genesys 10S UV-Vis spectrophotometer. Slit widths were fixed at 5 nm. A blank measurement with no sample in the sample holder was subtracted from all actual spectra to account for any error possible. UV-transparent quartz cuvette 136 (1 x 1 cm) was used for all experiments.

Stock solutions of concentration 1 mM of each compound were prepared in chloroform. UV-vis measurements were performed on 60 μM solutions. Molar absorptivity was determined using calibration curve technique for a set of 5 different concentrations (1 μM, 10 μM, 20 μM, 40 μM and 60 μM) for each compound. Stock solutions and all prepared concentrations were kept in the freezer and used the next day.

CHAPTER 3

COMPUTATIONAL MODELING AND

ELCTROCHEMISTRY OF 6,6'-DIARYLSUBSTITUTED

ISOINDIGO COMPOUNDS

3.1 Introduction

3.1.1 Computational Chemistry

Computational chemistry is a powerful tool since it can contribute to solving chemical problems through computer simulations.[69] It allows to calculate the structure and properties of molecules based on theoretical chemistry.[69,70] For example, it can estimate molecular geometry, energies of molecules, transition states, chemical reactivity and spectroscopy.[70] Therefore, computational chemistry quickly became a highly attractive and reliable tool in all fields of chemistry especially in molecular design[71,72] and interpretation of material chemistry.[73]

Generally, computational chemistry uses different methods depending on the type and accuracy of calculations desired.[74] For instance, molecular mechanics can predict and visualize the geometry of a molecule using geometry optimization in order to find the geometry with the lowest energy possible.[75] Moreover, molecular dynamics calculations can study the motion of molecules such as protein binding.[76] These methods are fast and are usually used for large molecules, such as DNA, proteins and enzymes. Whereas, other methods that rely on quantum mechanics[77] take longer times. Such methods, i.e. quantum mechanics methods,[78] are based on the fundamental equation of modern physics, the Schrödinger equation.[79] Since this equation cannot be solved exactly for molecules bearing

more than one electron, approximations are followed. For instance, in the pioneering work of Hartree and Fock, electron correlations were neglected.[80] Both ab initio and semiempirical calculations use the Schrödinger equation, however, ab initio calculations consider less approximations and thus take longer times.[70] Density functional theory (DFT)[81] is another method that relies on the Schrödinger equation. While both ab initio and semiempirical calculations solve the wavefunction, DFT derives directly the electron density function (i.e. the electron distribution).[70] In the recent years, DFT became one of the most reliable and popular methods in the prediction and interpretation of compounds used in materials science.[82] Hence, it works hand in hand with experimental methods, to confirm, to complement, to further predict trends in geometric, electronic, and spectroscopic properties and to offer some explanation and understanding to observed experimental results.[82]

3.1.2 Electrochemistry

Voltammetry is a known branch of electrochemistry that developed initially from the noble prized discovery of polarography in 1959.[83] Even though early techniques of voltammetry were quite difficult for routine analytical use, many remarkable advances were achieved in the recent years. The inexpensive instrumentation in addition to the enhanced sensitivity of measurements rendered voltammetry techniques reliable in numerous applications in organic and inorganic chemistry such as speciation, solution thermodynamics, determining oxidation parameters, studying surface absorption, electron transfer kinetics, reaction mechanisms, and transport processes.[84] Voltammetric techniques offer amenability to many solvents and electrolytes, at many temperatures. These techniques provide flexibility with rapid analysis times (on the order of one second), simultaneous determination of several analytes and kinetic and mechanistic parameters, well-understood physics that permits reasonable estimation of values of unknown parameters, and ease of determination of potential waveforms and using small currents.[84]

Generally, voltammetric methods measure the resulting current (i) of an electrochemical cell as a certain potential (E) is applied to an electrode.[84] The applied potential (E) can be varied white the current (i) is measured over time (t). Workers construct an electrochemical cell with two or three electrodes: a working electrode, a reference electrode, and possibly a counter electrode.[84]

Among the most important and widely used methods of voltammetry are cyclic voltammetry[85] and pulse voltammetry[86] methods. Learning about redox processes, identifying reaction intermediates, and studying reaction product stability are all applications of cyclic voltammetry (CV). This technique (at a known current) consistently varies the applied potential at the working electrode with current going in both direction between electrodes. This technique is amenable to full, partial, and multiple cycles.[85]

Pulse voltammetry methods were developed in order to enhance speed and sensitivity, such as normal pulse voltammetry (NPV), differential pulse voltammetry (DPV)[87,88] and square-wave voltammetry (SWV).[89] Normal pulse voltammetry (NPV) pulses the potential serially over increasing amplitudes. To avoid measurement of the charging current, current is measured at the end of each pulse.[84] Differential pulse voltammetry (DPV) follows the same procedure as normal pulse voltammetry while potential is also scanned over a series of pulses.[84] NPV differs further as each potential pulse has fixed small amplitude at around (10 to 100 mV).[84] Thus, in DPV, the resulting current resulting from a series of larger potential pulses is compared with the current at a constant baseline voltage.[84].

3.1.3 Aims and Objectives

As discussed in Chapter 2, isoindigo has emerged as an important building block for optoelectronic device applications mostly in organic photovoltaics and organic field-effect transistors.[90-94] Attempts to describe the absorption behavior and thus expected spectroscopic

properties of indigo and isoindigo compounds were covered by extensive benchmark studies involving density functional theory (DFT) and time-dependent (TD) DFT.[95-100] When considering oligomers, only a few studies have thus far been reported utilizing isoindigo for organic field-effect transistor applications.[101-111]

In this chapter, we investigate isoindigo derivatives modulated on positions 6 and 6' with electron density-modulating groups for their electronic properties as explored by differential pulse voltammetry along with a comprehensive computational study of the ground and excited states by utilizing density functional theory both in gas phase and solution. This work was achieved by our collaborator Prof. Brigitte Wex and her student Peter Nasr from the Lebanese American University (LAU). The compounds included in this study are shown in Figure 3.1.
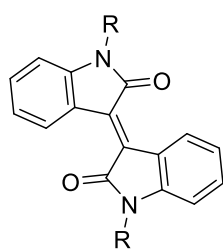
2.16: R = C$_6$H$_{13}$
2.17: R = 2-ethylhexyl
3.1: R = CH$_3$
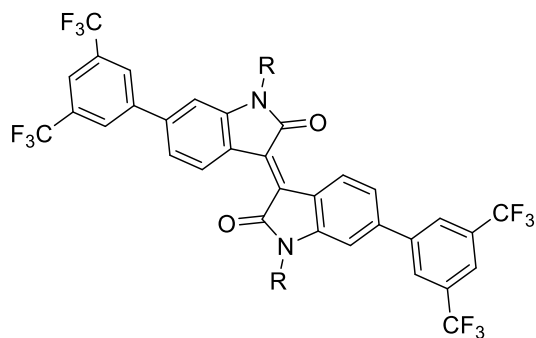
2.4: R = C$_6$H$_{13}$
2.5: R = 2-ethylhexyl
3.2: R = CH$_3$
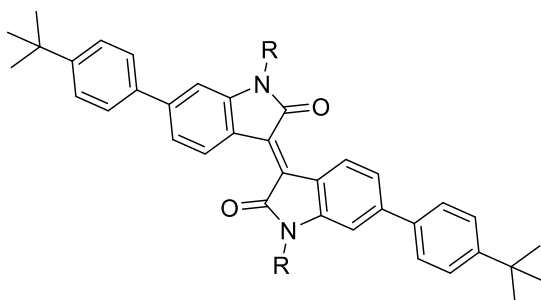
2.6: R = C$_6$H$_{13}$
2.7: R = 2-ethylhexyl
3.3: R = CH$_3$
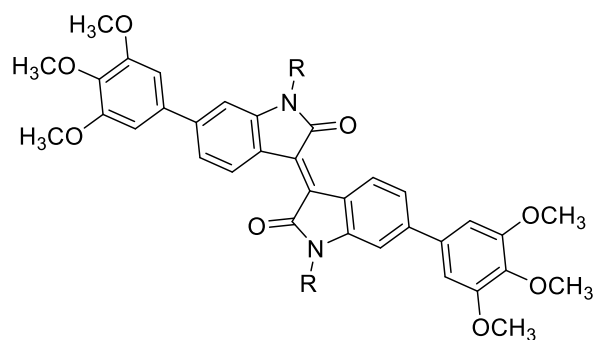
2.8: R = C$_6$H$_{13}$
2.9: R = 2-ethylhexyl
3.4: R = CH$_3$
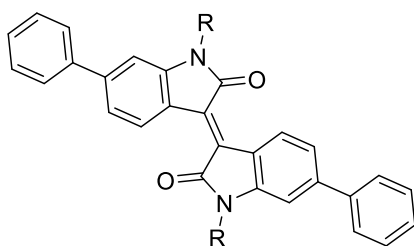
2.1: R = C$_6$H$_{13}$
3.5: R = CH$_3$

Figure 3.1. Chemical structures of the isoindigo derivatives.

3.2 Results and Discussion

The singlet ground state geometries were optimized using density functional theory at the B3LYP/6-311G(2d,p)//B3LYP/6-31G(d) level of theory. All alkyl chains were truncated to methyl groups (**3.1-3.5**). X-ray diffraction of N,N'-dimethylisoindigo revealed a twist of 22° between the oxindoles.[112] Estrada *et al.* determined the molecular geometries and packing behavior of N,N-dihexyl-6,6-diphenylisoindigo using X-ray diffraction.[113] The dihedral angles observed for the phenyl group with the oxindole group in **3.5** is reported as 39.2°, Figure 3.2. The resulting geometries were printed in Table 3.1 along with the dihedral angles between the oxindoles of the isoindigo core, which ranged from 12.2° to 13.2° and the dihedral angles phenyl-oxindole ranged from 34.6° to 36.3°. Using DFT calculations, Estrada *et al.*[113] showed that among the two local minima (planar system and a structure with a slight twist of 15° between the oxindoles) that the twisted system represents the global minimum with an energy difference of 0.33 kcal/mol at the B3LYP/6-311+G(d,p)//B3LYP/6-31G(d), which is in line with our results, Table 3.1.
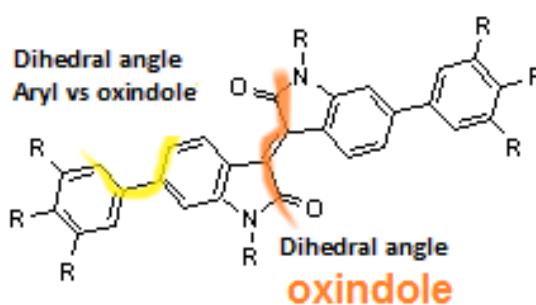
Figure 3.2. Definition of dihedral angles along the two oxindole groups and phenyl-oxindole group.

46

Table 3.1. Optimized geometries, dihedral angle along the two oxindole groups and phenyl-oxindole group of **3.2-3.4** at the B3LYP/6-311G(2d,p)//B3LYP/6-31G(d) level of theory.
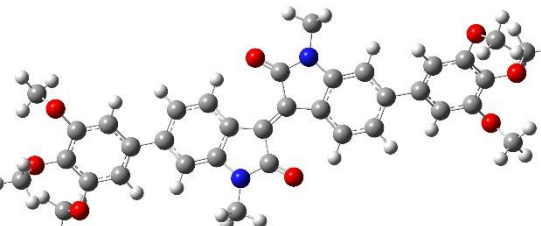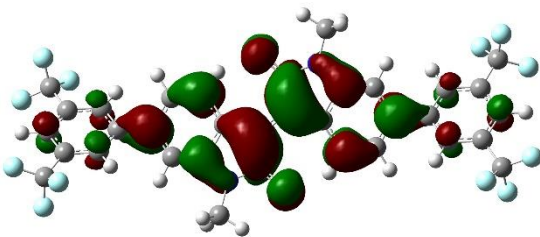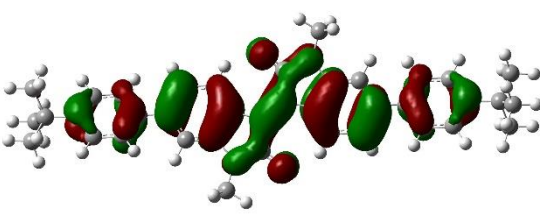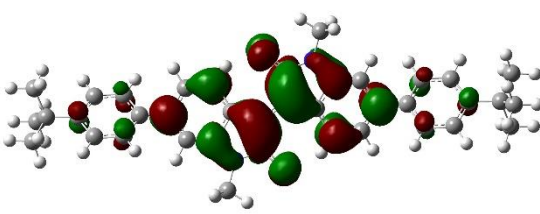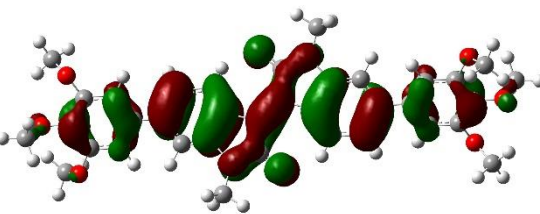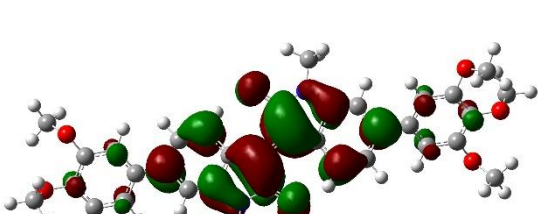
Compound	Optimized geometry 1	Dihedral angle (oxindole)	Dihedral angle (Aryl vs oxindole)
3.2		12.9°	36.3°
3.3		13.2°	35.3°
3.4		13.1°	34.6°

Table 3.2. Frontier molecular orbital energies of **3.1-3.5** as obtained at the B3LYP/6-311G(2d,p)//B3LYP/6-31G(d) level of theory.

Compound	HOMO (eV)	LUMO (eV)
3.1	-5.91[25]	-3.06[25]
3.2	-5.59	-2.98
3.3	-6.29	-3.58
3.4	-5.63	-3.02
3.5	−5.71[25]	−3.06[25]

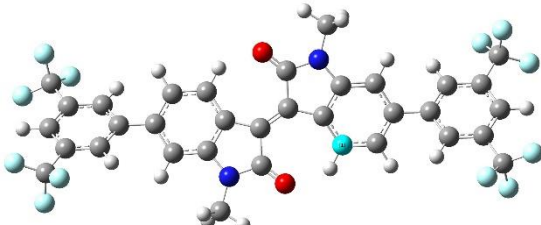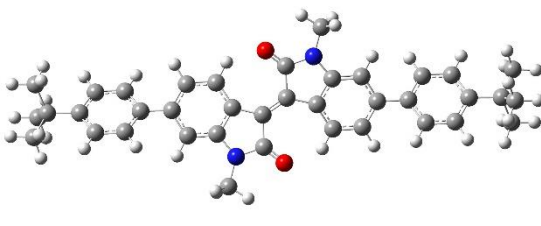At the B3LYP/6-311G+(2d,p)//B3LYP/6-31G(d) level of theory, isoindigo **3.1** exhibits HOMO and LUMO energy levels of -5.91 eV and -3.06 eV, respectively.[113] The HOMO and LUMO energy level of 6,6-diphenyl substituted isoindigo **3.5** were computed to be -5.71 eV and -3.06 eV at the same level of theory.[113] The electron-donating effects of *t*-butyl groups on **3.3** and trimethoxy groups on **3.4** as well as the electron-withdrawing effect of the trifluoromethyl groups on **3.2** are well reflected on HOMO and LUMO energy levels in comparison to the unsubstituted 6,6-diphenylisoindigo **3.5**, Table 3.2 and Table 3.3.

Table 3.3. Computed frontier molecular orbital maps of **3.2-3.4** at B3LYP/6-311G(2d,p)//B3LYP/6-31G(d) level of theory were printed at an isodensity value of 0.02 e/bohr^3.
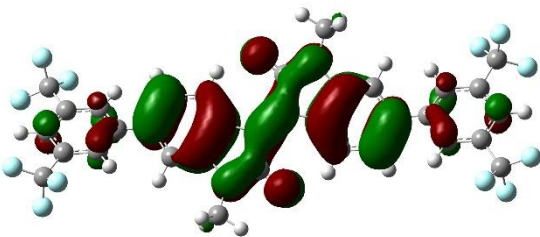
	HOMO	LUMO
3.2		
3.3		
3.4		
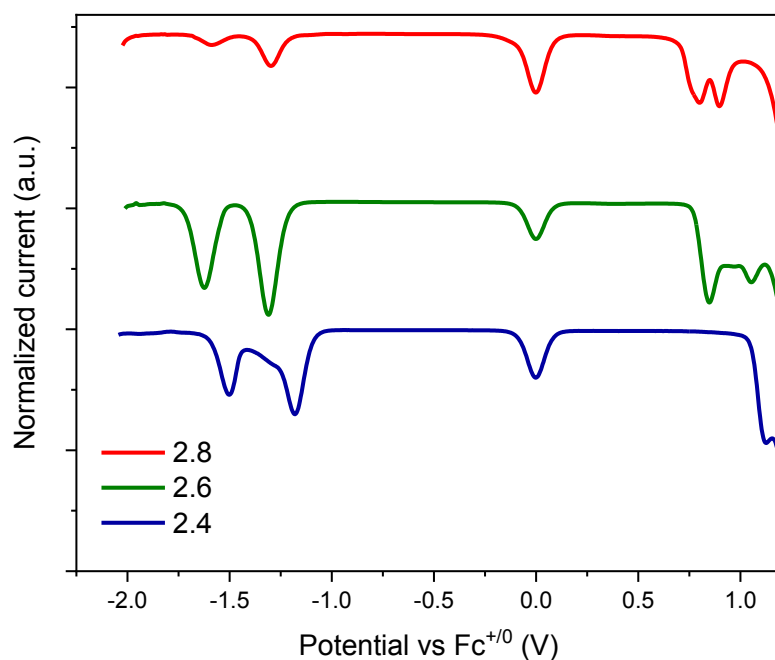
Figure 3.3. Differential pulse voltammograms of **2.4-2.8** determined in TBAP versus ferrocene.

Table 3.4. Average peak potentials of compounds **2.1-2.16** determined by differential pulse voltammetry versus ferrocene internal standard.

Compound	E_{ox}(peak) (V)[a]	E_{red1}(peak) (V)[b]	E_{red2}(peak) (V)[b]	HOMO (eV)[c]	LUMO (eV)[d]
2.16	--	-1.40[25]	-1.88[25]	--	-3.70[25]
2.4	1.17	-1.17	-1.49	-6.27	-3.93
2.6	0.85	-1.30	-1.62	-5.95	-3.80
2.8	0.81/0.89	-1.29	-1.58	-5.91	-3.81
2.1	--	-1.41[25]	-1.83[25]	--	-3.69[25]

For spectroscopic and electrochemical data compounds **2.1-2.16** were utilized. Differential pulse voltammetry was determined in 0.1 TBAP in DCM using ferrocene as internal standard. For computational data, compounds **3.1-3.5** were utilized. [a] Peak potential value for the first oxidation peak in volts against Fc/Fc$^+$. [b] Peak potential value for the first/second reduction peak in volts against Fc/Fc$^+$. [c] HOMO calculated using E_{ox1} vs Fc/Fc$^+$ in DCM, which is set at −5.1 eV vs vacuum; [d] LUMO calculated using E_{red1} vs Fc/Fc$^+$ in DCM, which is set at −5.1 eV vs vacuum.
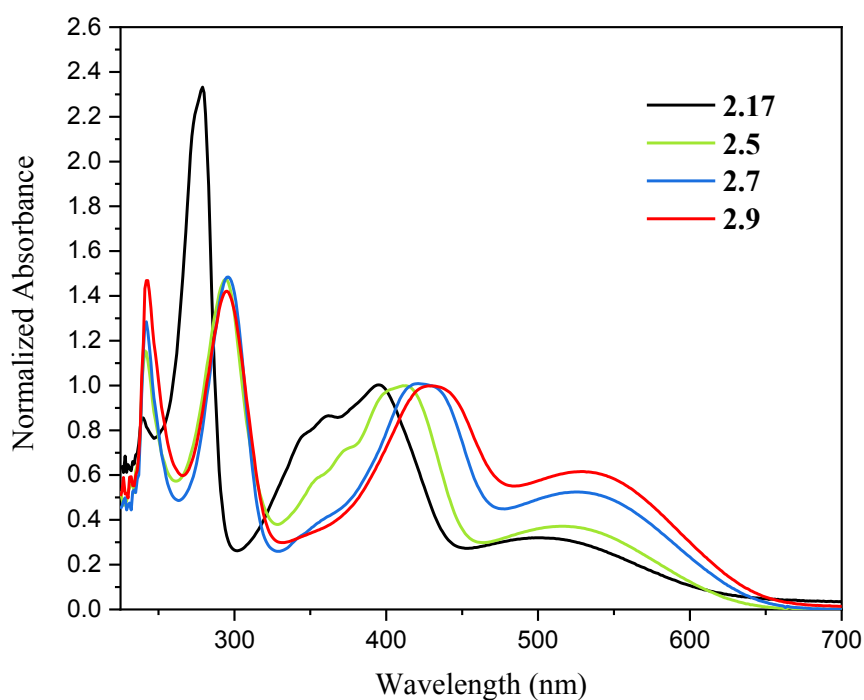
Figure 3.4. UV-Vis of **2.5**, **2.7**, **2.9** and **2.17** in CHCl$_3$.

Table 3.5. The absorption results of compounds **2.4-2.9** and **2.16-2.17** in chloroform.

Compound	λ_{max1} (nm)	ε (L.mol^{-1}.cm^{-1})	λ_{max2} (nm)	ε (L.mol^{-1}.cm^{-1})
2.16	396	12,900	519	3400
2.17	395	11,400	496	3075
2.4	411	26,000	522	9495.7
2.5	412	25,700	516	9538.5
2.6	420	25,600	522	13114
2.7	422	25,700	530	13342
2.8	426	25,800	522	15250
2.9	429	27,800	532	16771

In an effort to understand the absorption spectra, TD-DFT calculations were carried out for compounds **3.2-3.4** using B3LYP/6-311+G(2d,p)// B3LYP/6-31G(d,p) level of theory. Results are presented in Tables 3.6-3.8. In all cases, the lowest energy transition is composed of HOMO -> LUMO (>88%) with a minor component HOMO-2->LUMO (<12%). As shown below in Figures 3.5-3.7, the lowest energy transition is governed by shift of electron density attributed to a π-π* transition based on the orbitals involved.

Table 3.6. Optical properties of **3.2-3.5** in solution compared with the values for isolated molecules computed at the using TD-B3LYP/6-311+G(2d,p)//B3LYP/6-31G(d) level of theory.

	λ $(\pi-\pi^*)_{max}$ (nm)	ε ($\times 10^{-3}$ cm^{-1} M^{-1})	λ $(\pi-\pi^*)_{max}$ TDDFT (nm)	ΔE_{opt} (eV)	ΔE_{th} (eV) TD-DFT	f_{exp}	f TD-DFT	μ_{ge} exp (D)	μ_{ge} TD-DFT (D)
3.1	494[25]	3.69[25]	527[25]	2.51[25]	2.35[25]	0.07[25]	0.08[25]	2.88[25]	3.21[25]
3.2	526	7.54	550	2.36	2.25	0.128	0.323	2.94	5.84
3.3	548	10.83	559	2.26	2.22	0.152	0.504	2.95	9.28
3.4	544	12.58	559	2.28	2.22	0.187	0.495	3.61	9.12
3.5[11]3	517[a,b]	10.7[a]	553[a]	2.4[a,b]	2.24[a]	0.2[a]	0.38[a]	4.9[a]	6.67[a]

Legend: λ_{max} wavelength of longest wavelength absorption from deconvoluted spectrum (see Materials and Methods); ε molar decade extinction coefficient; **ΔE_{opt}** optical gap calculated from the lowest energy band in the UV$-$vis absorption spectrum; **ΔE_{th}; f** Oscillator strength, f_{exp} calculated through eq 1; μ_{ge} Transition dipole moment in Debyes; μ_{ge} $_{expt}$ calculated through eq. 2. Parameters listed with TDDFT were obtained by **TDDFT** calculations; [a] Value not deconvoluted, values taken from maximum of lowest energy UV-vis absorption band; [b] DCM else CHCl$_3$.

Table 3.7. Characteristics for the $S_n \leftarrow S_0$ vertical transitions of **3.3** as computed via TD-B3LYP/6-311+G(2d,p)//B3LYP/6-31G(d).

n	Energy (eV)	λ ($S_n \leftarrow S_0$) (nm)	f	μ				
1	2.22	559	0.5039	9.2769	HOMO-2	->	LUMO	6
					HOMO	->	LUMO	94
2	2.41	516	0.0000	0.0006	HOMO-3	->	LUMO	2
					HOMO-1	->	LUMO	98
3	2.86	434	0.6919	9.8795	HOMO-2	->	LUMO	94
					HOMO	->	LUMO	6
4	3.20	388	0.0042	0.0539	HOMO-3	->	LUMO	100
5	3.28	378	0.0648	0.8073	HOMO-7	->	LUMO	69
					HOMO-6	->	LUMO	5
					HOMO-4	->	LUMO	26

Table 3.8. Characteristics for the $S_n \leftarrow S_0$ vertical transitions of **3.2** as computed via TD-B3LYP/6-311+G(2d,p)//B3LYP/6-31G(d).

n	Energy (eV)	λ ($S_n \leftarrow S_0$) (nm)	f	μ				
1	2.25	550	0.3227	5.8413	HOMO-2	->	LUMO	6
					HOMO	->	LUMO	94
2	2.39	518	0.0001	0.0015	HOMO-1	->	LUMO	100
3	2.96	420	0.6459	8.9199	HOMO-4	->	LUMO	8
					HOMO-2	->	LUMO	87
					HOMO	->	LUMO	5
4	3.26	381	0.2332	2.9206	HOMO-4	->	LUMO	93
					HOMO-2	->	LUMO	7
5	3.50	354	0.0009	0.0100	HOMO-6	->	LUMO	13
					HOMO-5	->	LUMO	41
					HOMO-3	->	LUMO	43
					HOMO	->	LUMO+1	3

Table 3.9. Characteristics for the $S_n \leftarrow S_0$ vertical transitions of **3.4** as computed via TD-B3LYP/6-311+G(2d,p)//B3LYP/6-31G(d).

n	Energy (eV)	λ ($S_n \leftarrow S_0$) (nm)	f	μ				
1	2.22	559	0.4951	9.1173	HOMO-2	->	LUMO	6
					HOMO	->	LUMO	94
2	2.40	516	0.0000	0.0006	HOMO-3	->	LUMO	3
					HOMO-1	->	LUMO	97
3	2.84	436	0.6685	9.6006	HOMO-2	->	LUMO	94
					HOMO	->	LUMO	6
4	3.13	396	0.0022	0.0286	HOMO-3	->	LUMO	97
					HOMO-1	->	LUMO	3
5				not converged				

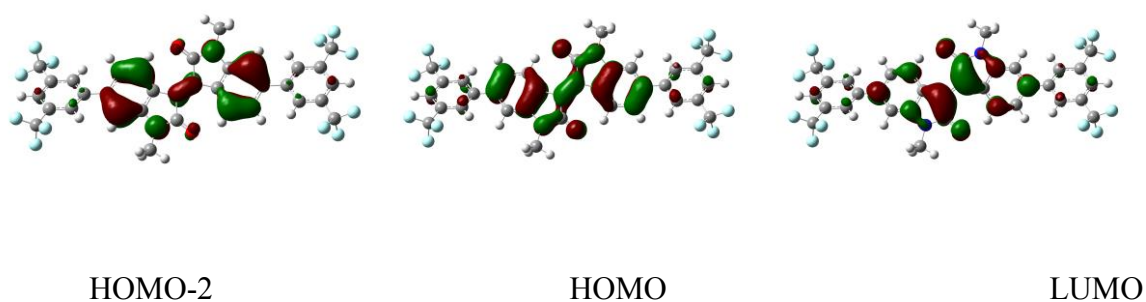| HOMO-2 | HOMO | LUMO |

Figure 3.5. Wave function maps of orbitals in the main vertical transitions of **3.2** at B3LYP/6-311G(2d,p) level of theory and plotted at isodensity 0.03 e/bohr^3.

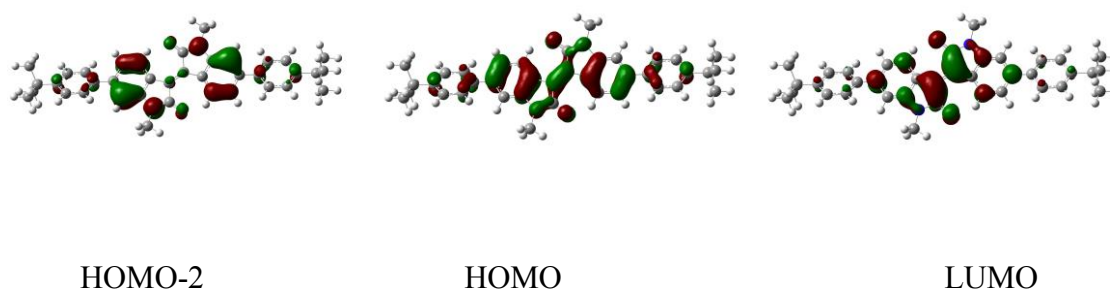| HOMO-2 | HOMO | LUMO |

Figure 3.6. Wave function maps of orbitals in the main vertical transitions of **3.3** at B3LYP/6-311G(2d,p) level of theory and plotted at isodensity 0.03 e/bohr^3.

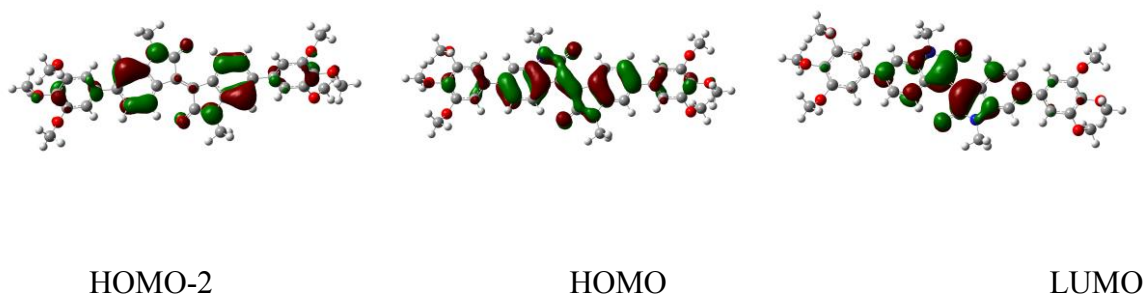| HOMO-2 | HOMO | LUMO |

Figure 3.7. Wave function maps of orbitals in the main vertical transitions of **3.4** at B3LYP /6-311G(2d,p) level of theory and plotted at isodensity 0.03 e/bohr^3.

3.3 Materials and Methods

3.3.1 Computations

Gaussian09 (rev.E.01) was used to perform all computations.[114] The starting geometry was based on (E)-1,1'-dimethyl-[3,3'-biindolinylidene]-2,2'-dione (iI-Me2) as reported by Estrada *et al.* and modified for the corresponding substitution pattern on positions 6 and 6' with 3,5-trifluoromethylphenyl (**3.2**), 4-*tert*-butylphenyl (**3.3**), and 3,4,5-trimethoxyphenyl (**3.4**) using GaussView 5.0.9. The substituted phenyl groups were arranged at a starting dihedral angle of 90° and the alkyl groups were replaced with methyl groups to keep computational cost at a minimum. Density functional theory was utilized to carry out unrestricted gas-phase geometry optimization with the hybrid functional B3LYP[115-117] and the modest basis set 6-31G(d)[118]. Minima were verified by the absence of imaginary frequencies at the same level of theory. The basis set was extended to 6-311+G(2d,p)[119,120] for single energy point calculations, thus B3LYP/6-311+G(2d,p)//B3LYP/6-31G(d) level of theory was applied. Computed frontier molecular orbital maps of B3LYP/6-311+G(2d,p)//B3LYP/6-31G(d) level of theory were printed at an isodensity value of 0.02 e/bohr^3. Experimental absorption spectra were deconvoluted using Peak analysis tool using a Gaussian fit model in Origin 2015, R^2 and Anova analysis. Oscillator strengths (f) and transition dipole moments (μ_{ge}) were calculated using the following two equations (Eq. 1 and Eq. 2) relating theoretical data computed by TD-DFT to experimental absorption data for the lowest energy transition ($S_1 \leftarrow S_0$).[121] In Eqs 1 and 2, ε_{max} is the molar absorptivity at the maximum of that transition, $\Delta\nu_{1/2}$ is the full width at half-maximum (in cm^{-1}), and ν is the peak maximum wavenumber (in cm^{-1}).

$$f = \frac{\varepsilon_{max}\Delta\overline{\nu}_{1/2}}{2.5x10^8} \qquad \text{Eq. 1}$$

$$\mu_{ge} = \sqrt[2]{\frac{e^2 \varepsilon_{max} \Delta \bar{v}_{1/2}}{2.5 x 10^{19} \bar{v}_{1/2}}}$$ Eq. 2

3.3.2 Electrochemistry

Tetrabutylammonium hexafluorophosphate (TBAP, 1.937g) was dissolved in dry dichloromethane (DCM) in a 50 mL volumetric flask. A three-electrode setup consistent of Ag/AgCl reference electrode, glassy carbon or platinum working electrode, and platinum wire as counter electrode was utilized. Ferrocene was utilized as internal standard. The solution was stirred via a magnetic stirrer and purged with Argon bubbling for 10 min. The scan range was set approximately from -1.6V to 1.6V, with a sampling width of 0.1s, and a sensitivity of 10^{-5} A/V. Three independent differential pulse voltammetry scans were performed. The ferrocene standard potential is -5.1 eV vs. vaccum.[113] Recorded reduction and oxidation potentials are averaged peak potentials across recoded scans.

CHAPTER 4

ISOINDIGO ALDEHYDES: POTENTIAL BUILDING BLOCKS FOR COVALENT ORGANIC FRAMEWORKS (COFS)

4.1 Introduction

Covalent Organic Frameworks (COFs) are relatively new emerging field of organic porous materials, that form crystalline structures through strong covalent bonds between organic building blocks.[122,123] The most noticeable innovation in this field was introduced by Yaghi *et al.* in 2005, with the construction of an organic crystalline porous polymer, the first 2D COF material.[124] Later, in 2007, Yaghi *et al.* synthesized the first 3D COF materials, Figure 4.1.[125] In light of the pioneering work of Yaghi and co-workers, dramatic progress in the synthesis and applications of these organic porous materials has taken place in recent years.[123] Interest in developing new COFs emerged because of the several advantages they have over other types of porous materials such as larger surface area, lower density, controlled tailoring to different structures and pore sizes, and choice of composition by various available organic building blocks and tunable functionalities of these organic building blocks.[123] COFs provide the ability to design new porous materials for numerous desired applications, including adsorption,[126] catalysis,[127] optoelectricity,[128] and gas storage.[129]
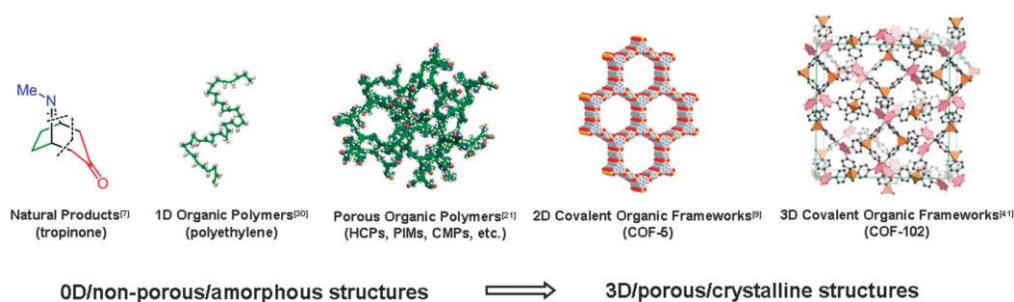

Figure 4.1. Examples of organic assemblies to construct chemical architectures.[123]

Although the synthesis and applications of COFs evolved rapidly in the recent years, yet there remain challenges in obtaining desired crystalline materials.[123] In order to design COF materials, there are three major concerns; porosity, structural regularity and functionality. Pore size is governed by the length of each building block and structural regularity is related to the reversible formation of covalent bonds. To address the design requirements, three types of synthesized COFs are developed: boron-containing COFs, triazine-based COFs, and imine-based COFs. Boron-containing COFs can be obtained either through self-condensation[124] or co-condensation.[125] They are the most commonly synthesized COFs and offer the main advantages of high surface area, low densities and high thermal stabilities. However, these COFs are unstable in air[130] and water as structures can lose their regularity through hydrolysis.[131] Triazine-based COFs have good chemical and thermal stabilities, but they exhibit lower crystallinity compared to boron-containing COFs with potential application in catalysis.[132] Most imine-based COFs belong to two types: the hydrazone-linked that are synthesized from the co-condensation of aldehydes and hydrazides,[133] and the Schiff base type that are synthesized from the co-condensation of aldehydes and amines, Figure 4.2.[134] Imine-based COFs exhibit analogous crystallinity with boron-based COFs. Their insensitivity to water and good stability in most common organic solvents make them highly advantageous over the other types of COFs.[135] However, attaining improved crystallinity and surface areas remains desirable.
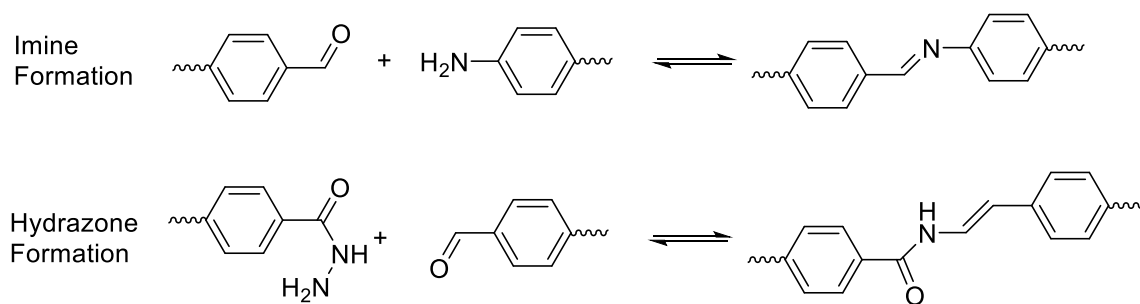

Figure 4.2. Reactions of the two types of imine-based COF materials.[123]

In 2017, Ditchel and coworkers reported the first synthesis of thienoisoindigo based COFs.[136] The synthesis was done through a metal triflates catalyzed imine-linked covalent bond between thienoisoindigo dialdehyde (**4.1**) and 1,3,5-tris(4aminophenyl)benzene (TAPB) (**4.2**), Scheme 4.1.[136] Their reported COF showed good crystallinity as well as surface area compared to reported imine-linked COFs derived from simple aldehyde and aniline monomers.[135]
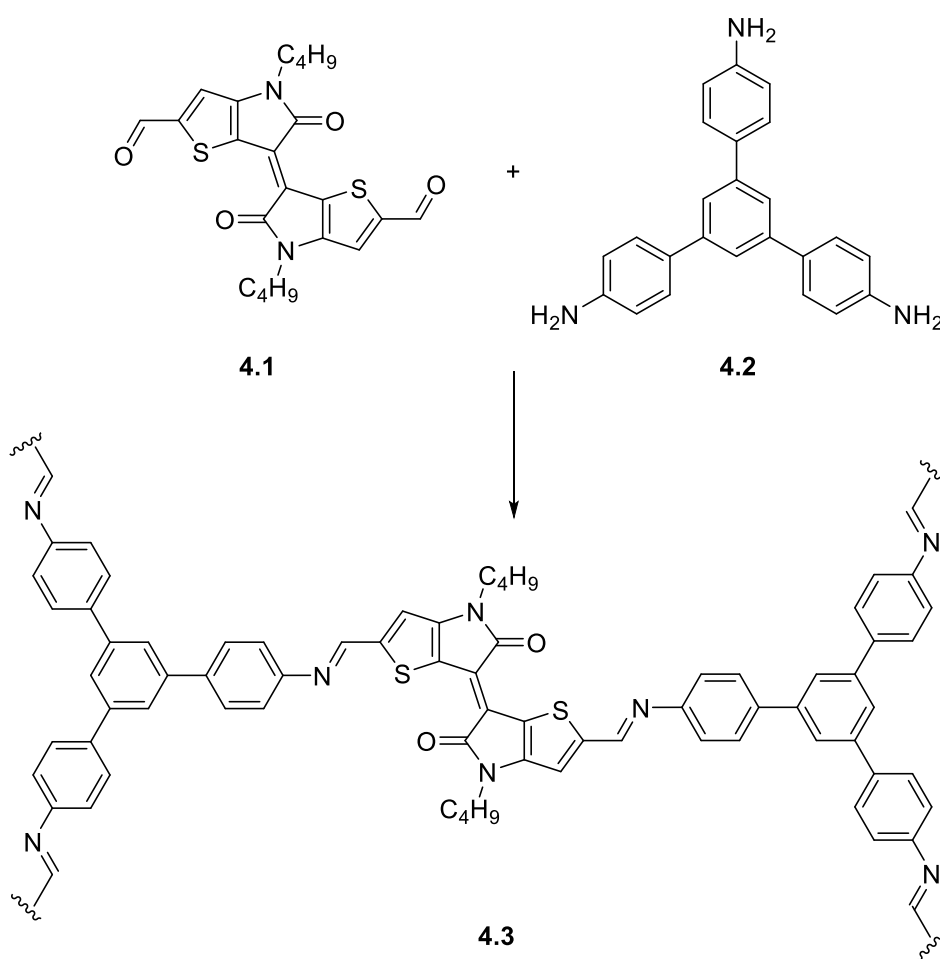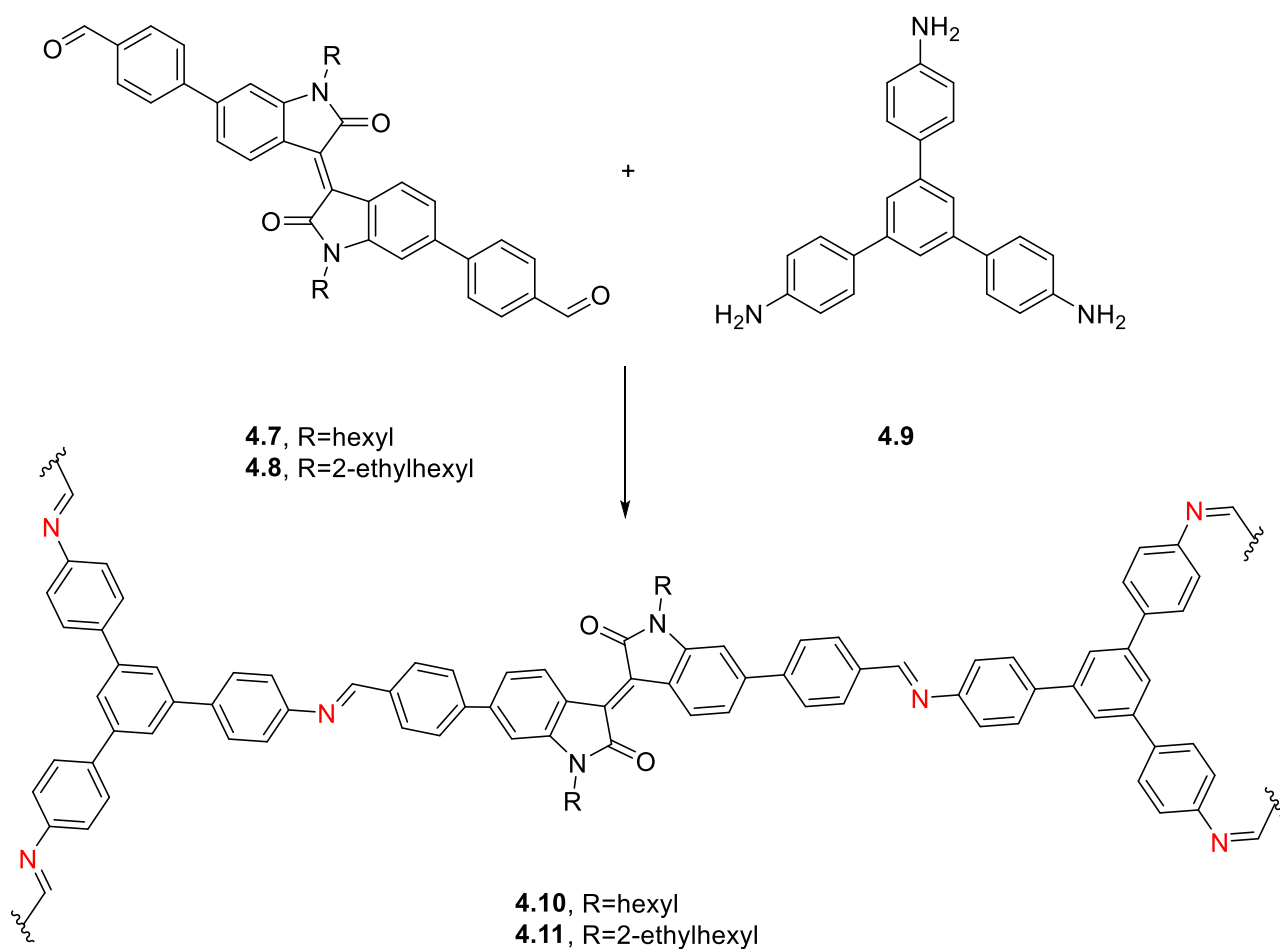

Scheme 4.1. The condensation of thienoisoindindigo dialdehyde(**4.1**) with TAPB (**4.2**).[136]

Soon afterwards, Bein and co-workers reported the first 2D COF-based UV to NIR-responsive photodetector, Scheme 4.2.[137] Their incorporation of donor-acceptor type isoindigo- and thienoisoindigo-based moieties allowed a very high absorption as well as good porosity and stability.[137] Hence, the remarkable absorbance properties obtained when including isoindigo units in donor-acceptor COFs structures is promising for future investment in optoelectronic applications.
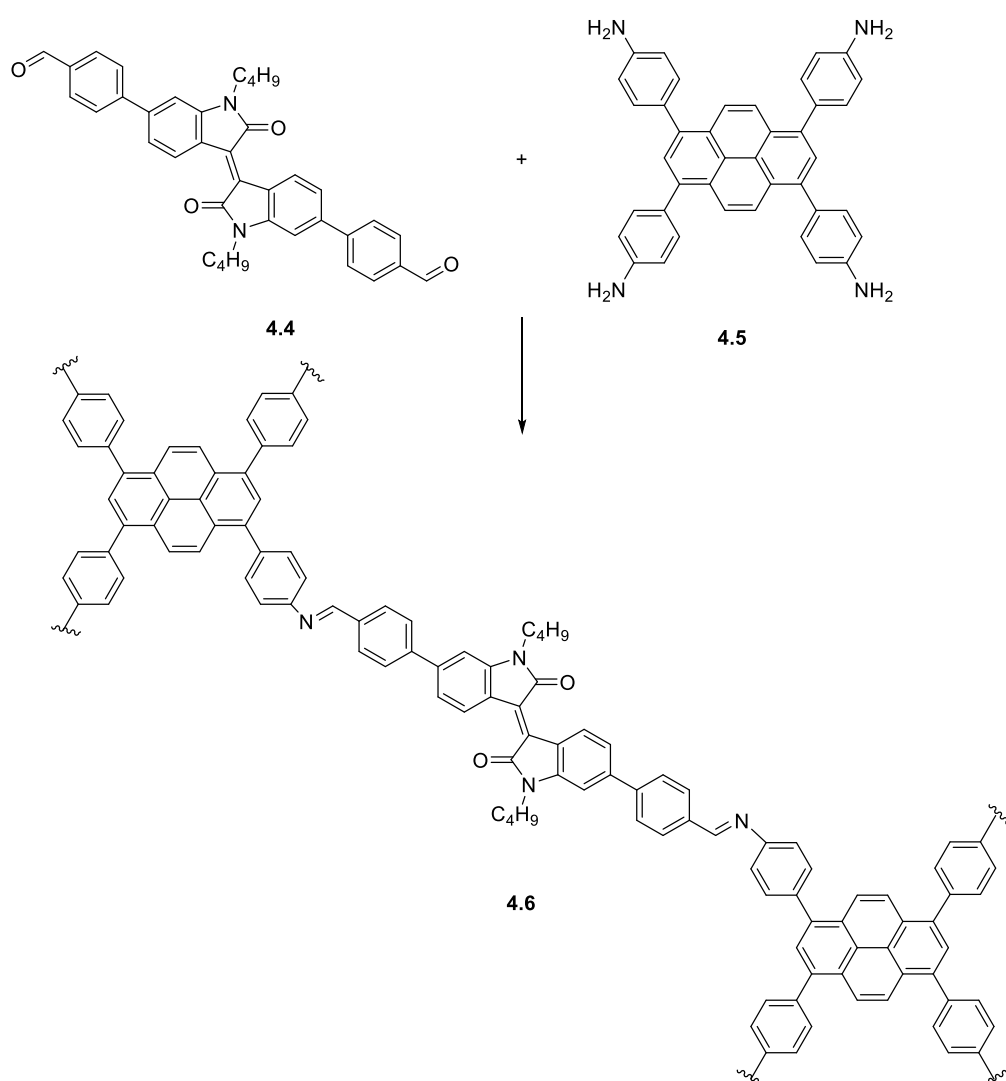
Scheme 4.2. The condensation of isoindigo dialdehyde (**4.2**) with **4.3**.[136]

In this chapter, we report the synthesis of two isoindigo dialdehydes derivatives as building blocks for COFs, Scheme 4.3. The two compounds (**4.1-4.2**) were synthesized through Suzuki coupling reactions, purified and characterized by ^{1}H and ^{13}C NMR and elemental analysis. Our collaborator Prof. Ali Trabolsi from the New York University in Abu Dhabi is currently exploring these two isoindigo dialdehydes for the synthesis various COF materials. The condensation reaction of isoindigo dialdehydes (**4.1- 4.2**) and 1,3,5-tris(4-aminophenyl)benzene (TAPB) (**4.3**) successfully led to the formation of **COF 4.10** and **COF 4.11**. The properties of these two COFs are currently under investigation. The synthesis of other COFs using **4.7** and **4.8** is also ongoing.


Scheme 4.3. The condensation of isoindindigo dialdehydes (**4.7-4.8**) with **4.9** to afford COFs (**4.10-4.11**).

4.2 Results and Discussion

4.2.1 Synthesis

The two isoindigo aldehydes were synthesized through Suzuki coupling reaction between alkylated dibromoisoindigo derivatives and 4-formylphenylboronic acid, Scheme 4.4. After several attempts to optimize the reaction conditions, toluene was found to be a better solvent than THF to have higher yields. A competition between the formation of the monosubstituted aldehyde and the disubstituted aldehyde was governed by temperature and time. Running the reaction between 80-85 °C for 24 hours gave monosubstituted aldehyde as major product, while running the reaction at 100-110 °C for 48 hours resulted with the disubstituted aldehyde as major product with traces of the monoaldehyde. However, higher temperatures gave an undesired side product very close in polarity to the dialdehyde which made the purification process by column chromatography more difficult. Yet, more challenging purification payed off with overall higher yields.


2.18: R=hexyl
2.19: R=2-ethylhexyl

4.12

4.7: R=hexyl
4.8: R=2-ethylhexyl
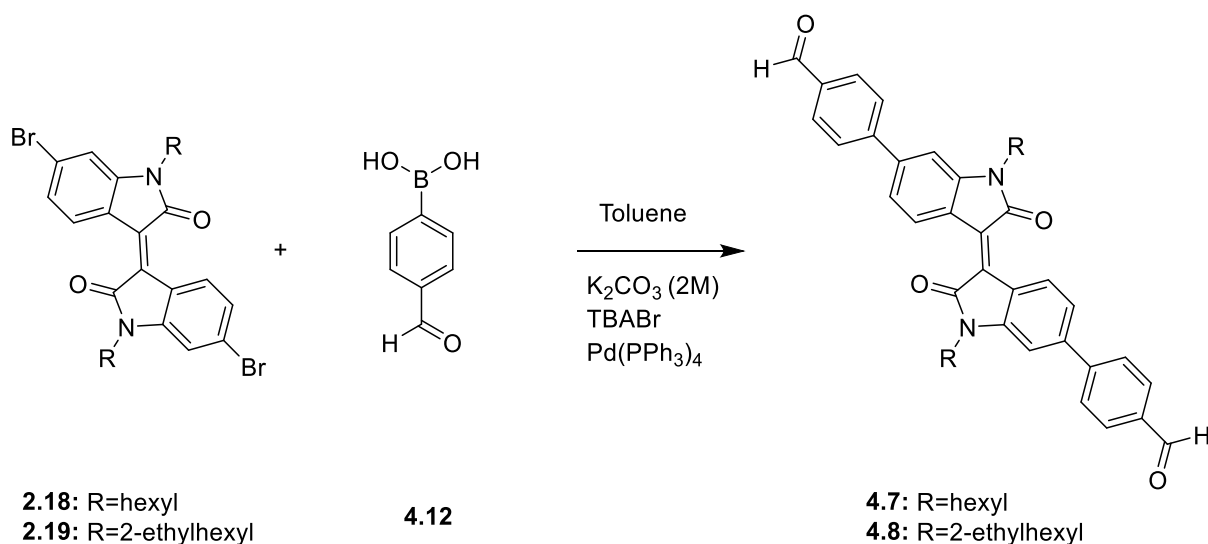
Scheme 4.4. Synthesis of isoindigo aldehydes (**4.7-4.8**).

4.3 Experimental

4.3.1 Synthesis

(*E*)-4,4'-(1,1'-dihexyl-2,2'-dioxo-[3,3'-biindolinylidene]-6,6'-diyl)dibenzaldehyde (4.7)

The title compound was synthesized according to a modified literature procedure.[63] Compound **2.18** (0.35 g, 0.60 mmol), (4-formylphenyl)boronic acid **4.12** (0.38 g, 2.50 mmol, 4.2 eqv), potassium carbonate 2M solution (4 mL), and tetrabutylammonium bromide (10 mg) were added to 40 mL toluene. The mixture was purged with argon gas for 30 minutes. Freshly synthesized tetrakis(triphenylphosphine)-palladium (0) (50 mg) was then added, and the reaction was refluxed at 100 °C for 48 hours under argon and in the dark. The reaction was then quenched with distilled water, then extracted with chloroform. The combined organic layer was dried over Na_2SO_4 and the solvent was removed under reduced pressure. The desired compound was separated using silica gel column chromatography with hexane: DCM (4:6) as mobile phase and recrystallized from toluene-hexane. **4.7** (0.29 g, 76%) was isolated as a shiny purple brown solid. ^1H NMR (500 MHz, $CDCl_3$): δ 10.09 (s, 2H), 9.32 (d, *J*=8.5 Hz, 2H), 8.01 (d, *J*=8.5 Hz, 4H), 7.82 (d, *J*=8.5 Hz, 4H), 7.34 (dd, *J₁*=8 Hz, *J₂*=1.5 Hz, 2H), 7.02 (d, *J*=1.5 Hz, 2H), 3.88 (t, *J*=7.5 Hz, 4H), 1.79 (p, *J*=7 Hz, 4H), 1.47 (p, *J*=7.5 Hz, 4H), 1.34 (m, 8H), 0.90 (t, *J*=7 Hz, 6H). ^{13}C NMR (125 MHz, $CDCl_3$): δ 191.69, 168.04, 146.31, 145.57, 143.65, 135.84, 132.97, 130.62, 130.34, 127.71, 121. 91, 121.31, 106.51, 40.22, 31.53, 27.56, 26.77, 22.57, 14.03. Anal. Calcd for $C_{42}H_{42}N_2O_4$: C, 78.97; H, 6.63; N, 4.39. Found: C, 78.93; H, 6.55; N, 4.37.

4.7
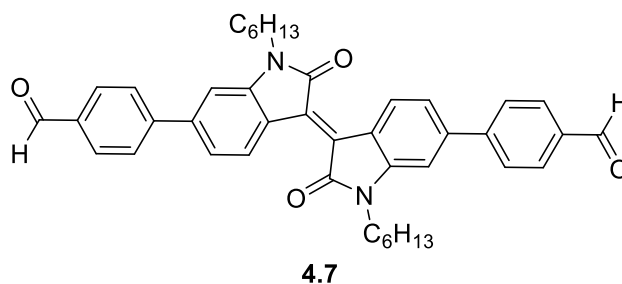
(*E*)-4,4'-(1,1'-bis(2-ethylhexyl)-2,2'-dioxo-[3,3'-biindolinylidene]-6,6'-diyl)dibenzaldehyde (4.8)

The title compound was synthesized according to a modified literature procedure.[63] Compound **2.19** (0.30 g, 0.47 mmol), (4-formylphenyl)boronic acid **4.12** (0.29 g, 1.96 mmol, 4.2 eqv), potassium carbonate 2M solution (3 mL), and tetrabutylammonium bromide (10 mg) were added to 30 mL toluene. The mixture was purged with argon gas for 30 minutes. Freshly synthesized tetrakis(triphenylphosphine)-palladium (0) (50 mg) was then added, and the reaction was refluxed at 100 °C for 48 hours under argon and in the dark. The reaction was quenched with distilled water and extracted with chloroform. The combined organic layer was dried over Na_2SO_4 and the solvent was removed under reduced pressure. The desired compound was separated using silica gel column chromatography with hexane: DCM (4:6) as mobile phase and recrystallized from toluene-hexane. Compound **4.8** (0.18 g, 56%) was isolated as a shiny purple brown solid. ^{1}H NMR (500 MHz, CDCl$_3$): δ 10.09 (s, 2H), 9.32 (d, *J*=8.5 Hz, 2H), 8.01 (d, *J*=8.5 Hz, 4H), 7.82 (d, *J*=8.5 Hz, 4H), 7.34 (dd, *J$_1$*=8 Hz, *J$_2$*=1.5 Hz, 2H), 7.02 (d, *J*=1.5 Hz, 2H), 3.88 (t, *J*=7.5 Hz, 4H), 1.79 (p, *J*=7 Hz, 4H), 1.44 (m, 4H), 1.34 (m, 8H), 0.90 (t, *J*=7 Hz, 6H). ^{13}C NMR (125 MHz, CDCl$_3$): 191.64, 168.40, 146.23, 145.95, 143.45, 135.83, 132.88, 130.45, 130.35, 127.56, 121.87, 121.22, 106.72, 44.28, 37.74, 30.78, 28.80, 24.20, 23.09, 14.09, 10.79. Anal. Calcd for $C_{46}H_{50}N_2O_4$: C, 79.51; H, 7.25; N, 4.03. Found: C, 79.36; H, 7.41; N, 4.04.

4.8
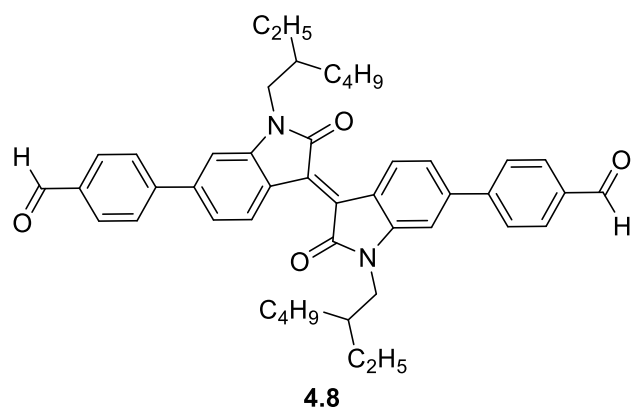
CHAPTER 5

NAPHTHALENE DIIMIDE (NDI) DERIVATIVES FOR

ELECTRONIC APPLICATIONS

5.1. Introduction

In the scope of designing organic architectures for high performance electronic applications, synthetic chemists usually choose conjugated aromatic molecules as building blocks since these are well-known for their large planarity, defined spectroscopic and redox properties.[33] From this class of organic molecules, pyrene[138] and rylene diimides (RDIs)[139] are well-explored examples. RDIs are a deficient class of aromatic compounds that have been studied for years mainly due to their exceptional fluorescent properties, good charge carrier mobility, and high stability,[140,141] which makes them suitable candidates for electronic applications. The two most studied subclasses of RDIs, are perylene diimides (PDIs)[142] and naphthalene diimides (NDIs), Figure 5.1.[143]
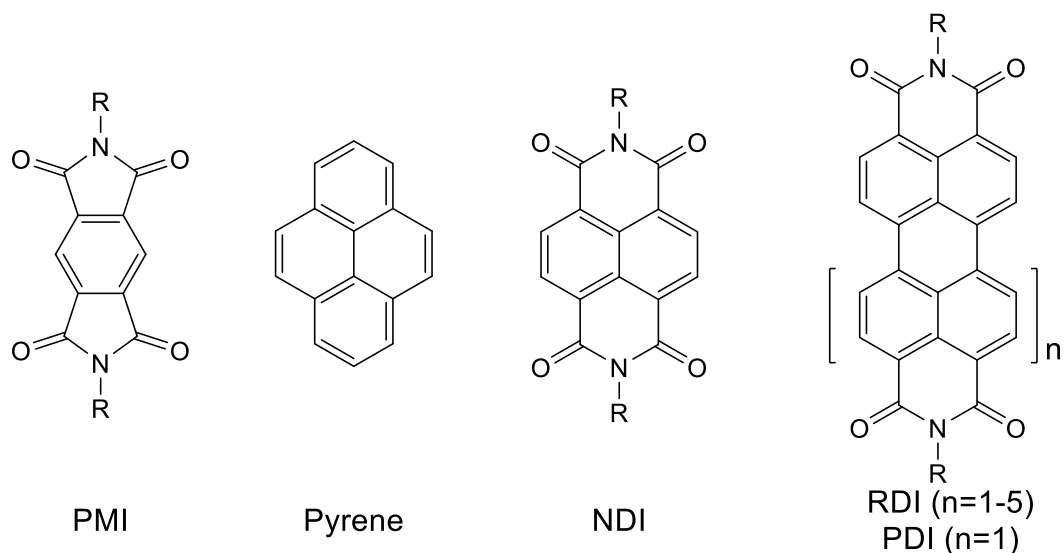
Figure 5.1. The structures of some explored aromatic compounds in electronics.

NDI, the smallest homologue of RDIs, found popularity in the 1930s after the pioneering work of Vollman *et al*.[144] However, focused studies on functionalizing NDI with

different ways did not evolve until after 2002, where Würthner group showed that core

substituted NDIs (cNDIs) can manifest a great variety of optical properties and colors,[30] as

well as diverse ranges of frontiers molecular orbital levels.[31] Thereafter, core substituted

NDIs became really attractive and rapidly emerged in the era of solar cells, artificial

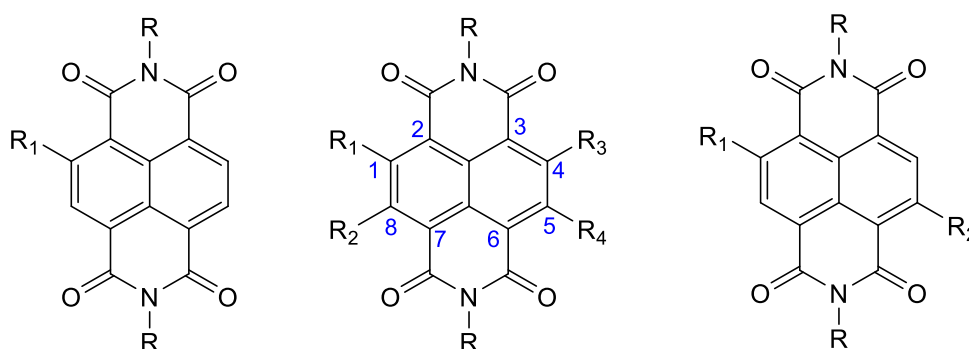photosynthesis, and supramolecular chemistry.[32,33] The structures of cNDIs are shown in

Figure 5.2.

Figure 5.2. The general structures of cNDIs (i.e. 1,4,5,8-naphththalenediimides with one or
more substituents in position 2, 3, 6 and 7).

NDI is characterized by a planar, large, robust, electron deficient core. The

hydrophilic (four carbonyl groups) and hydrophobic (naphthyl core) functionality on

naphthalene diimides (NDIs) leave solubility to depend on the substituents on the imide

groups.[33,145] Notably, substituting long and bulky aliphatics on imide nitrogens leads to

higher solubilities of NDIs both in solution and solid forms.[145] Stacking of these compounds

is stabilized by hydrogen bonds and π-π interactions between aromatic regions.[33,146] These

interactions offer varied challenges and possibilities in the scope of supramolecular

applications[147-149] as they aid the formation of continuous stacks but make solubility more

challenging.[32,33] Yet, such stacking allows electron transport with high charge mobility which

proved to be promising for air-stable n-semiconductors in OFETs.[31,150]

Hence, diimide substitution is important for stacking and alignment, which favors charge transport for electronic applications. On the other hand, core substitution allows to fine tune the HOMO and LUMO energy levels depending on the type of substituent. For instance, functionalizing the core with electron donating groups forms push-pull systems since NDI core is electron deficient, whereas core substitution with electron withdrawing groups forms π-acidic systems which are desirable for n-type semiconductors.[151] Furthermore, researchers can investigate orbital gaps near the HOMOs and LUMOs of cNDIs with DFT studies, cyclic voltammetry (CV), differential pulse voltammetry, absorption and fluorescence spectroscopy.[15]

In this Chapter, we report three core substituted NDI derivatives (Figure 5.3) through a three-step synthetic pathway. The aim of the synthesis was to first add an alkyl group at the imide nitrogen atoms to enhance its solubility and stacking, and second, to core-functionalize it with three different aromatic substituents through Suzuki coupling in order to study and better understand the subsequent effect of different electron donating and withdrawing groups on the energy levels, photophysical properties, charge-carrier mobilities, stacking, and overall performance as potential materials for organic field effect transistors.
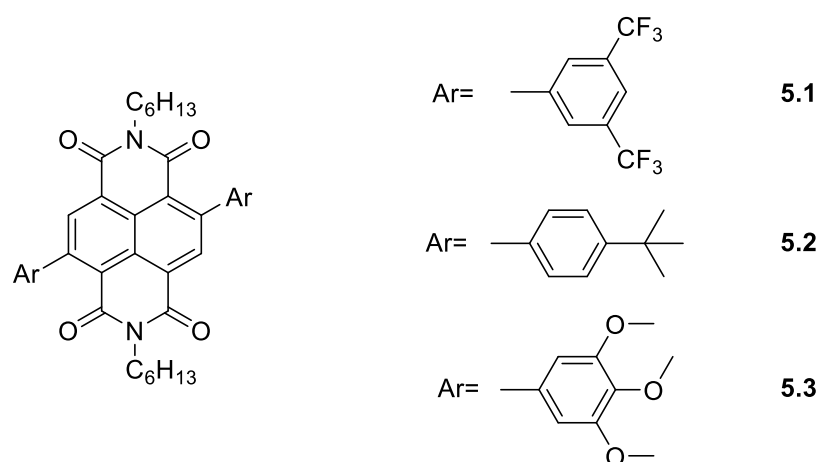

Figure 5.3. The structures of the synthesized NDI derivatives.

5.2. Results and Discussion

5.2.1. Synthesis

The synthesis of naphtalenetetracarboxylic diimide derivatives **5.1-5.3** starts from the bromination of naphtalenetetracarboxylic acid **5.4** according to a modified literature procedure,[152] by reacting it with dibromoisocyanuric acid in sulfuric acid at 130 °C for 15 hours. Compound **5.5** was washed with water and methanol and obtained with 91% yield without further purification. In the second step, compound **5.5** and hexylamine were refluxed in acetic acid for 1 hour to afford an oily residue which was purified over silica gel using column chromatography to obtain compound **5.6**.[153] The last step was to couple compound **5.6** with three different boronic acids via Suzuki coupling reaction.[154] The reactants were refluxed with potassium carbonate, tetra-n-butylammonium bromide and freshly synthesized tetrakis(triphenylphosphine)palladium(0) catalyst in toluene for 48 hours. Compounds **5.1-5.3** were obtained and were confirmed by ^{1}H,^{13}C NMR and elemental analysis. The synthetic pathway to afford NDI derivatives **5.1-5.3** is depicted in Scheme 5.1.
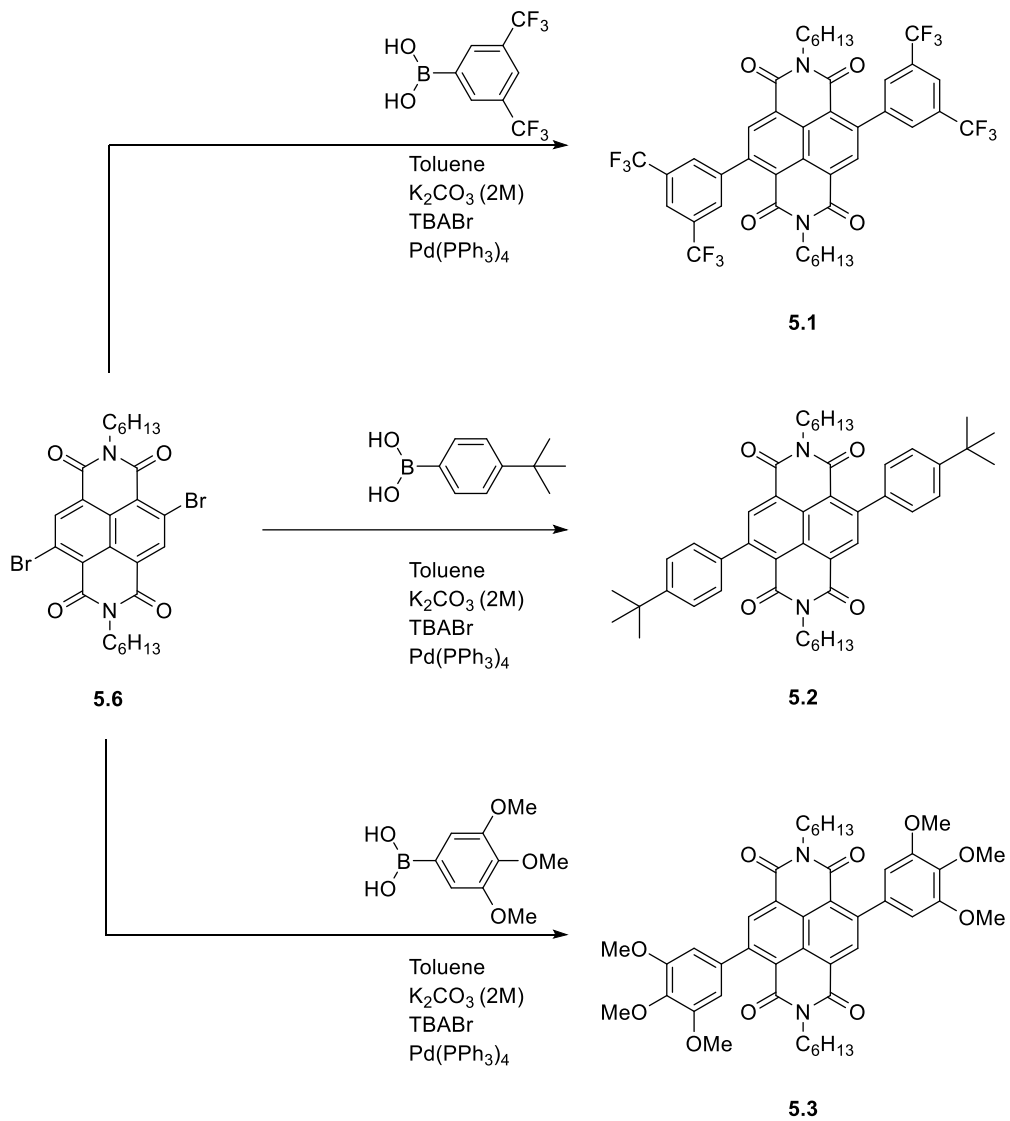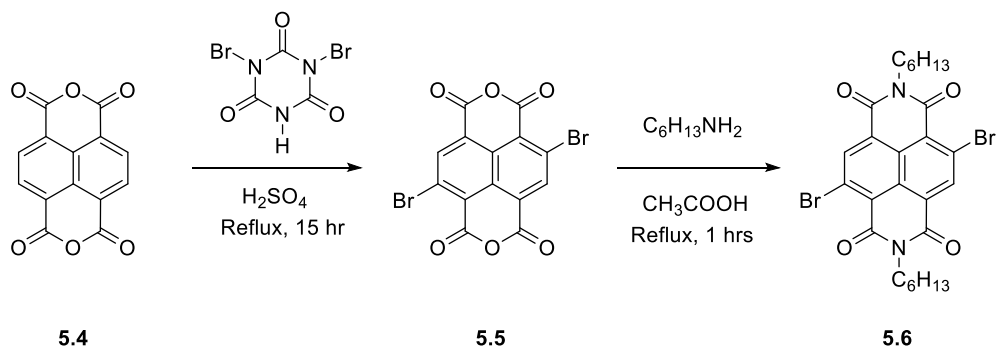
Scheme 5.1. Synthetic scheme of NDI derivatives **5.1-5.3**.

5.2.2. Absorption Properties

The representative absorption spectra of compounds **5.1-5.3** are depicted in Figure 5.4. The transition at around 360-380 nm is clearly insensitive to core substitution, since no shift is observed when the substituents are varied, which is in line with literature observations.[155] However, the lower energy band is indeed dependent on the substituent. We observe no absorption band for the compound bearing electron withdrawing substituent **5.1** which is indicative of no charge transfer,[155] and a red shifted band going from the compound bearing a moderately electron donating group (*tert*-butyl) **5.2** ($\lambda_{max3} = 445$ nm) to the one bearing strong electron donating group (trimethoxy) **5.3** ($\lambda_{max3} = 470$ nm). This is explained by the push–pull character of the cNDIs where the charge transfer band gets more red-shifted as the electron donating effect increases. It is worthy to mention that this is reflected through the color variation of cNDIs making them desirable candidates for various applications.[156] In this work, we observed the color change of cNDIs, ranging from pale yellow **5.1**, to orange **5.2**, to red **5.3**. The results of the absorption spectra are summarized in Table 5.1.
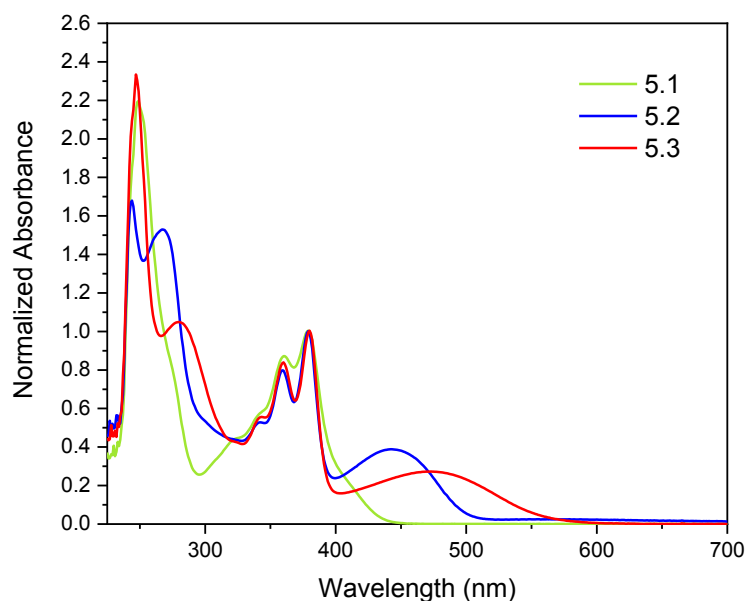
Figure 5.4. Normalized absorption spectrum of compounds **5.1-5.3** in chloroform.

70

Table 5.1. The absorption results of compounds **5.1-5.3** in chloroform.

Compound	λ_{max1} (nm)	ε (L.mol^{-1}.cm^{-1})	λ_{max2} (nm)	ε (L.mol^{-1}.cm^{-1})	λ_{max3} (nm)	ε (L.mol^{-1}.cm^{-1})
5.1	360	20702	379	23879	--	--
5.2	359	18364	379	23202	445	8741.9
5.3	360	19497	380	23356	470	6237.9

5.2.3. DFT Calculations and Electrochemistry

For computational analysis, alkyl groups were truncated to methyl groups except for *tert*-butyl groups in compound **5.10**, as shown in Figure 5.5.
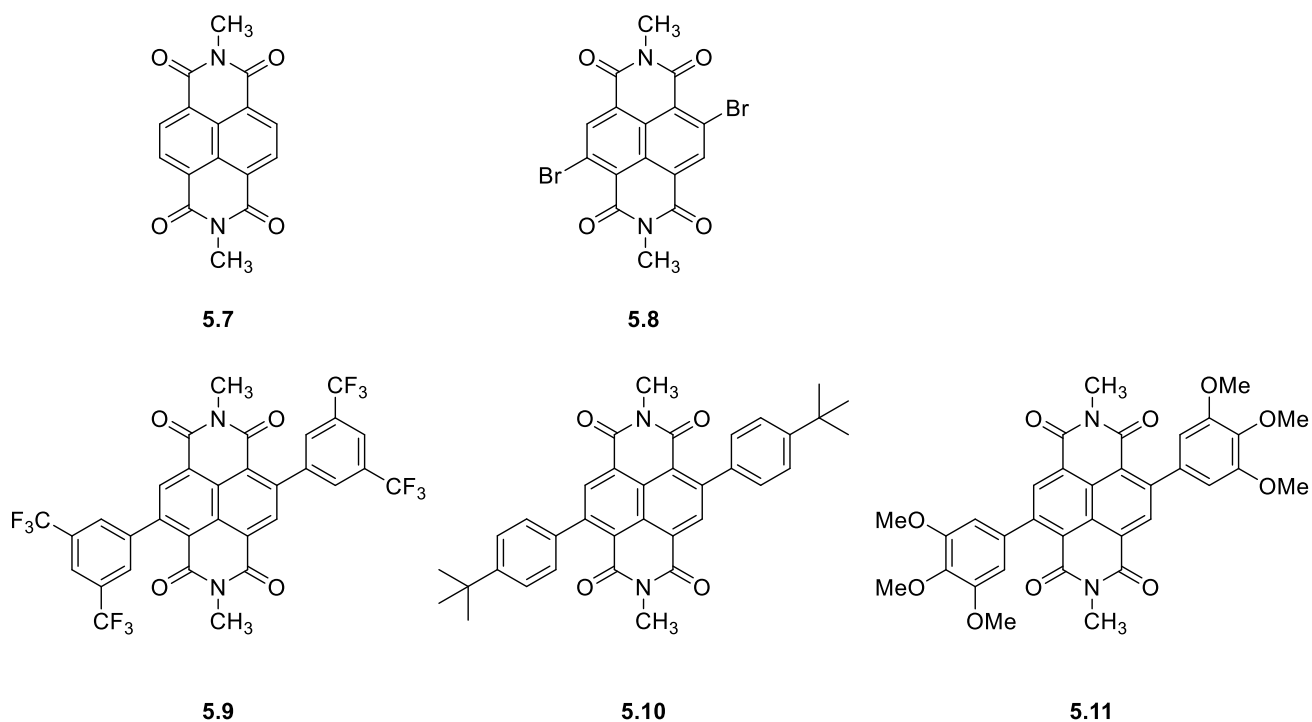
Figure 5.5. Chemical Structures of the naphthalenediimide derivatives **5.7-5.11** used for computational analysis.

In effort to better understand the effect of the substituents on the frontiers molecular orbitals, maps of the HOMOs and LUMOs were computed and represented in Table 5.2 and summarized in Table 5.3 and Figure 5.6.

Table 5.2. Computed HOMOs and LUMOs at the B3LYP/6-31G(d) level of theory for compounds **5.7-5.11**.
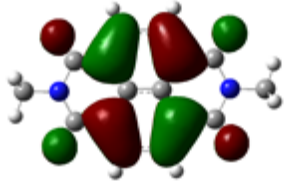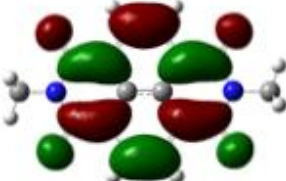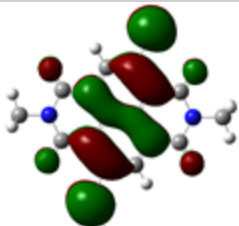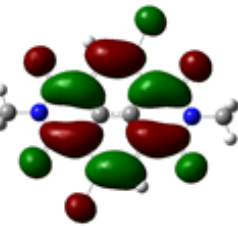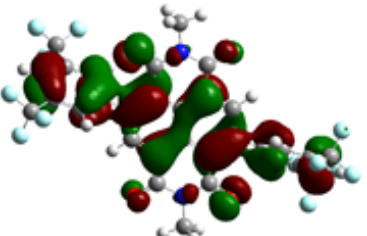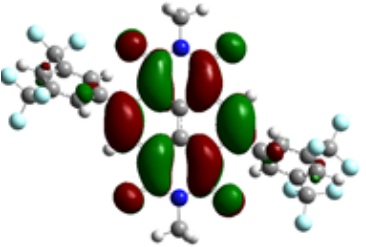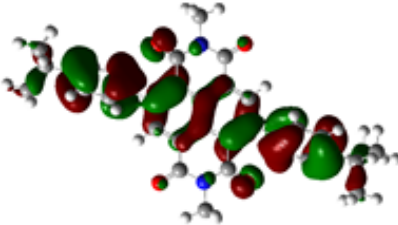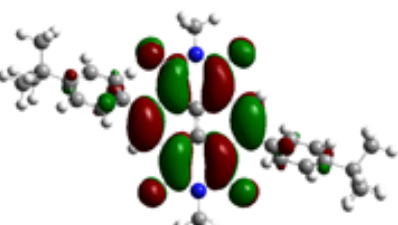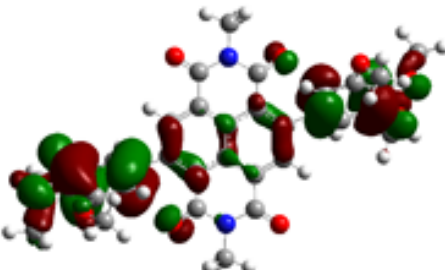
	HOMO	LUMO
5.7		
5.8		
5.9		
5.10		
5.11		

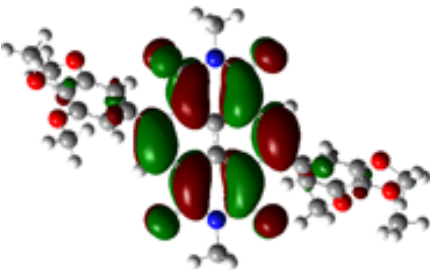**Table 5.3.** Frontier molecular orbitals as calculated at the B3LYP/6-31G(d) level of theory of compounds **5.7-5.11**.

Compound	HOMO (eV)	LUMO (eV)
5.7[157]	-7.3[157]	-4.3[157]
5.7	-7.03	-3.41
5.8	-7.07	-3.61
5.9	-7.21	-3.8
5.10	-6.16	-3.2
5.11	-5.76	-3.19
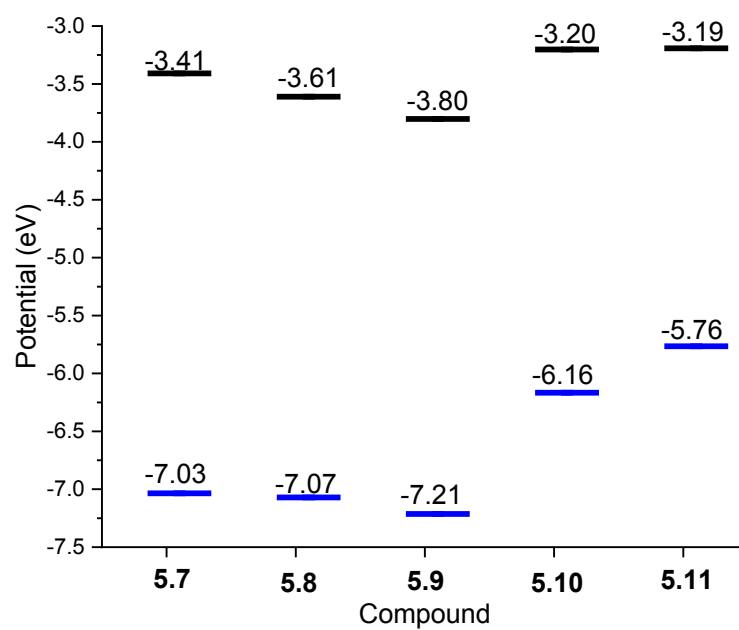
Figure 5.6. Graphical presentation of the frontier molecular energy levels as computed at the

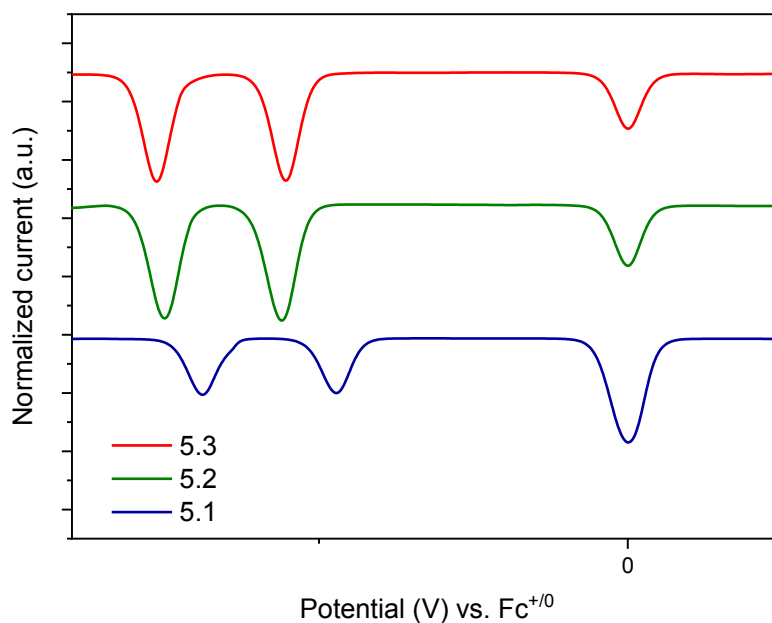B3LYP/6-31G(d) level of theory for compounds **5.7-5.11**.

Figure 5.7. Reductive differential pulse voltammograms of compounds **5.1-5.3** in CH$_2$Cl$_2$/0.1 M ^{n}Bu$_4$NPF$_6$ with ferrocene as internal standard (feature at 0 V).

Table 5.4. Reduction potentials of compounds **5.1-5.3** as determined in 0.1 M nBu$_4$NPF$_6$ in CH$_2$Cl$_2$ vs. Fc$^+$/Fc.

Compound	Potentials vs. Fc (V)	
	^{0}/-	-/-
5.1	-0.94	-1.37
5.2	-1.12	-1.49
5.3	-1.1	-1.51

Table 5.5. Characteristics of the transition states of compounds **5.7-5.11** determined at the LC-ωPBE[158-160] and cc-pVTZ[161] level of theory observed with significant oscillator strengths.

Compound	State	Energy (eV)	Wavelength (nm)	Oscillator strength	Dipole moment (D)	Contribution
5.7	S2	3.56	348	0.339	3.8829	HOMO →LUMO 100
5.8	S3	3.34	371	0.179	2.1898	HOMO-3 →LUMO (5) HOMO-3 →LUMO+2 (3) HOMO →LUMO (91)
	S4	3.69	336	0.232	2.5663	HOMO-3 →LUMO (87) HOMO →LUMO (8) HOMO →LUMO+2 (4)
5.9	S3	3.29	377	0.126	1.5594	HOMO-3 →LUMO (22) HOMO-2 →LUMO (49) HOMO →LUMO (27)
	S4	3.43	362	0.175	2.0882	HOMO-11 →LUMO (2) HOMO-3 →LUMO (69) HOMO-2 →LUMO (25) HOMO →LUMO (3)
	S8	4	310	0.138	1.4046	HOMO-9 →LUMO (35) HOMO-5 →LUMO (57) HOMO-2 →LUMO+2 (3) HOMO →LUMO+2 (2)

5.10	S1	2.77	448	0.153	2.2554	HOMO-5 →LUMO (2) HOMO-2 →LUMO (4) HOMO-1 →LUMO+1 (2) HOMO →LUMO (90)
	S4	3.41	363	0.238	2.8438	HOMO-5 →LUMO (38) HOMO-4 →LUMO (22) HOMO-3 →LUMO (10) HOMO-2 →LUMO (28)
5.11	S1	2.61	475	0.132	2.0686	HOMO-9 →LUMO (2) HOMO-6 →LUMO (2) HOMO-5 →LUMO (3) HOMO-2 →LUMO (3) HOMO-1 →LUMO+1 (2) HOMO →LUMO (85)
	S6	3.41	363	0.118	1.4160	HOMO-9 →LUMO (4) HOMO-8 →LUMO (4) HOMO-7 →LUMO (23) HOMO-6 →LUMO (28) HOMO-4 →LUMO (36) HOMO-1 →LUMO (2)
	S7	3.42	362	0.137	1.6310	HOMO-9 →LUMO (5) HOMO-8 →LUMO (4) HOMO-7 →LUMO (37) HOMO-5 →LUMO (8) HOMO-4 →LUMO (40) HOMO-3 →LUMO (3)

5.2.4. Thermal Analysis

TGA experiments were performed on compounds **5.1-5.3** using a Bruker TGA-IR Tensor 27 at a scanning rate of 10 °C min^{-1} under nitrogen atmosphere. The decomposition temperature was determined from the first derivative of the TGA curve. The results showed that the three compounds exhibit good thermal stability between 399.6 °C and 486.1 °C. Fluorinated compound **5.1** exhibited the lowest decomposition temperate although it had the highest molecular weight. The results for the TGA analysis of compounds **5.1-5.3** are summarized in Table 5.6 And depicted in Figure 5.8.

Table 5.6. Decomposition temperatures of compounds **5.1-5.3**.

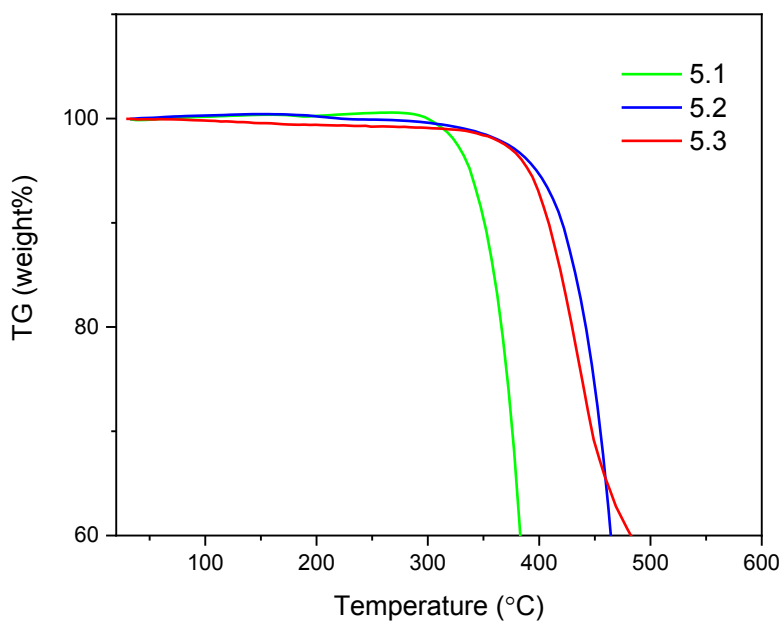| Compound	Empirical Formula	Molecular weight, (g.mol^{-1})	T_d (°C)
5.1	$C_{42}H_{34}F_{12}N_2O_4$	858.72	399.6
5.2	$C_{46}H_{54}N_2O_4$	698.95	486.1
5.3	$C_{44}H_{50}N_2O_{10}$	766.89	465.4

Figure 5.8. TGA results showing the thermal decomposition process of compounds **5.1-5.3**.

DSC experiments were performed on compounds **5.1-5.3** using TA instrument. Heat/cool/heat cycles were carried out while maintaining a heating/cooling rate of 10 °C min^{-1} under nitrogen atmosphere. Heating cycles were set around 90 degrees below the corresponding decomposition temperatures determined by TGA. Figures 5.9-5.11 show the collected DSC curves of the 2nd heating and the 1st cooling cycles of the compounds **5.1-5.3** Noting that the 1st heating cycle was carried out to remove the thermal history of the compounds. The melting point increased as the electron withdrawing effect increased. The results of the DSC analysis are summarized in Table 5.7.

Table 5.7. DSC results for compounds **5.1-5.3**.

	Mol wt, (g.mol⁻¹)	Transition	Onset temp (°C)	Maximum temp (°C)	Area, (J.g⁻¹)	Molar enthalpy (kJ.mol⁻¹)
5.1	858.72	crystallization	153.61	174.14	10.28	8.83
		melting	179.76	184.89	8.74	7.50
5.2	698.95	crystallization	157.88	168.30	11.16	7.80
		melting	204.18	226.36	8.82	6.17
5.3	766.89	crystallization	245.35	252.48	30.25	23.20
		melting	281.84	294.71	31.81	24.40
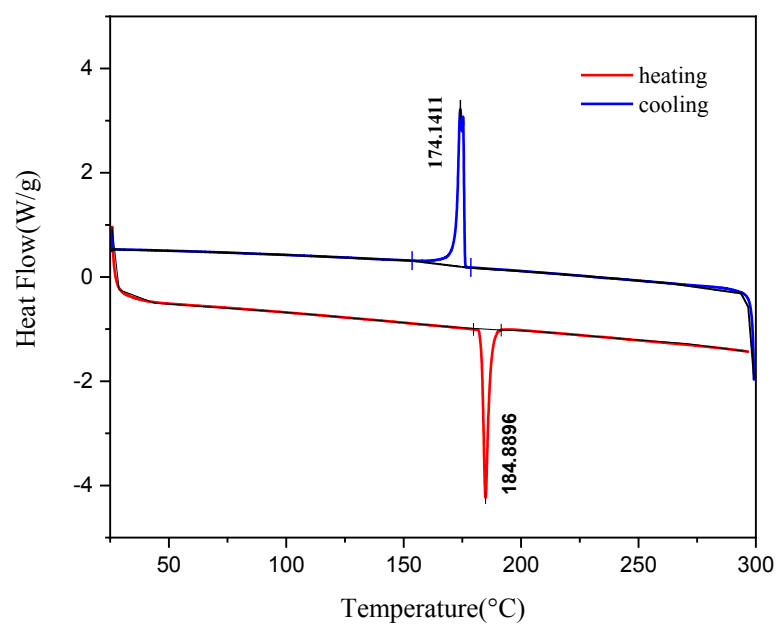
Figure 5.9. DSC analysis of compound **5.1**

80
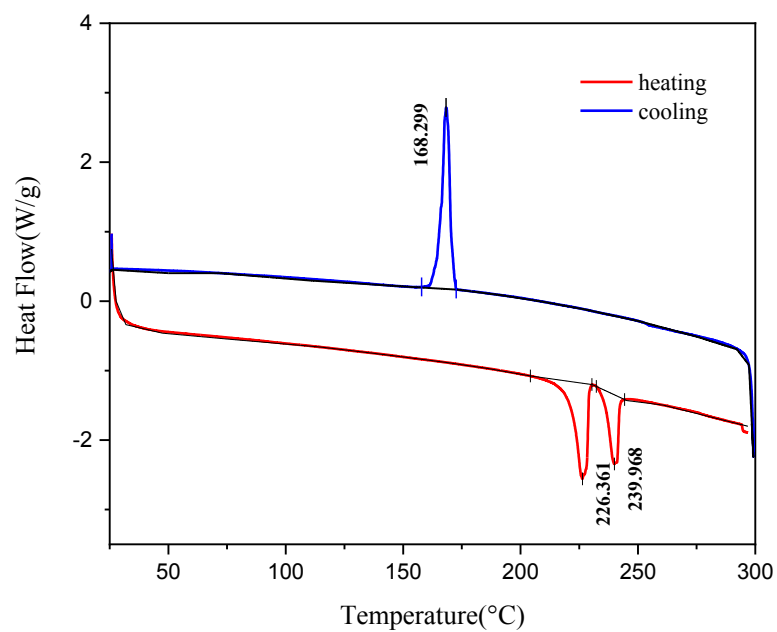
Figure 5.10. DSC analysis of compound **5.2.**
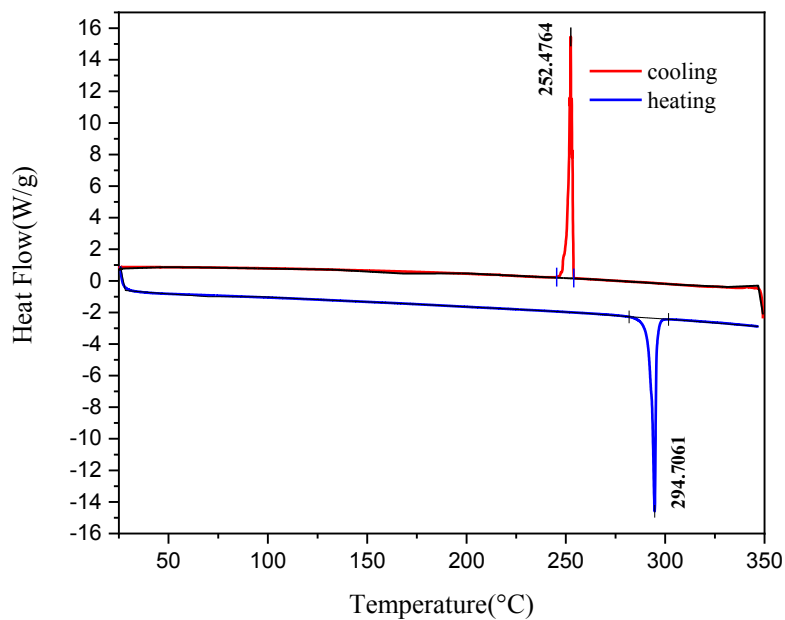
**Figure 5.11.** DSC analysis of compound **5.3**.

5.3. Experimental

5.3.1. Synthesis

All reactions were run using clean and oven dried glassware. Decomposition temperatures (T_d) were determined using a NETZSCH thermogravimetric analyzer and were defined to be as a loss of 5% of the initial sample mass upon heating at a 20 °C/min rate; under continuous flow of nitrogen gas in order to ensure a completely inert atmosphere inside the heating chamber during measurements. Melting temperatures were determined using a TA Instruments, Q2000 differential scanning calorimeter. NMR spectra were acquired using a 500 MHz Bruker NMR machine. Elemental analyses were performed at Atlantic Microlab, Inc., Norcross, USA.

**2,6-Dibromo-naphthalene-1,4,5,8-tetracarboxylic acid (5.5)**

The title compound was synthesized according to a modified literature procedure.[162] In a round-bottom-flask, **5.4** (1.00 g, 3.73 mmol) was dissolved in 6 mL sulfuric acid. Dibromoisocyanuric acid (2.10 g, 7.49 mmol) was dissolved in 6 mL sulfuric acid and then added slowly to the reaction mixture. The mixture was stirred at 130 ºC for 16 hours. The mixture was cooled to room temperature then poured over 100 mL cold distilled water. The precipitate was filtered. Compound **5.5** (0.78 g, 91%) was obtained as a yellow olive solid and was washed with water followed by methanol. ^{1}H NMR (500 MHz, DMSO-d_6): δ 11.18 (s, 4H), δ 8.71 (s, 2H).
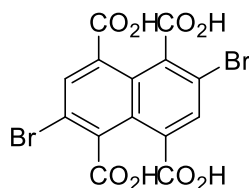
5.5

4,9-dibromo-2,7-dihexylbenzo[*lmn*][3,8]phenanthroline-1,3,6,8(*2H,7H*)-tetraone (5.6)

The title compound was synthesized according to a modified literature procedure.[162] In a round-bottom-flask **5.5** (1.00 g, 2.16 mmol) was dissolved in 60 mL acetic acid. Hexylamine (2.19 g, 21.64 mmol) was then added. The reaction mixture was refluxed for 1 hour then cooled to room temperature and filtered. The obtained crude was recrystallized from acetic acid. Compound **5.6** (0.30 g, 23%) was obtained as a gold yellow solid. ^{1}H NMR (500 MHz, CDCl$_3$): δ 8.97 (s, 2H), 4.18 (t, 4H), 1.71 (p, *J*=7 Hz, 4H), 1.32 (m, 4H), 1.23 (m, 8H), 0.89 (t, *J*=7 Hz, 6H).
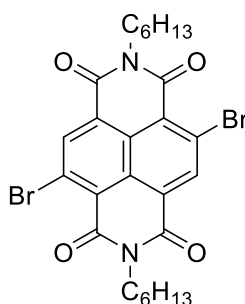
5.6

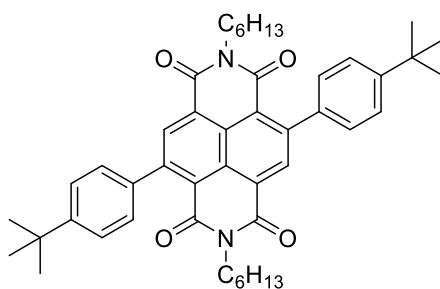**4,9-bis(3,5-bis(trifluoromethyl)phenyl)-2,7-dihexylbenzo[*lmn*][3,8]phenanthroline-1,3,6,8(*2H,7H*)-tetraone (5.1)**

The title compound was synthesized according to a modified literature procedure.[63] Compound **5.6** (0.25 g, 0.42 mmol), 3,5-bis(trifluoromethyl)phenylboronic acid (0.33 g, 1.27 mmol, 3 eqv), potassium carbonate 2M solution (3 mL), and tetrabutylammonium bromide (10 mg) were added to 30 mL toluene. The mixture was purged with argon gas for 30 minutes. Freshly synthesized tetrakis(triphenylphosphine)-palladium (0) (50 mg) was then added, and the reaction was refluxed at 110 ºC for 48 hours under argon and in the dark. The reaction was then quenched with distilled water, then extracted with DCM. The combined organic layer was dried over Na$_2$SO$_4$ and the solvent was removed under reduced pressure.

The desired compound was separated using silica gel column chromatography with hexane: DCM (1:1) as mobile phase and recrystallized from toluene. Compound **5.1** (0.25 g, 69%) was isolated as a pale-yellow solid. ^{1}H NMR (500 MHz, CDCl$_3$): δ 8.63 (s, 2H), 8.03 (s, 2H), 7.86 (s, 4H), 4.09 (t, *J*=7.5 Hz, 4H), 1.67 (p, *J*=7.5 Hz, 4H), 1.36 (m, 4H), 1.29 (m, 8H), 0.88 (t, *J*=7 Hz, 6H). ^{13}C NMR (125 MHz, CDCl$_3$): 161.87, 144.63, 142.16, 135.12, 132.11, 131.84, 128.47, 127.58, 126.38, 124.35, 123.60, 122.33, 122.18, 41.29, 31.43, 27.95, 26.65, 22.46, 13.92. Anal. Calcd for C$_{42}$H$_{34}$F$_{12}$N$_2$O$_4$: C, 58.75; H, 3.99; N, 3.26. Found: C, 58.91; H, 3.88; N, 3.30.
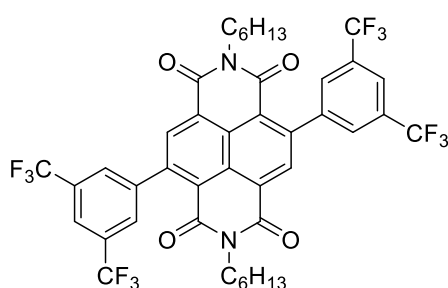
5.1

4,9-bis(4-(*tert*-butyl)phenyl)-2,7-dihexylbenzo[*lmn*][3,8]phenanthroline-1,3,6,8(*2H*,*7H*)-tetraone (5.2)

The title compound was synthesized according to a modified literature procedure.[35] Compound **5.6** (0.28 g, 0.47 mmol), 4-*tert*-butylphenylboronic acid (0.25 g, 1.42 mmol, 3 eqv), potassium carbonate 2M solution (3 mL), and tetrabutylammonium bromide (10 mg) were added to 30 mL toluene. The mixture was purged with argon gas for 30 minutes. Freshly synthesized tetrakis(triphenylphosphine)-palladium (0) (50 mg) was then added, and the reaction was refluxed at 110 ^{o}C for 48 hours under argon and in the dark. The reaction was then quenched with distilled water and extracted with dichloromethane. The combined organic layer was dried over MgSO$_4$ and solvent was removed under reduced pressure. The dark brownish residue was obtained and purified by silica gel column chromatography using

84

hexane: dichloromethane (3:2) as mobile phase. Compound **5.2** (0.29 g, 88%) was isolated as a bright orange solid. ^{1}H NMR (500 MHz, CDCl$_3$): δ 8.66 (s,2H), 7.56 (d, J = 8.5 Hz, 4H), 7.40 (d, J = 8.5 Hz, 4H), 4.12 (t, J = 7.5 Hz, 4 H), 6.85 (d, J = 1.5 Hz, 2H), 4.12(t, J = 7.5 Hz, 4H), 1.68 (p, J = 7.5 Hz, 4H), 1.35 (s, 18H), 1.30 (p, 12H), 0.89 (t, J = 7 Hz, 6H). ^{13}C NMR (125 MHz, CDCl$_3$): 162.62, 162.46, 151.21, 147.66, 137.55, 136.30, 128.07, 127.20, 125.46, 125.40, 122.70, 40.93, 34.79, 31.54, 31.39, 28.00, 26.74, 22.60, 14.07. Anal. Calcd for C$_{46}$H$_{54}$N$_2$O$_2$: C, 79.05; H, 7.79; N,4.01. Found: C, 79.03; H, 8.01; N, 3.91.

5.2

2,7-dihexyl-4,9-bis(3,4,5-trimethoxyphenyl)benzo[*lmn*][3,8]phenanthroline-1,3,6,8(*2H,7H*)-tetraone (5.3)

The title compound was synthesized according to a modified literature procedure.[63] Compound **5.6** (0.32 g, 0.54 mmol), 3,4,5-trimethoxyphenylboronic acid (0.34 g, 1.62 mmol, 3 eqv), potassium carbonate 2M solution (3 mL), and tetrabutylammonium bromide (10 mg) were added to 30 mL toluene. The mixture was purged with argon gas for 30 minutes. Freshly synthesized tetrakis(triphenylphosphine)-palladium (0) (50 mg) was then added, and the reaction was refluxed at 110 ºC for 48 hours under argon and in the dark. The reaction was then quenched with distilled water, then extracted with DCM. The combined organic layer was dried over Na$_2$SO$_4$ and the solvent was removed under reduced pressure. The desired compound was separated using silica gel column chromatography with DCM as mobile phase and finally washed with hot hexane. Compound **5.3** (0.283 g, 68%) was isolated

as a maroon solid. ^{1}H NMR (500 MHz, CDCl$_3$): δ 8.66 (s, 2H), 6.61 (s, 4H), 4.11 (t, *J*=7.5 Hz, 4H), 3.97 (s, 6H), 3.89 (s, 12H), 1.69 (p, *J*=7.5 Hz, 4H), 1.38 (m, 4H), 1.29 (m, 8H), 0.88 (t, *J*=7 Hz, 6H). ^{13}C NMR (125 MHz, CDCl$_3$): δ 162.38, 162. 09, 153.28, 147.53, 138.15, 135.80, 135.78, 127.10, 125. 30, 122.74, 105.59, 62.03, 56.23, 41.03, 31.52, 31.38, 28.04, 26.71, 22.53, 14.04. Anal. Calcd for C$_{44}$H$_{50}$N$_2$O$_{10}$: C, 68.91; H, 6.57; N, 3.65. Found: C, 68.88; H, 6.51; N, 3.62.

5.3

5.3.2. Photophysical Studies

Absorption spectra were measured using a Thermo scientific Genesys 10S UV-Vis spectrophotometer. Slit widths were fixed at 5 nm. A blank measurement with no sample in the sample holder was subtracted from all actual spectra to account for any error possible. UV-transparent quartz cuvette 136 (1 x 1 cm) was used for all experiments.

Stock solutions of concentration 1 mM of each compound were prepared in chloroform. UV-vis measurements were performed on 60 μM solutions. Molar absorptivity was determined using calibration curve technique for a set of 5 different concentrations (1 μM, 10 μM, 20 μM, 40 μM and 60 μM) for each compound. Stock solutions and all prepared concentrations were kept in the freezer and used the next day.

5.3.3. Computations

For compound **5.7**, X-ray crystal structure 1029338[157] was downloaded from CCDC. The cif-file was opened with Mercury (a single molecule was exported as .mol file). The chemical structures of compounds **5.7-5.11** were exported from Chemdraw. Quantum chemical calculations using density functional theory (DFT) and time-dependent DFT (TD-DFT) approaches were completed using Gaussian09 Revision D01.[163] Geometry optimizations were completed at B3LYP/6-31G(d) level of theory.[164,165] Analysis of frequency calculations verified geometries are minima. A single point calculation was carried out at the same level of theory and the Gaussian utility was used to create HOMO-LUMO frontier molecular orbitals plots. Then, TD-DFT calculations using Range-separated functional LC-ωPBE/6-31G(d) level of theory were completed.[158-160] Omega tuning[166-168] was completed to achieve omega values of compound **5.7** (w=0.2221), compound **5.8** (w=0.2221), compound **5.9** (w=0.1761), compound **5.10** (w=0.1727), and compound **5.11** (w=0.1757).

5.3.4 Electrochemistry

TBAP (1.937g) was dissolved in dichloromethane (DCM) in a 50 mL volumetric flask. A three-electrode setup consistent of Ag/AgCl reference electrode, glassy carbon working electrode, and platinum wire as counter electrode was utilized. A capillary tube's worth of compound was added to the solution along with a capillary tube's worth of ferrocene. The solution was stirred via a magnetic stirrer and purged with Argon bubbling for 10 min. The scan range was set from -1.6V to 1.6V, with a sampling width of 0.1s, and a sensitivity of 10^{-5}A/V. Three independent differential pulse voltammetry scans were performed.

CHAPTER 6

SUPPORTING DATA

In this Chapter, we include the spectral data (^{1}H and ^{13}C NMR) of the compounds reported throughout this thesis, as well the elemental analysis thereof. Appendix A contains ^{1}H NMR, Appendix B contains ^{13}C NMR, and Appendix C contains elemental analysis results.

PROTON NMR SPECTRA

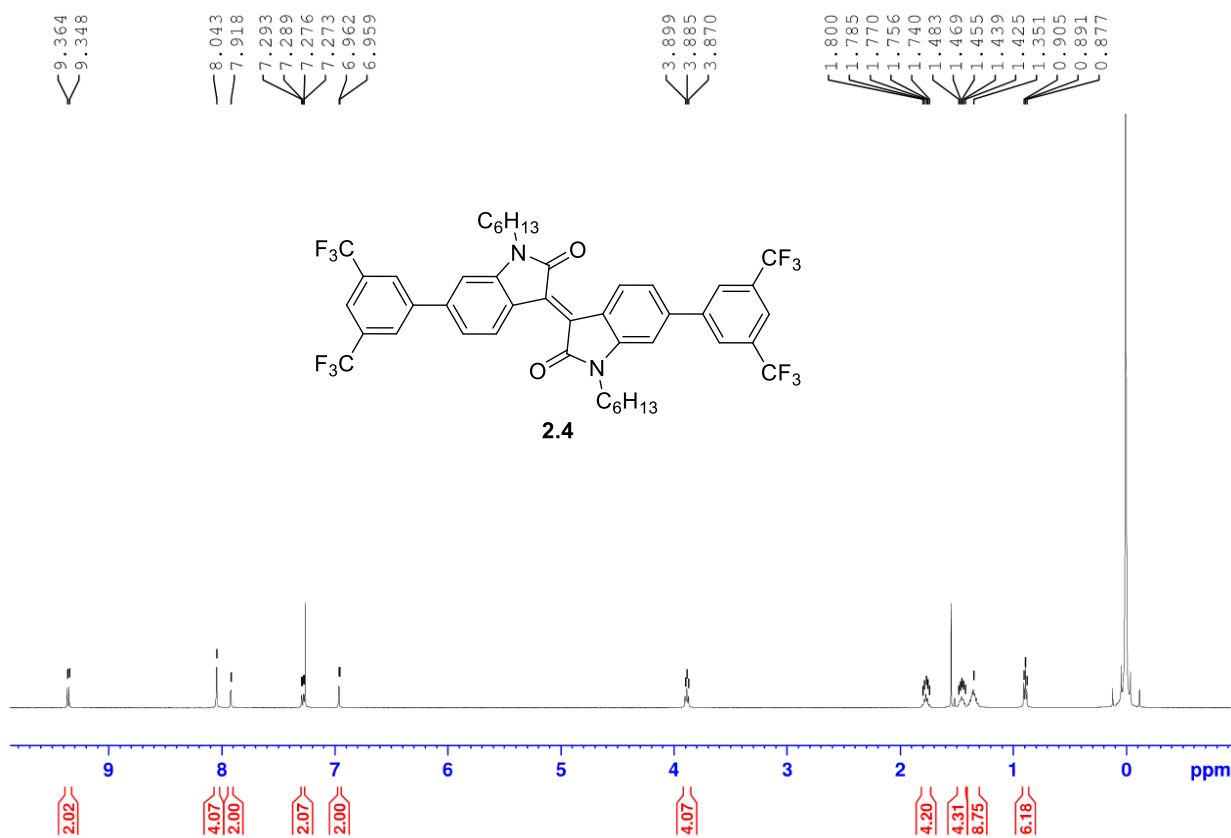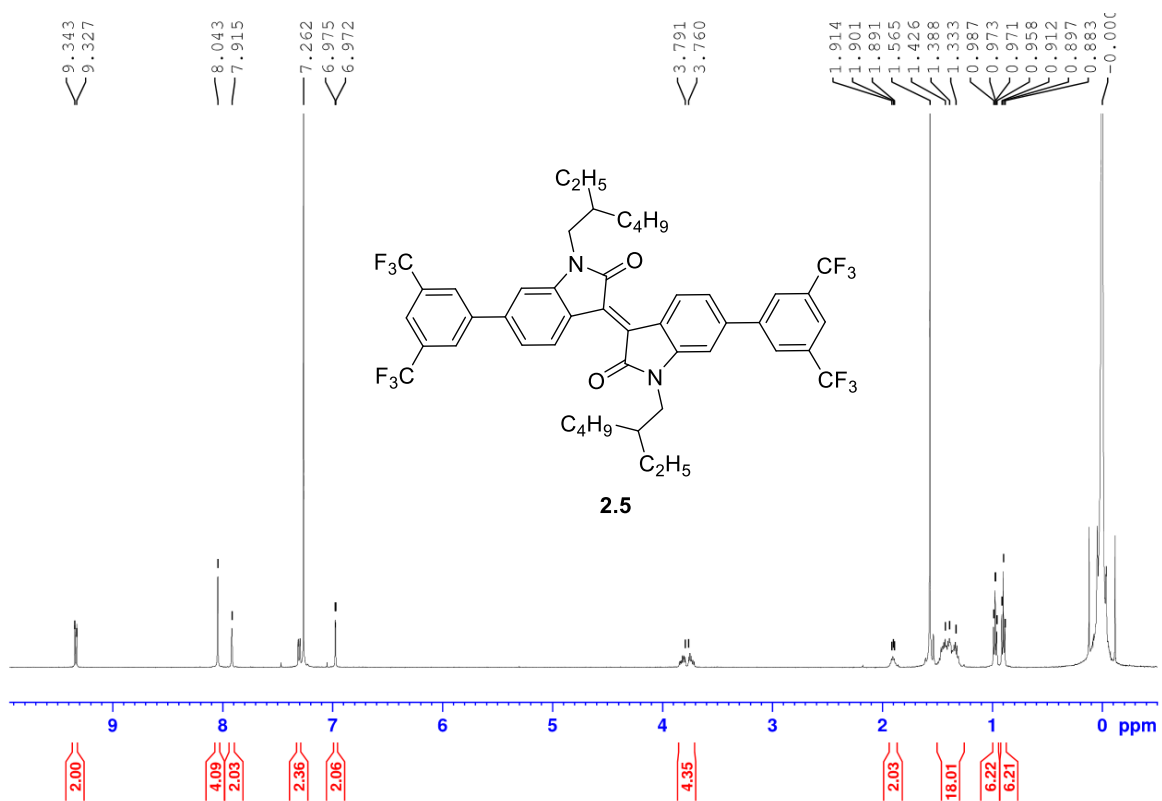**Figure 6.1.** ^{1}H NMR of **2.4** in CDCl$_3$ at 500 MHz.

Figure 6.2. ^{1}H NMR of **2.5** in CDCl$_3$ at 500 MHz.
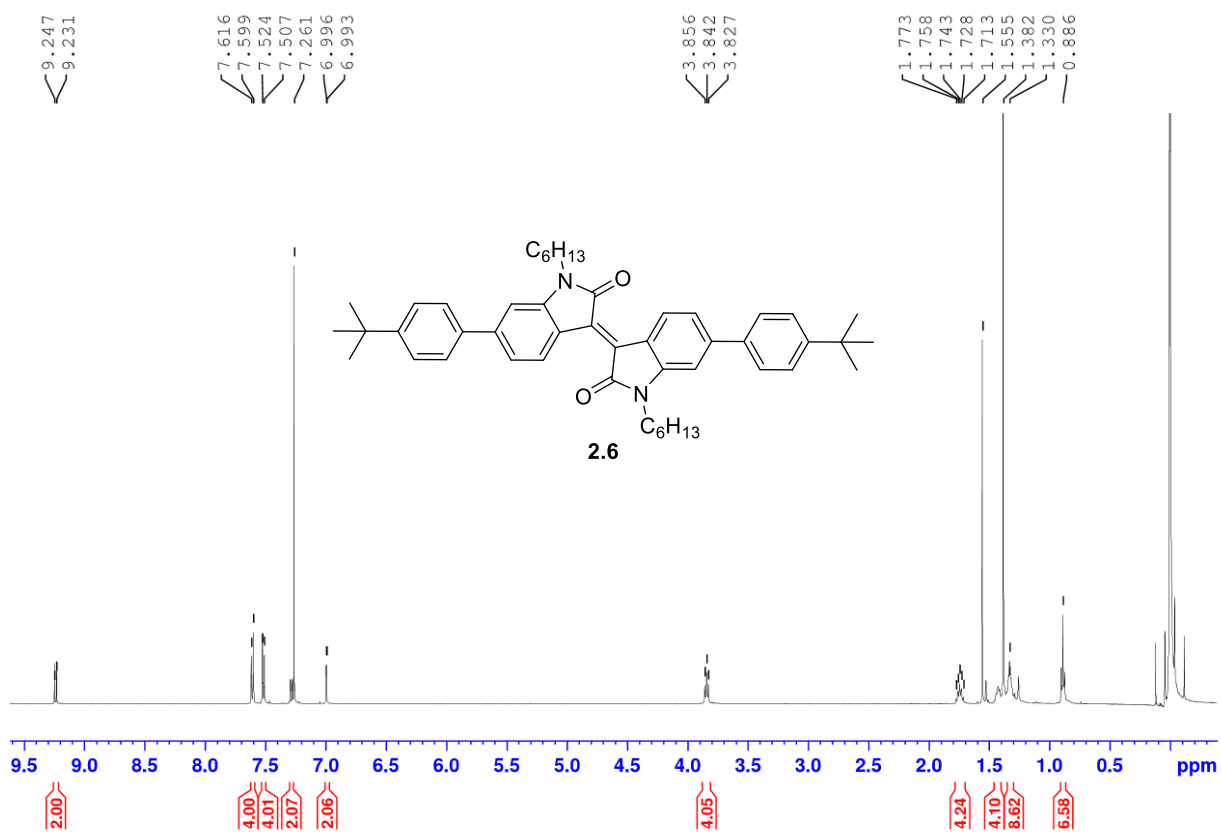
Figure 6.3. ^{1}H NMR of **2.6** in CDCl$_3$ at 500 MHz.
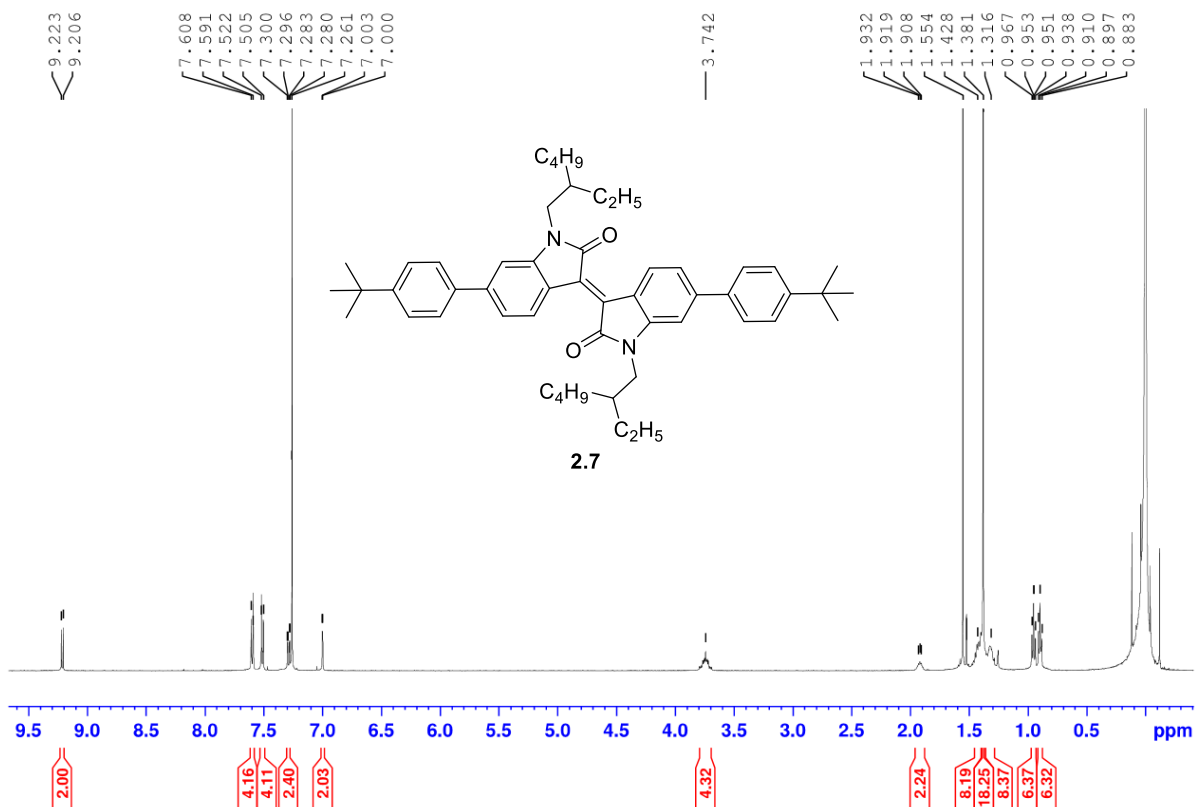
Figure 6.4. ^{1}H NMR of **2.7** in CDCl$_3$ at 500 MHz.
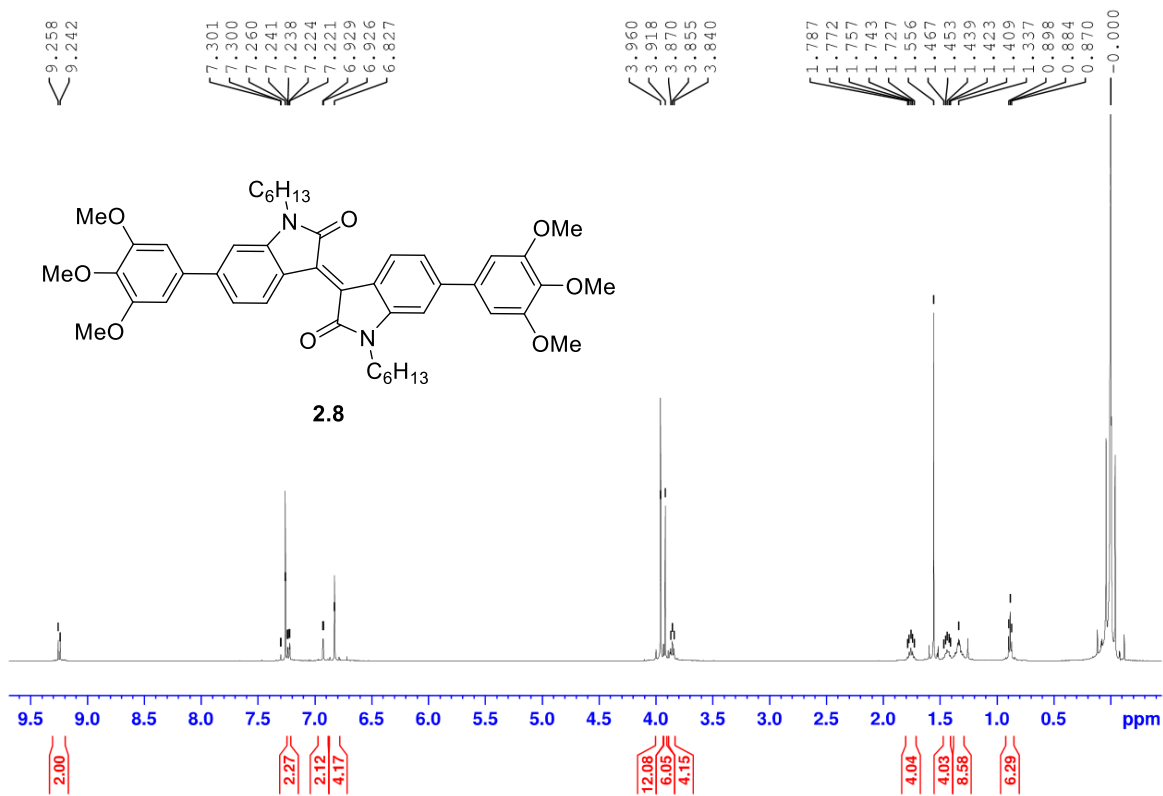
Figure 6.5. ^{1}H NMR of **2.8** in CDCl$_3$ at 500 MHz.
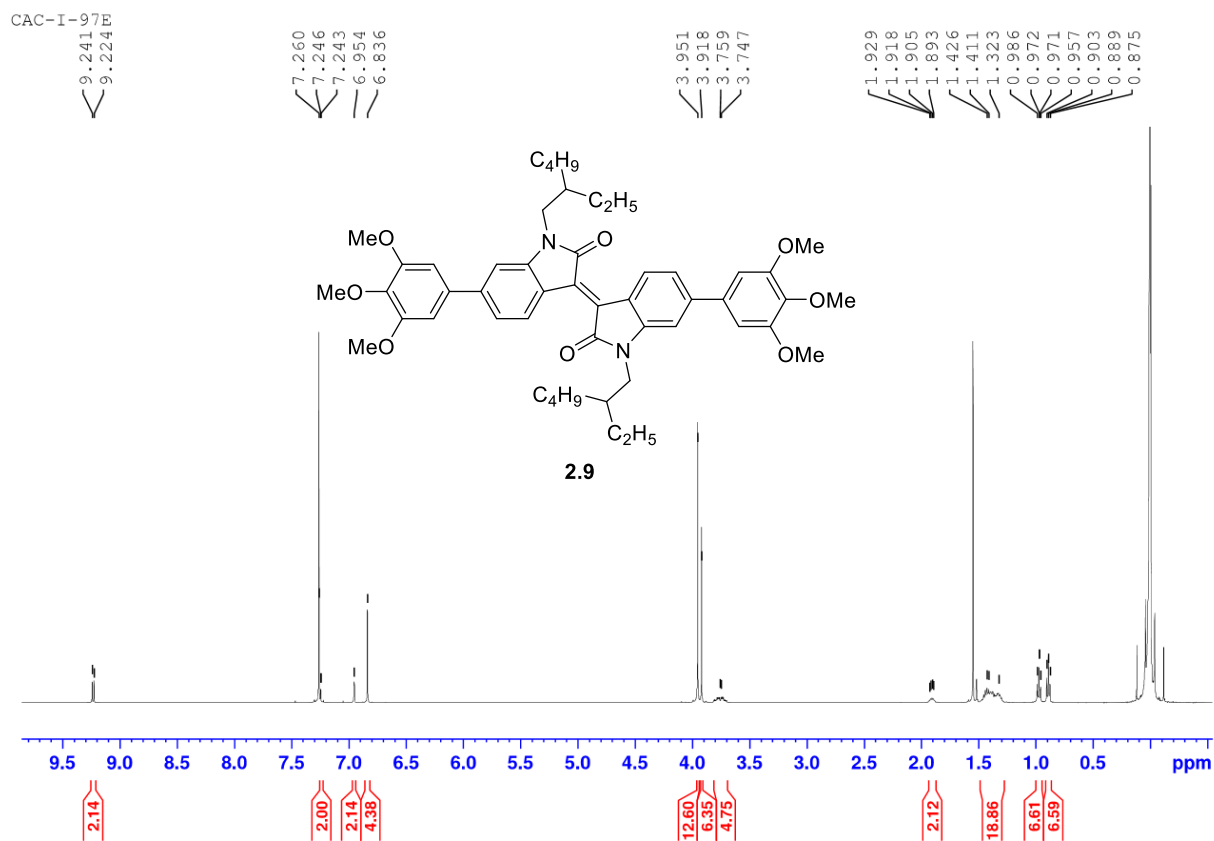
Figure 6.6. ^{1}H NMR of **2.9** in CDCl$_3$ at 500 MHz.
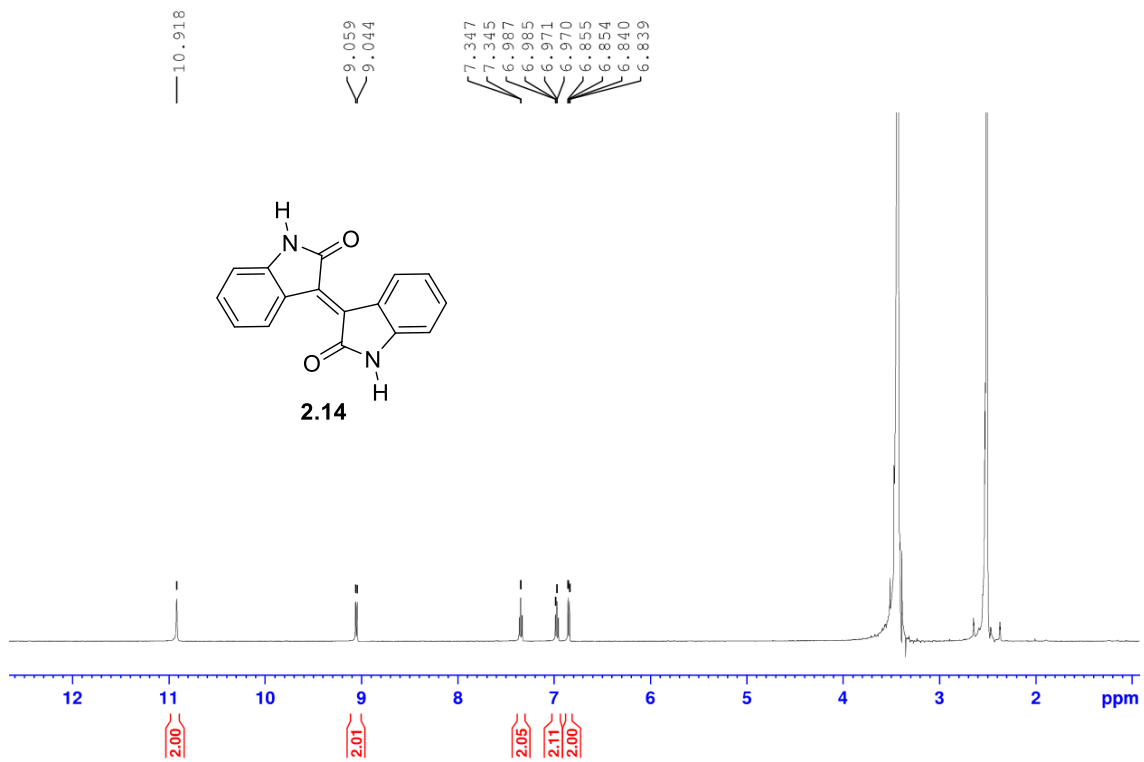
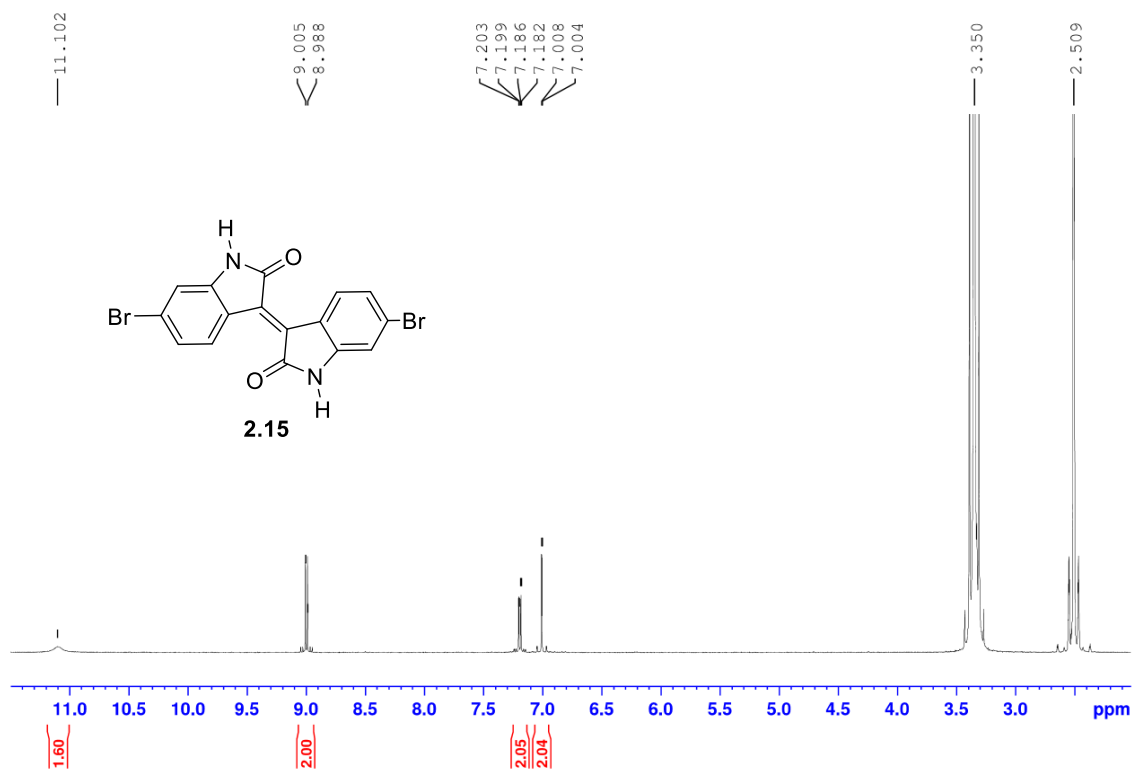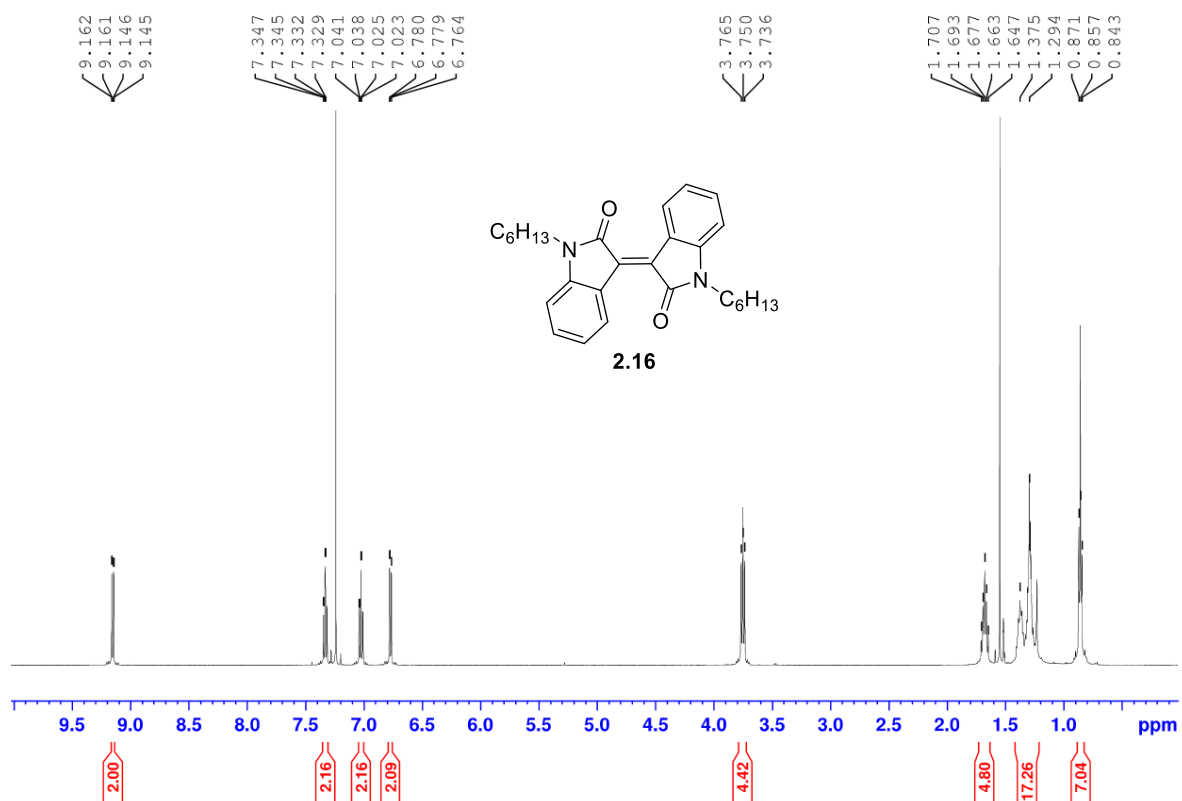**Figure 6.7.** ^{1}H NMR of **2.14** in DMSO-d_6 at 500 MHz.

Figure 6.8. ^{1}H NMR of **2.15** in DMSO-*d₆* at 500 MHz.

Figure 6.9. ^{1}H NMR of **2.16** in CDCl$_3$ at 500 MHz.
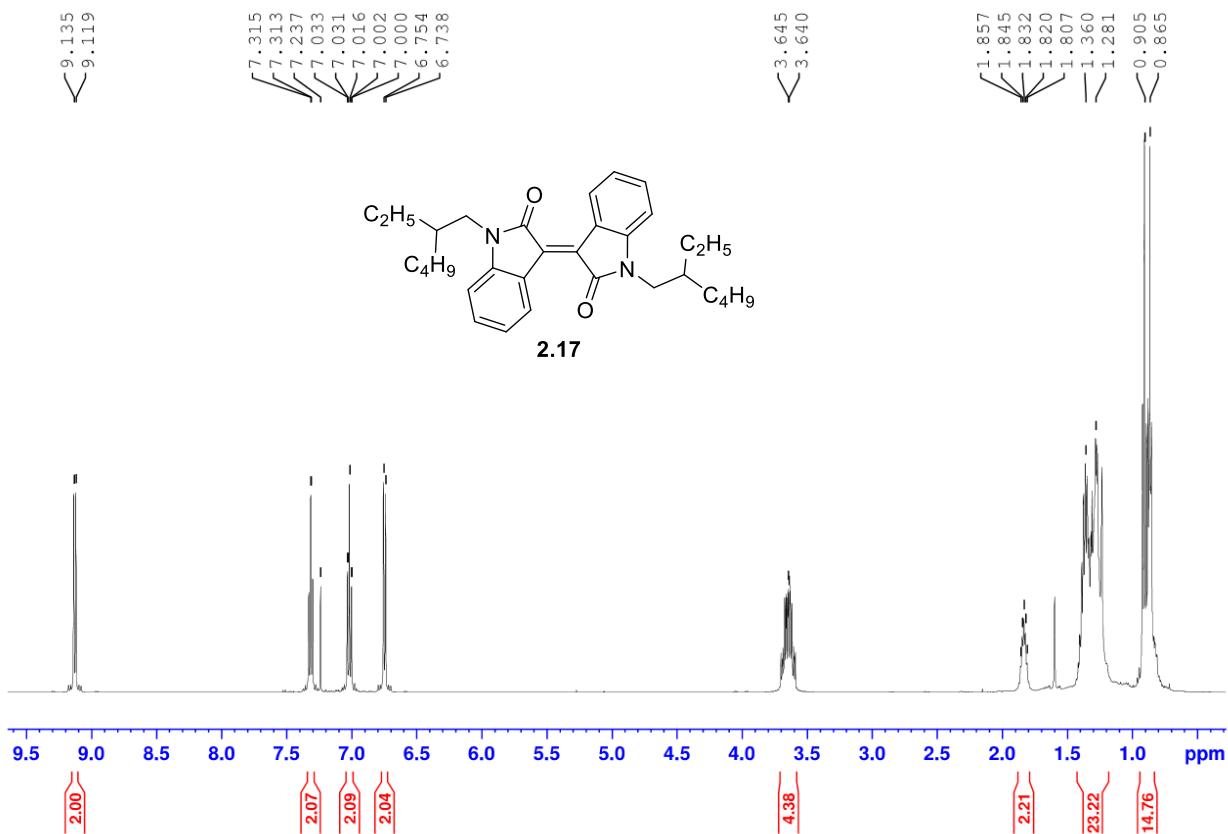
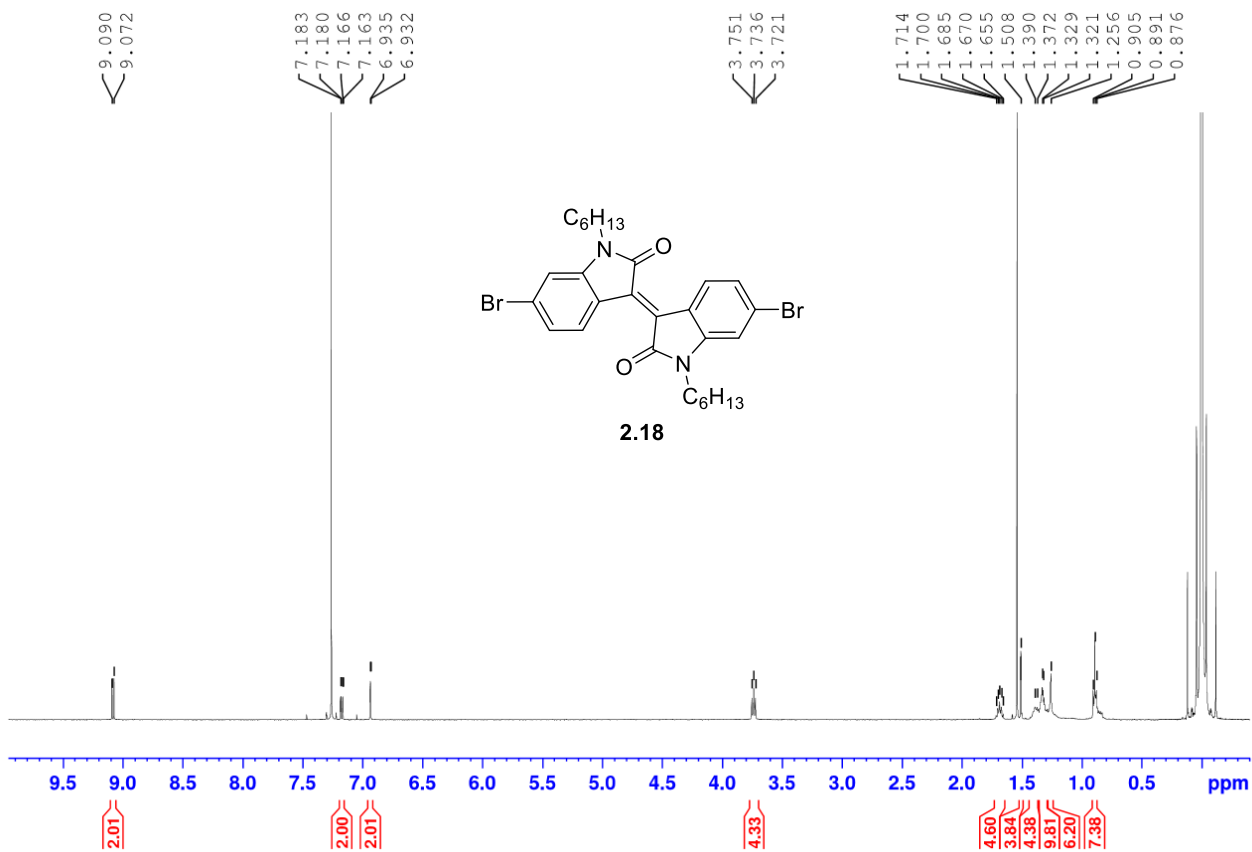**Figure 6.10.** ^{1}H NMR of **2.17** in CDCl$_3$ at 500 MHz.

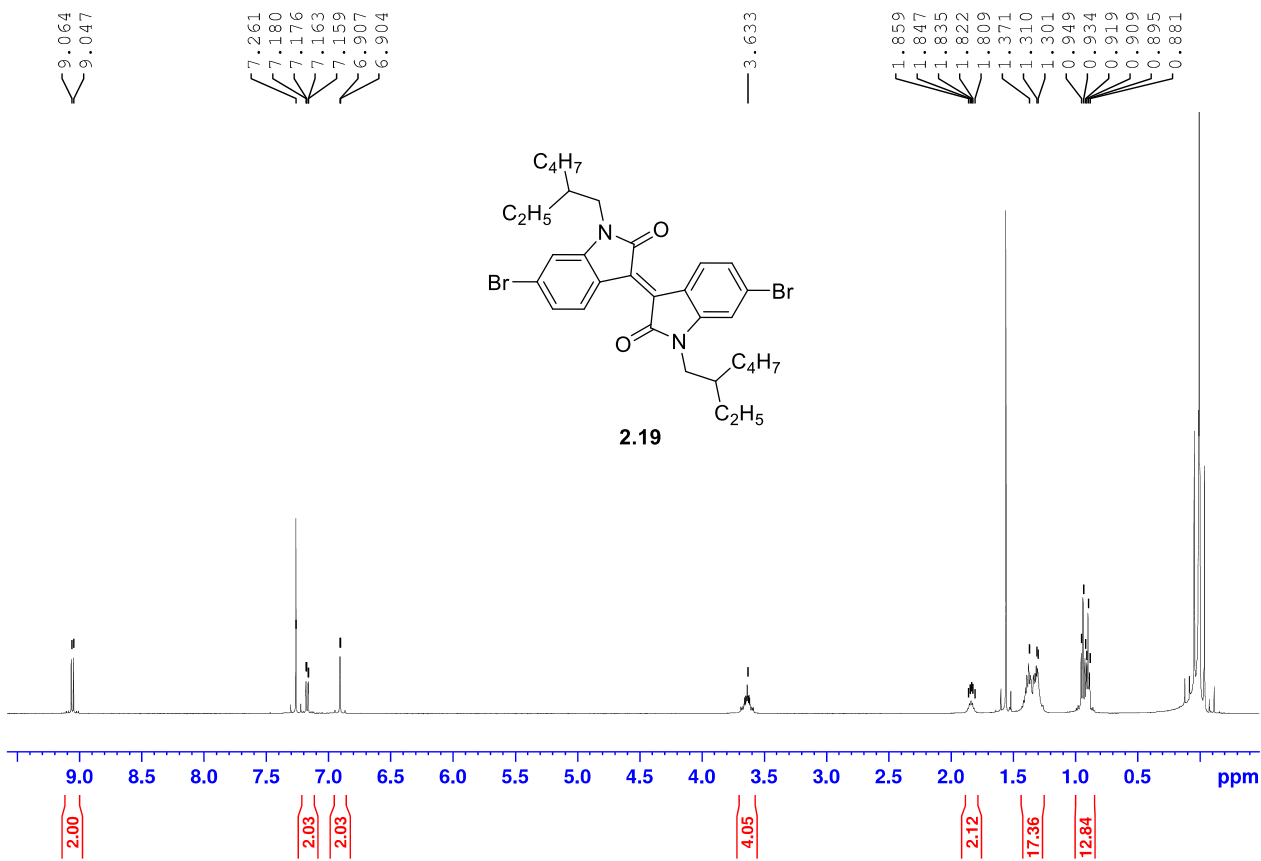**Figure 6.11.** ^{1}H NMR of **2.18** in CDCl$_3$ at 500 MHz.

Figure 6.12. ^{1}H NMR of **2.19** in CDCl$_3$ at 500 MHz.
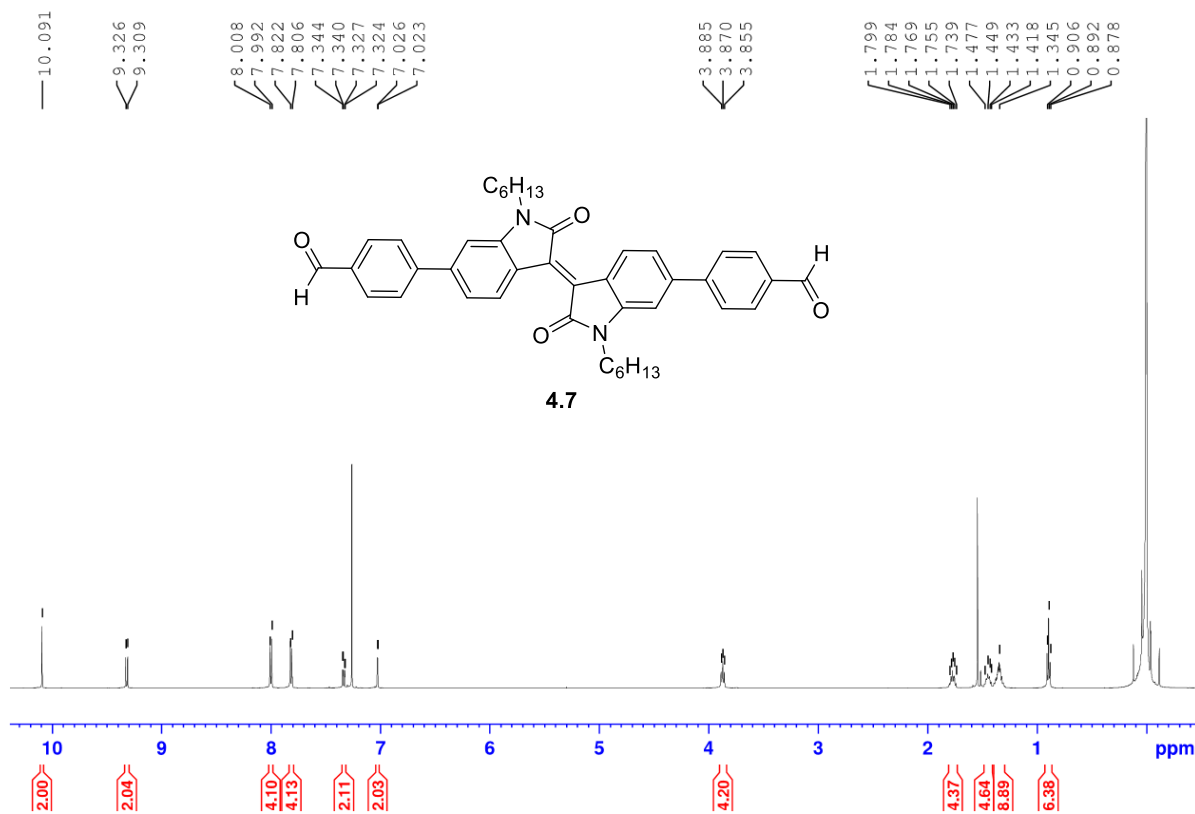
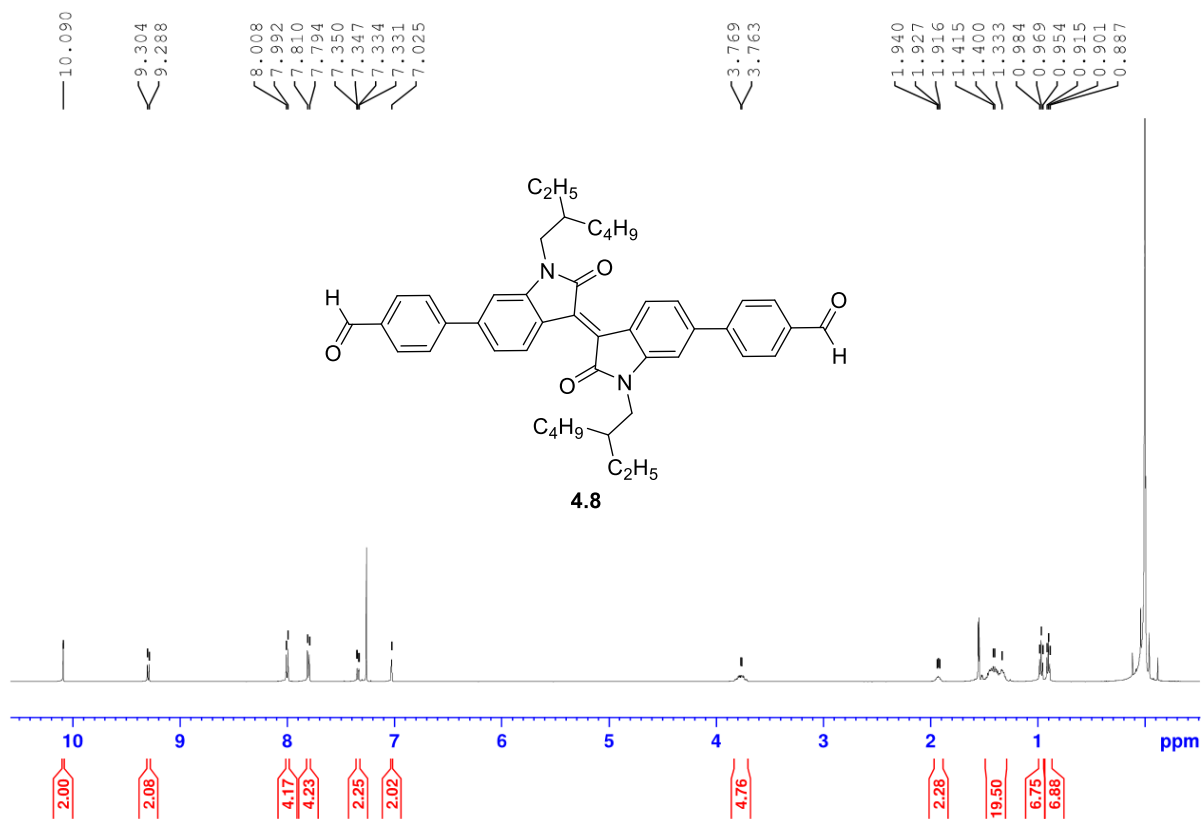**Figure 6.13.** ^{1}H NMR of **4.7** in CDCl$_3$ at 500 MHz.

Figure 6.14. ^{1}H NMR of **4.8** in CDCl$_3$ at 500 MHz.
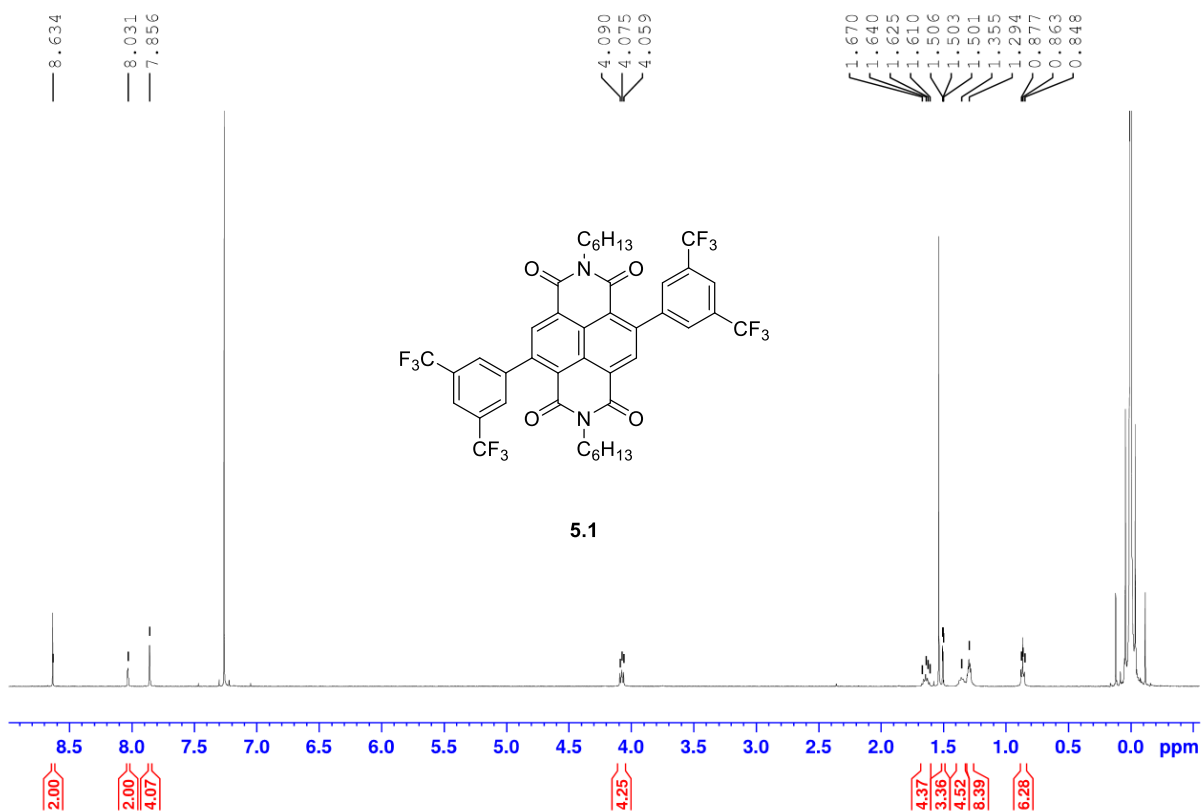
Figure 6.15. ^{1}H NMR of **5.1** in CDCl$_3$ at 500 MHz.
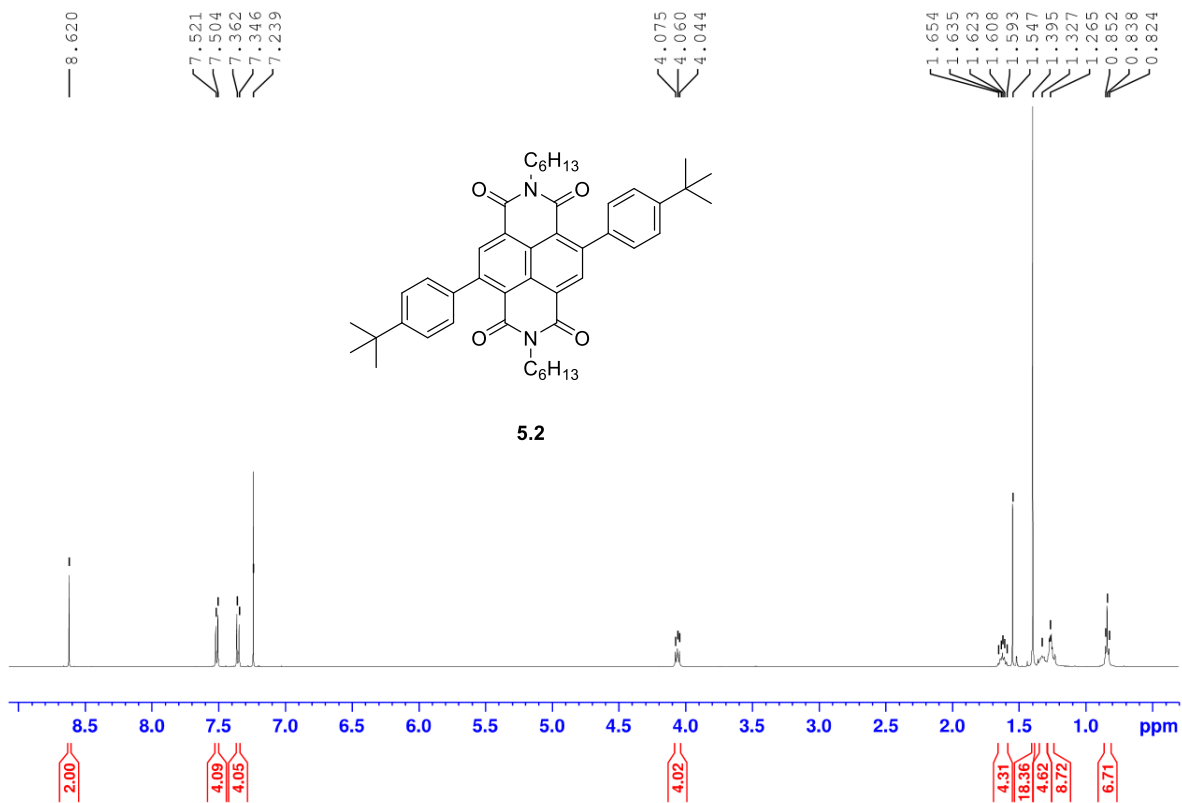
Figure 6.16. ^{1}H NMR of **5.2** in CDCl$_3$ at 500 MHz.
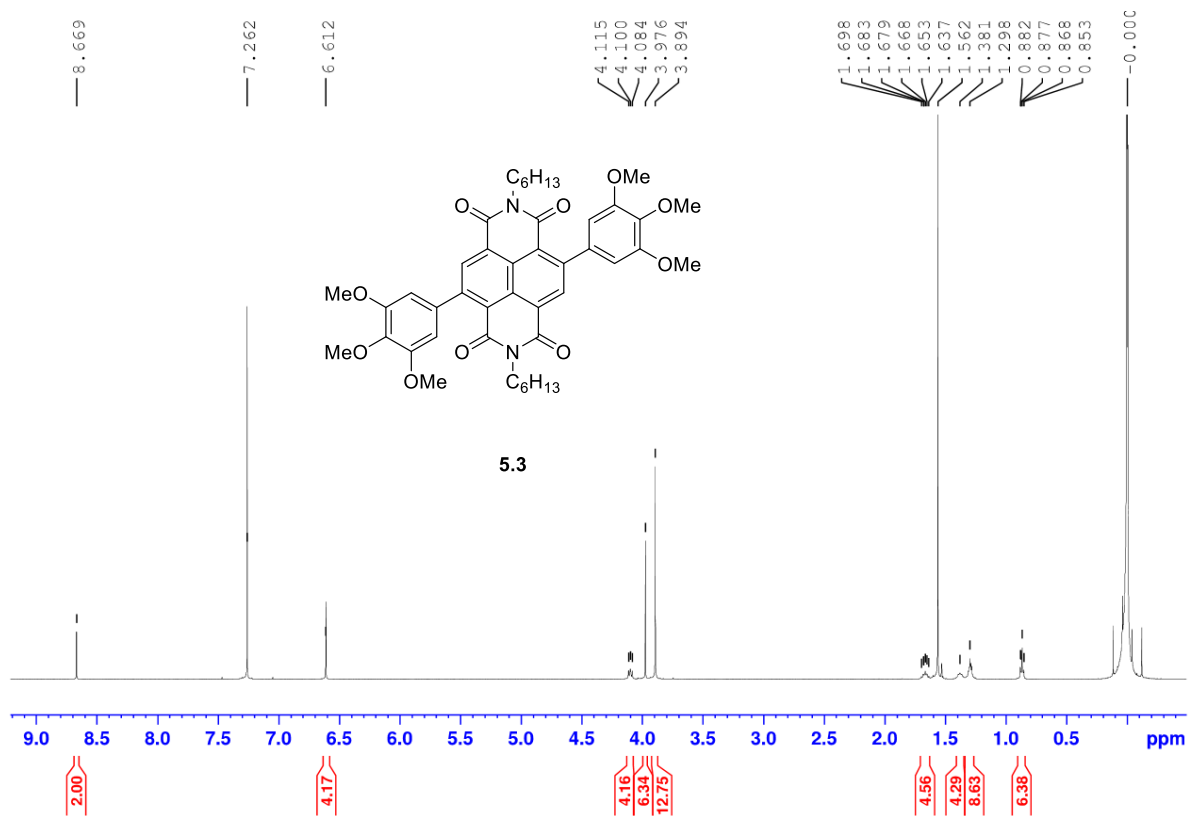
Figure 6.17. ^{1}H NMR of **5.3** in CDCl$_3$ at 500 MHz.
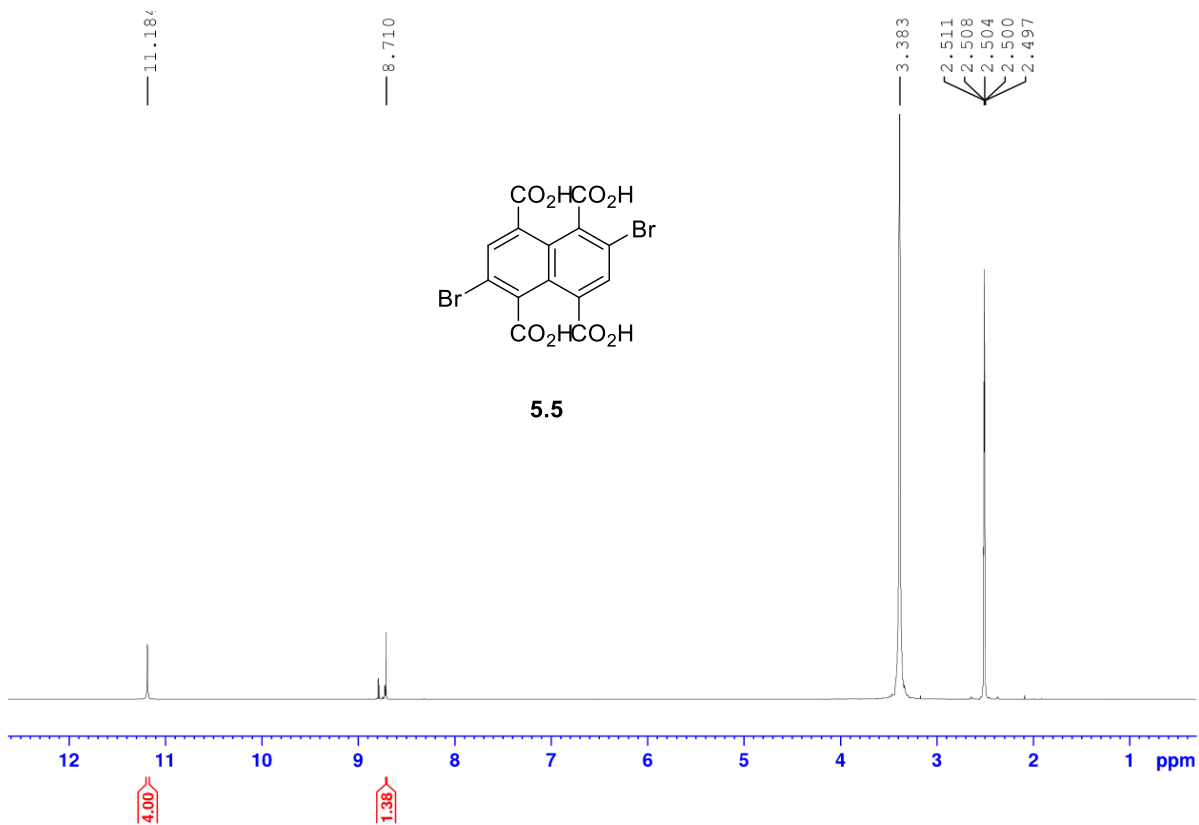
Figure 6.18. ^{1}H NMR of **5.5** in DMSO-d_6 at 500 MHz.
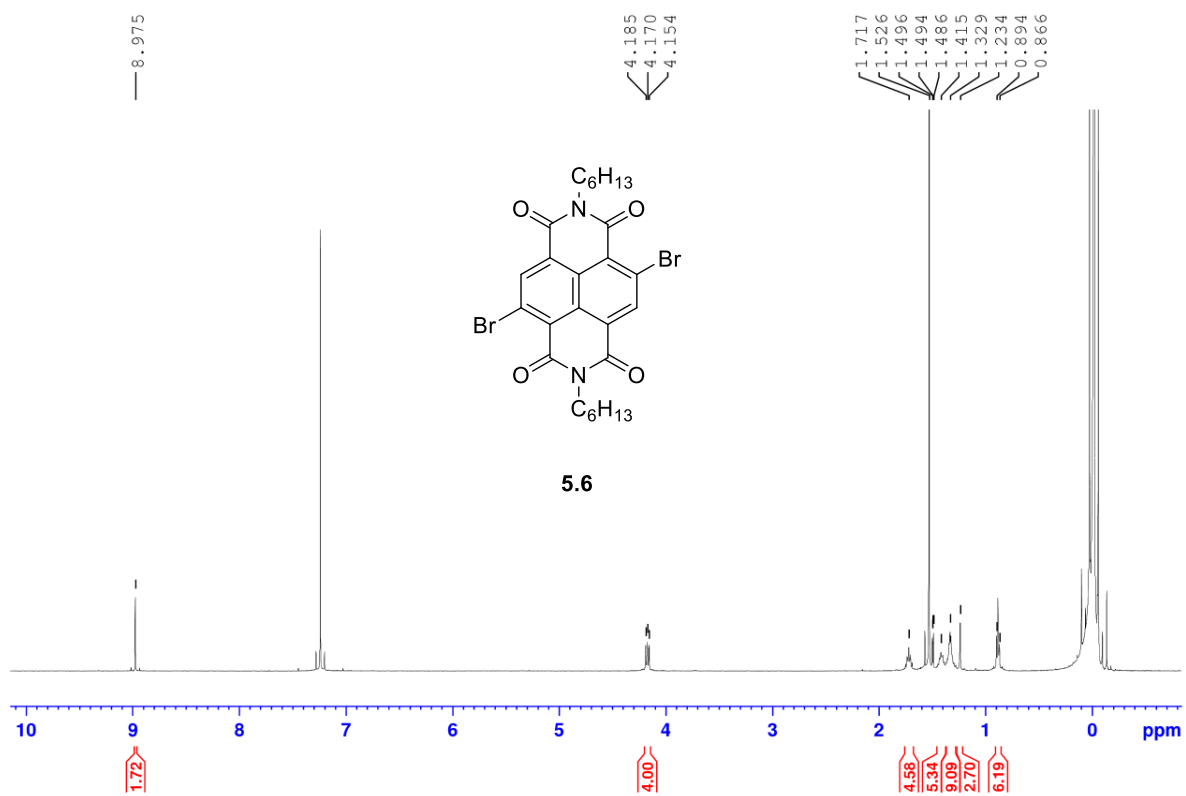
Figure 6.19. ^{1}H NMR of **5.6** in CDCl$_3$ at 500 MHz.

CARBON-13 NMR SPECTRA
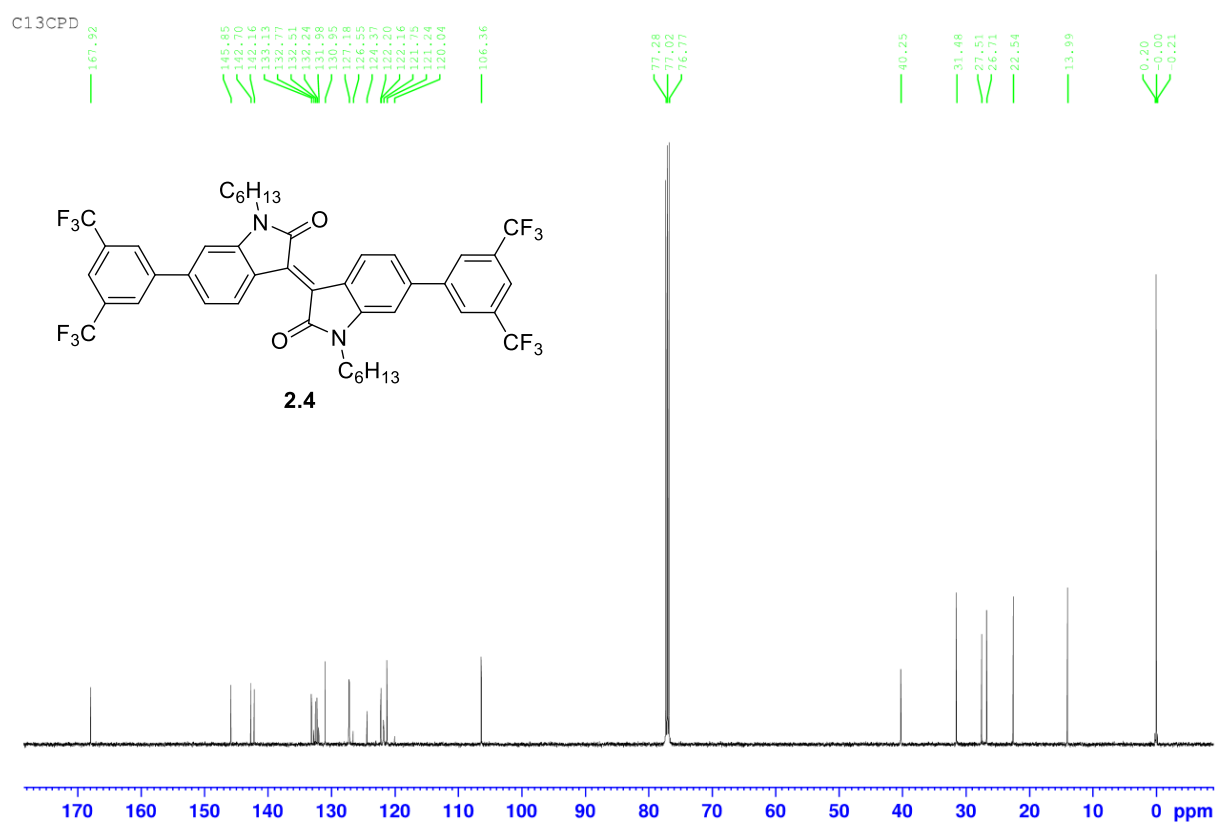
Figure 6.20. ^{13}C NMR of **2.4** in CDCl$_3$ at 125 MHz.
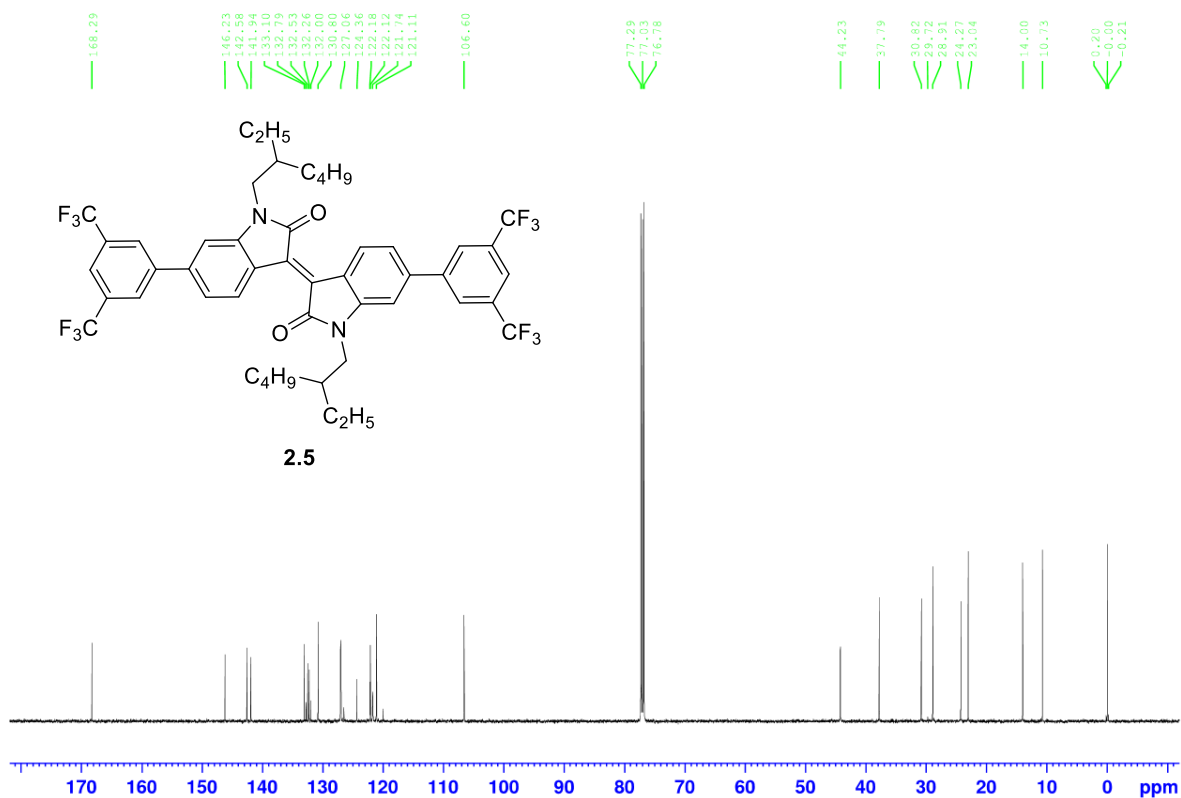
Figure 6.21. ^{13}C NMR of **2.5** in CDCl$_3$ at 125 MHz.
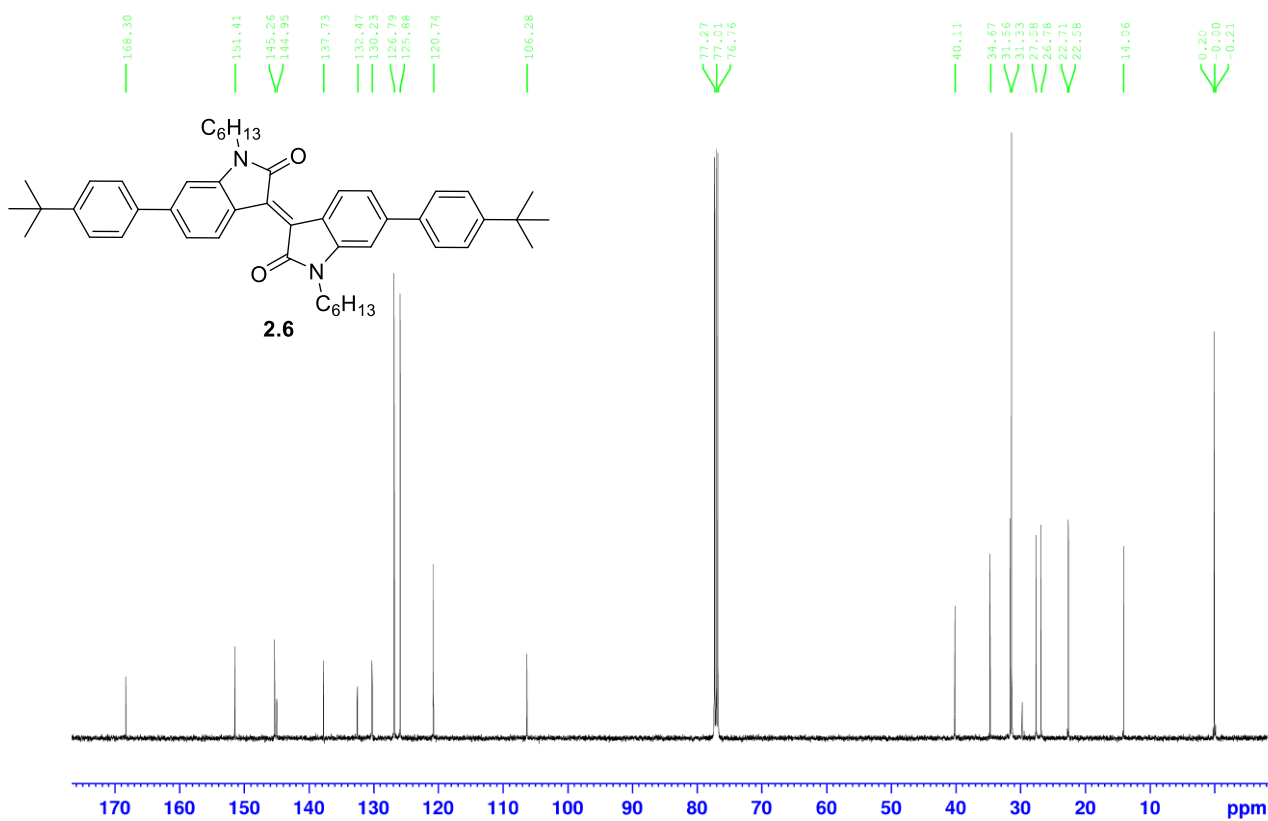
Figure 6.22. ^{13}C NMR of **2.6** in CDCl$_3$ at 125 MHz.
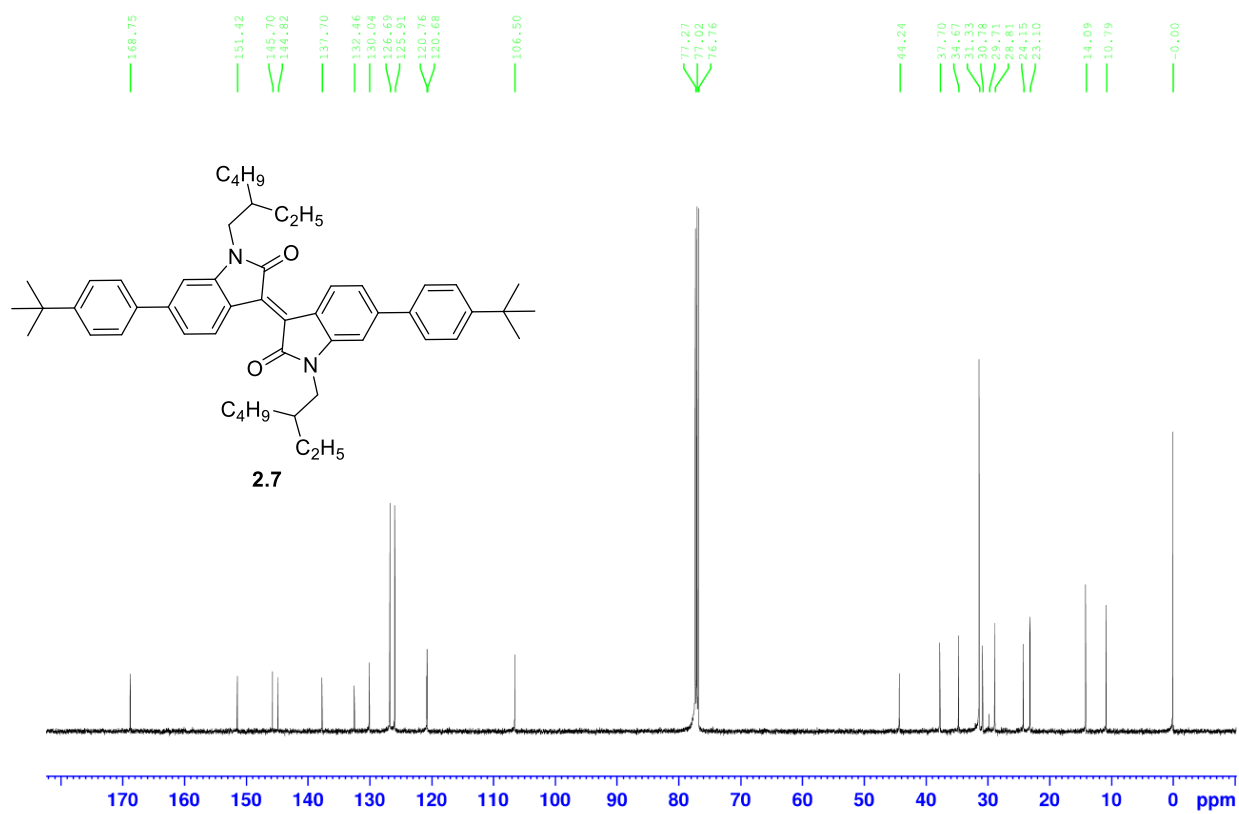
Figure 6.23. ^{13}C NMR of **2.7** in CDCl$_3$ at 125 MHz.
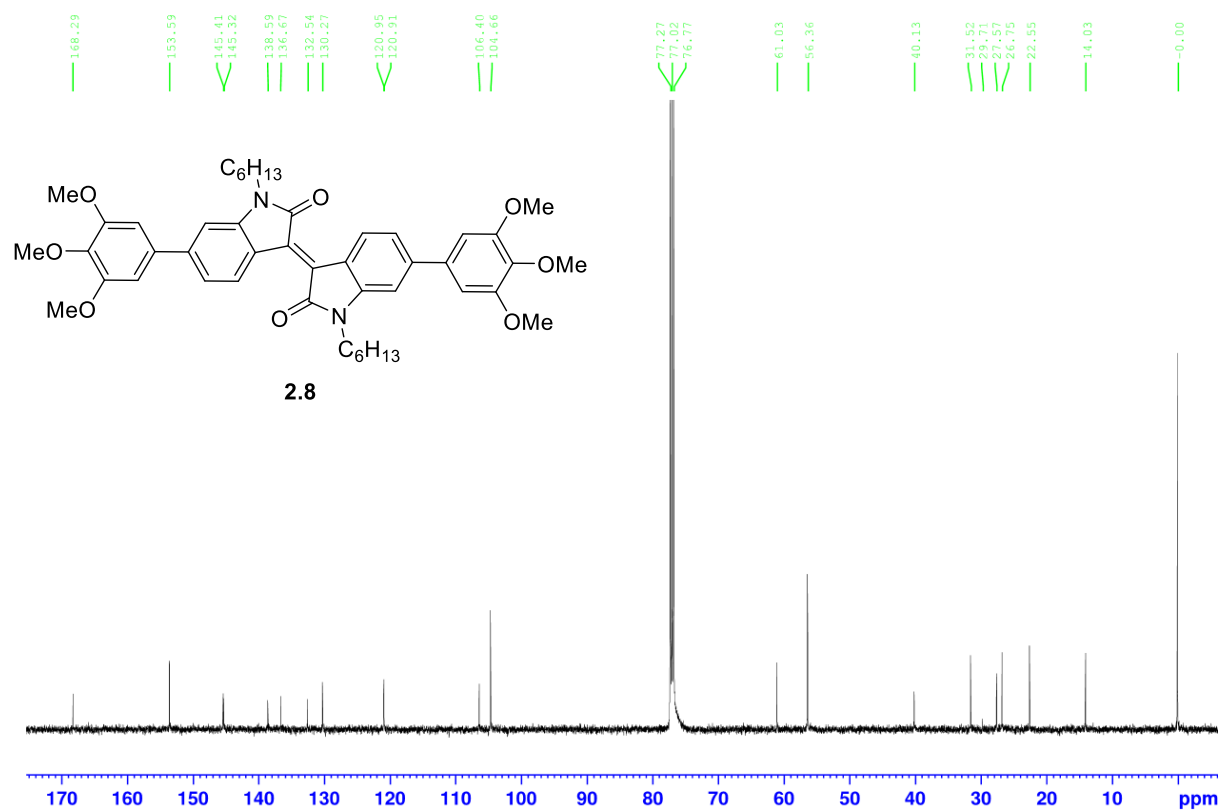
Figure 6.24. ^{13}C NMR of **2.8** in CDCl$_3$ at 125MHz.
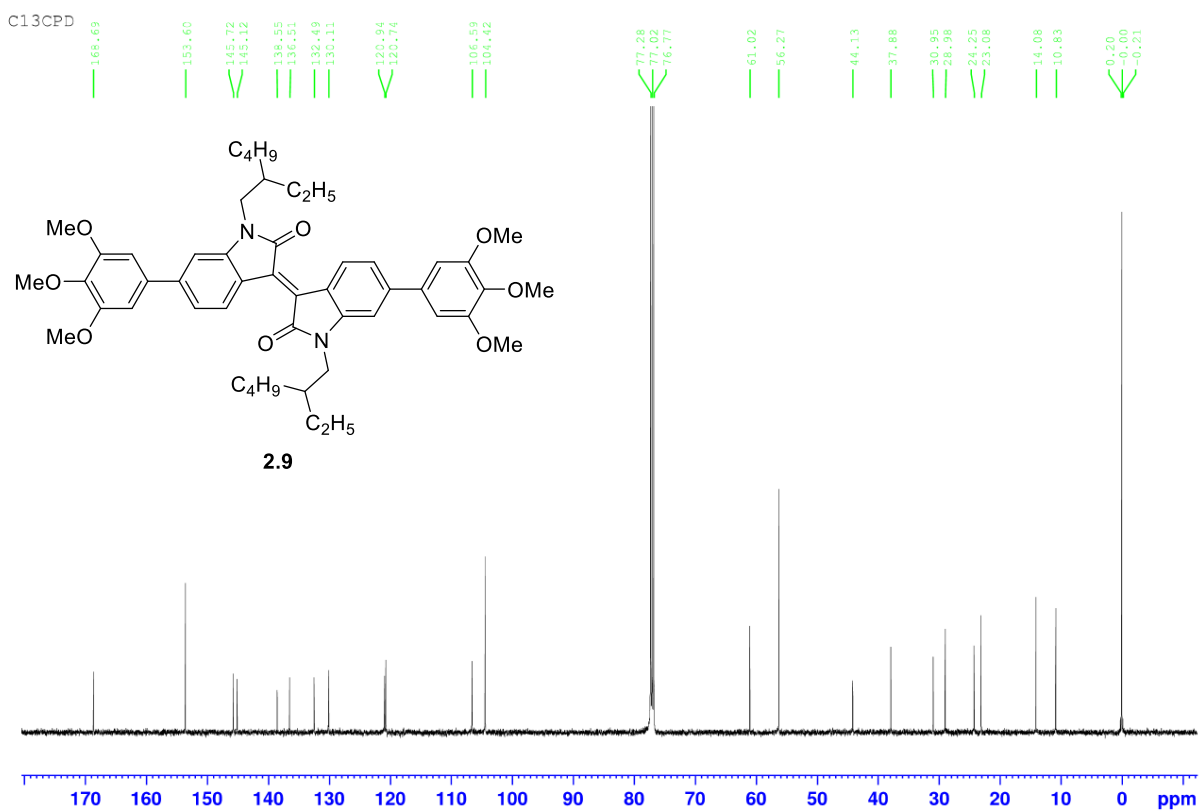
Figure 6.25. ^{13}C NMR of **2.9** in CDCl$_3$ at 125MHz.
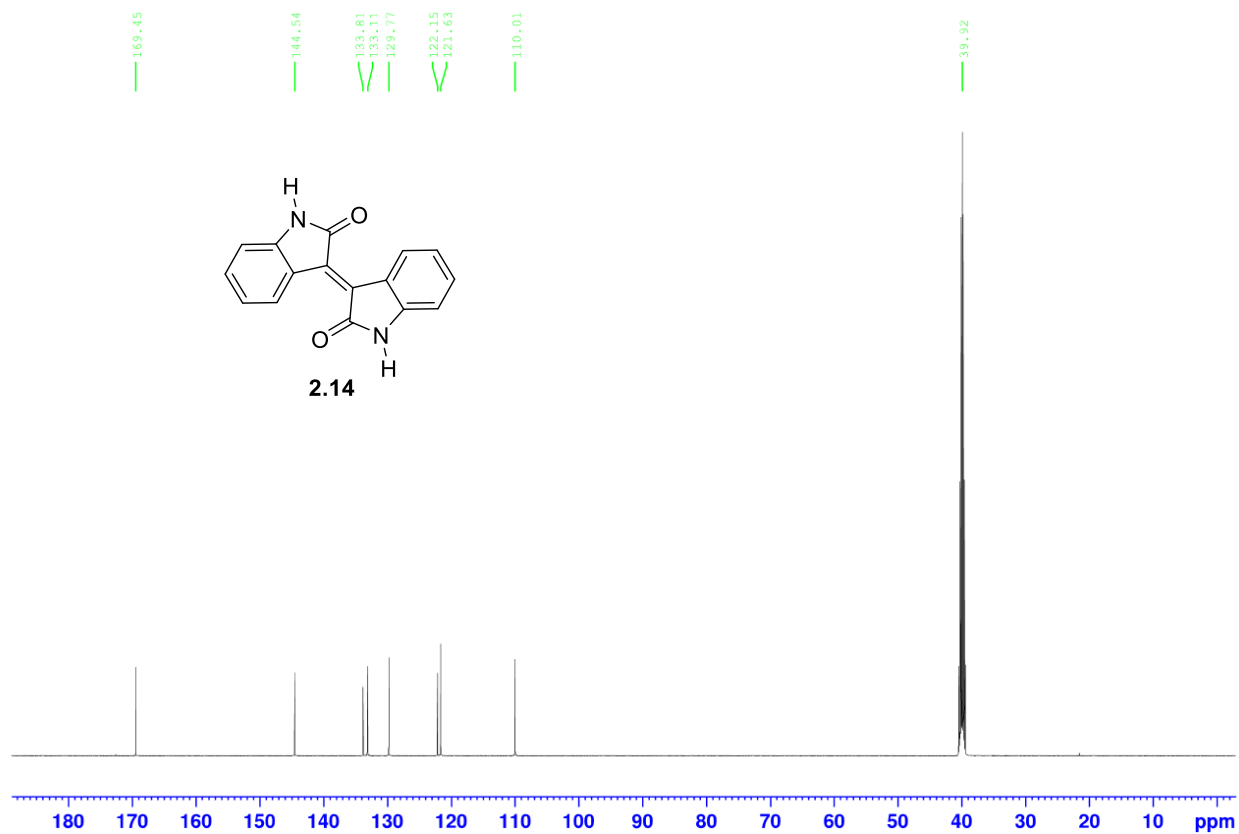
Figure 6.26. ^{13}C NMR of **2.14** in DMSO-d_6 at 125MHz.
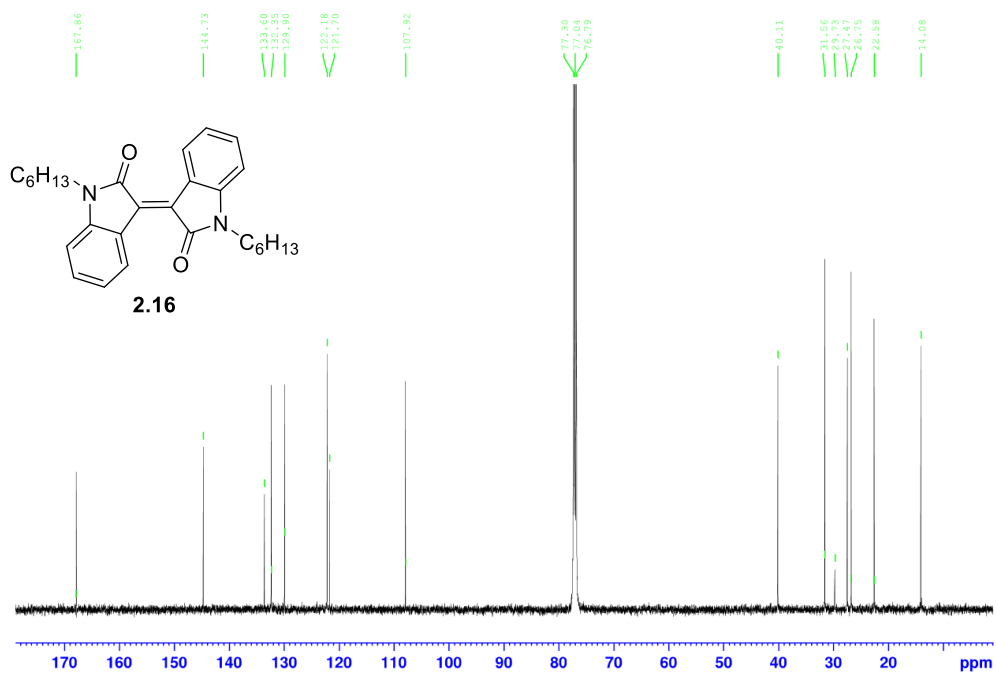
Figure 6.27. ^{13}C NMR of **2.16** in CDCl$_3$ at 125MHz.
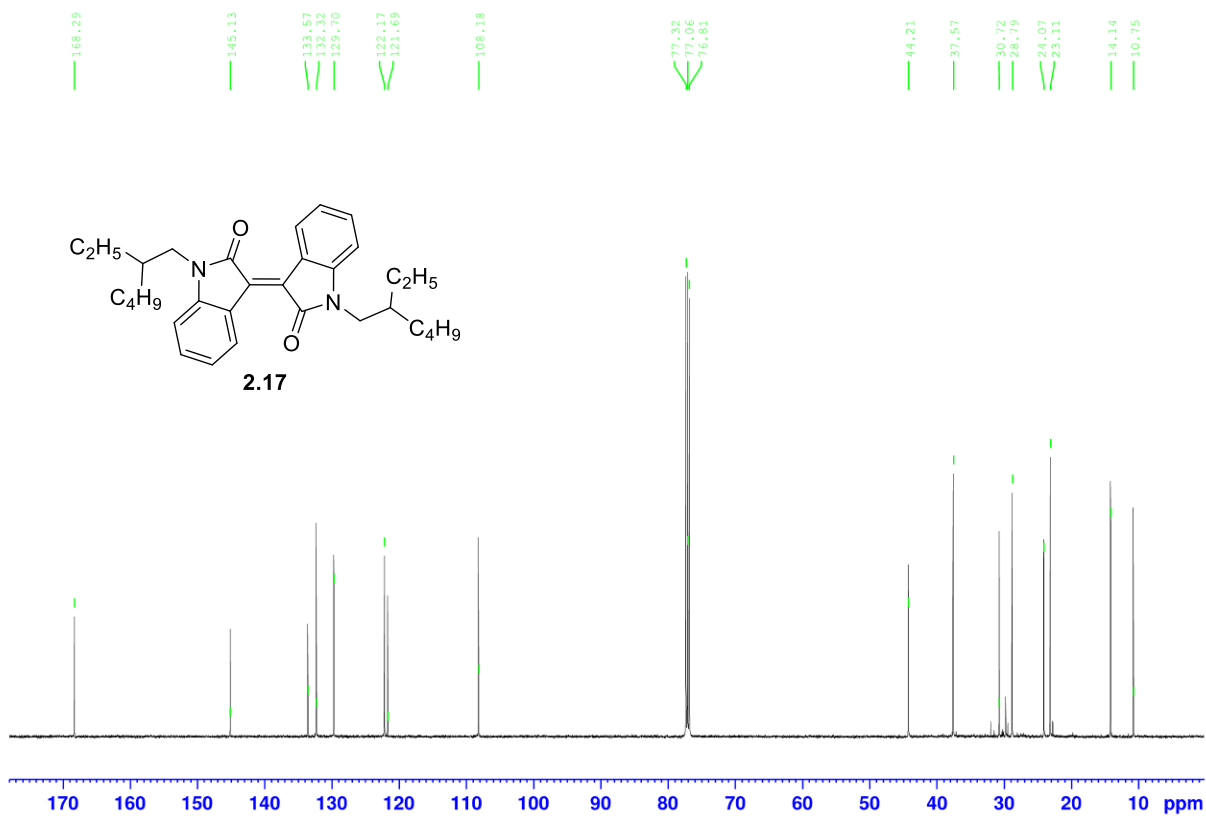
Figure 6.28. ^{13}C NMR of **2.17** in CDCl$_3$ at 125MHz.
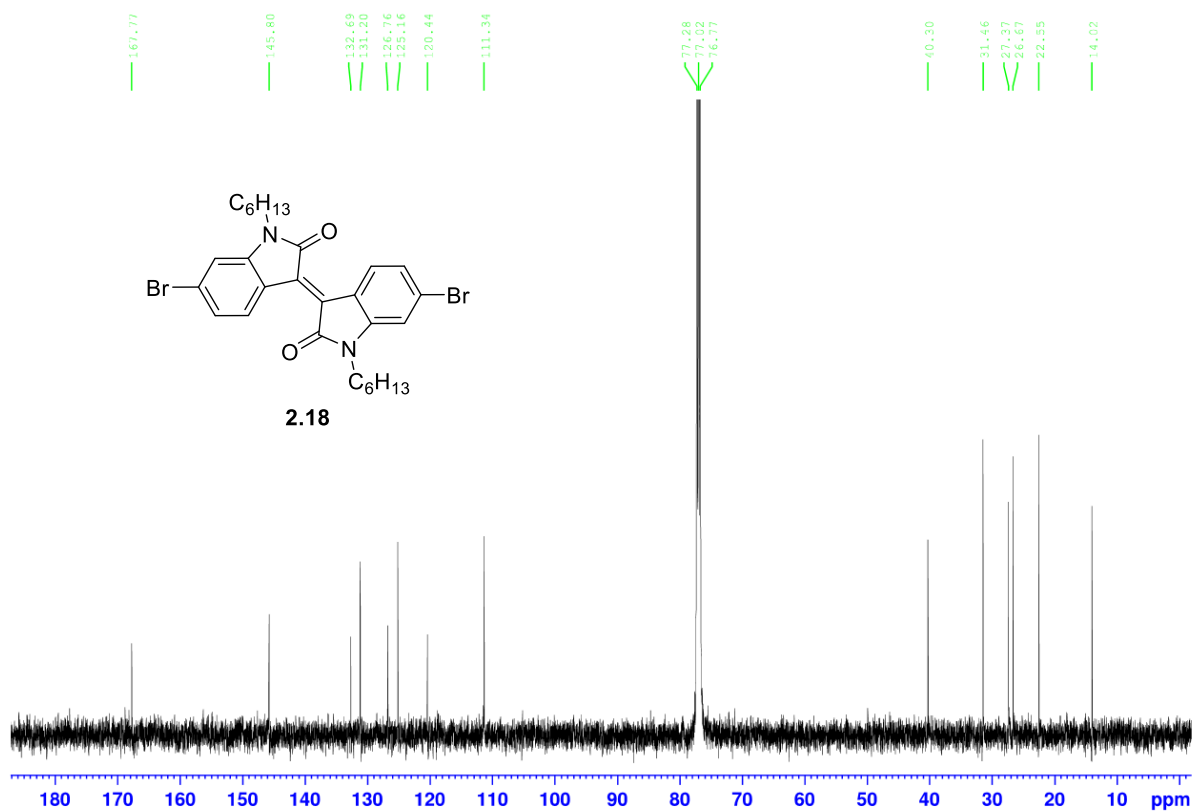
Figure 6.29. ^{13}C NMR of **2.18** in CDCl$_3$ at 125MHz.
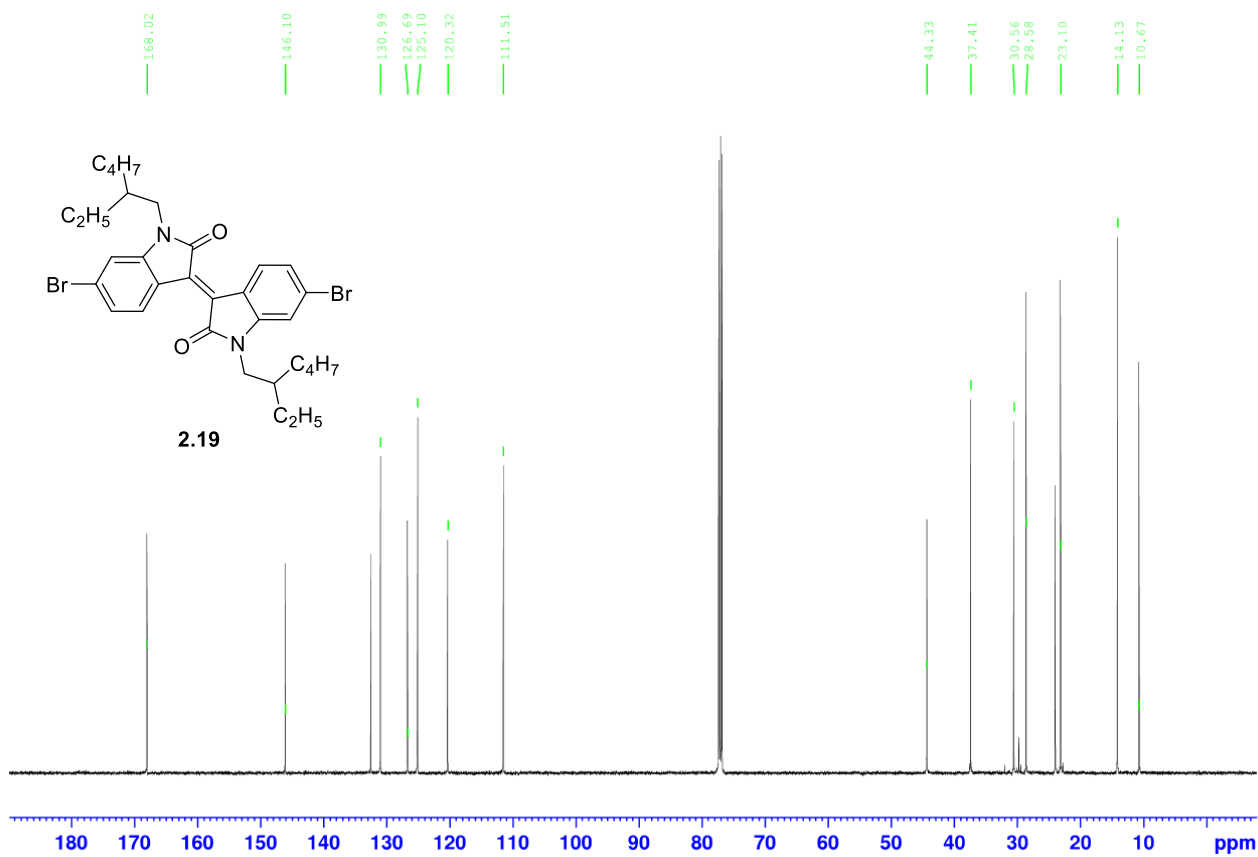
Figure 6.30. ^{13}C NMR of **2.19** in CDCl$_3$ at 125MHz.
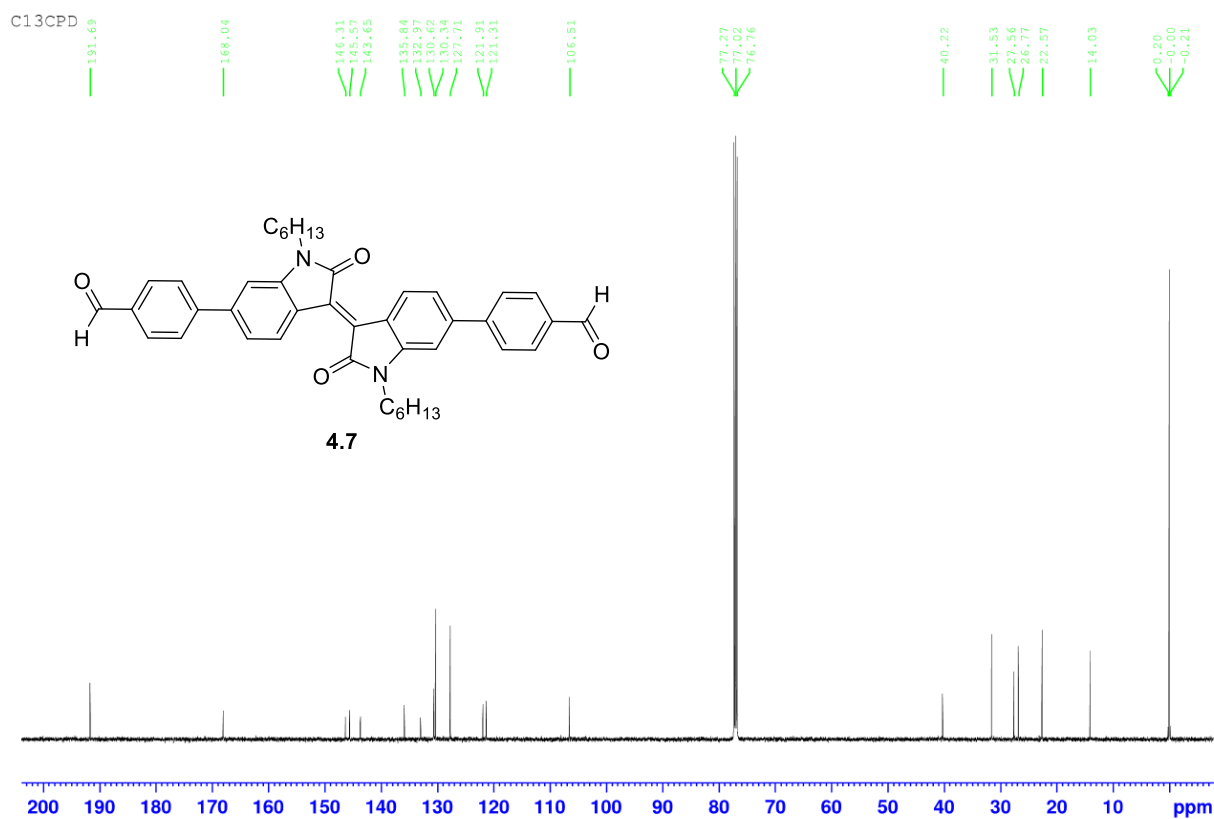
Figure 6.31. ^{13}C NMR of **4.7** in CDCl$_3$ at 125MHz.
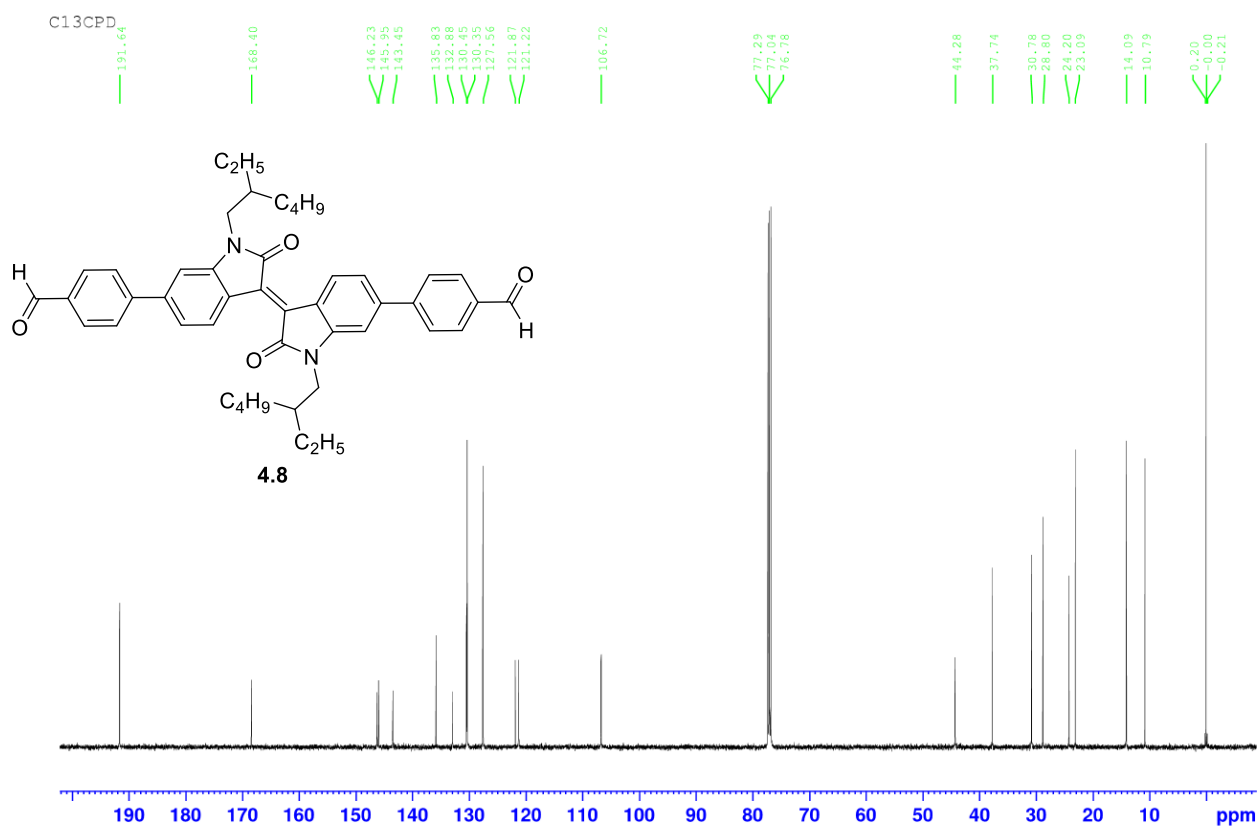
Figure 6.32. ^{13}C NMR of **4.8** in CDCl$_3$ at 125MHz.

Figure 6.33. ^{13}C NMR of **5.1** in CDCl$_3$ at 125MHz.
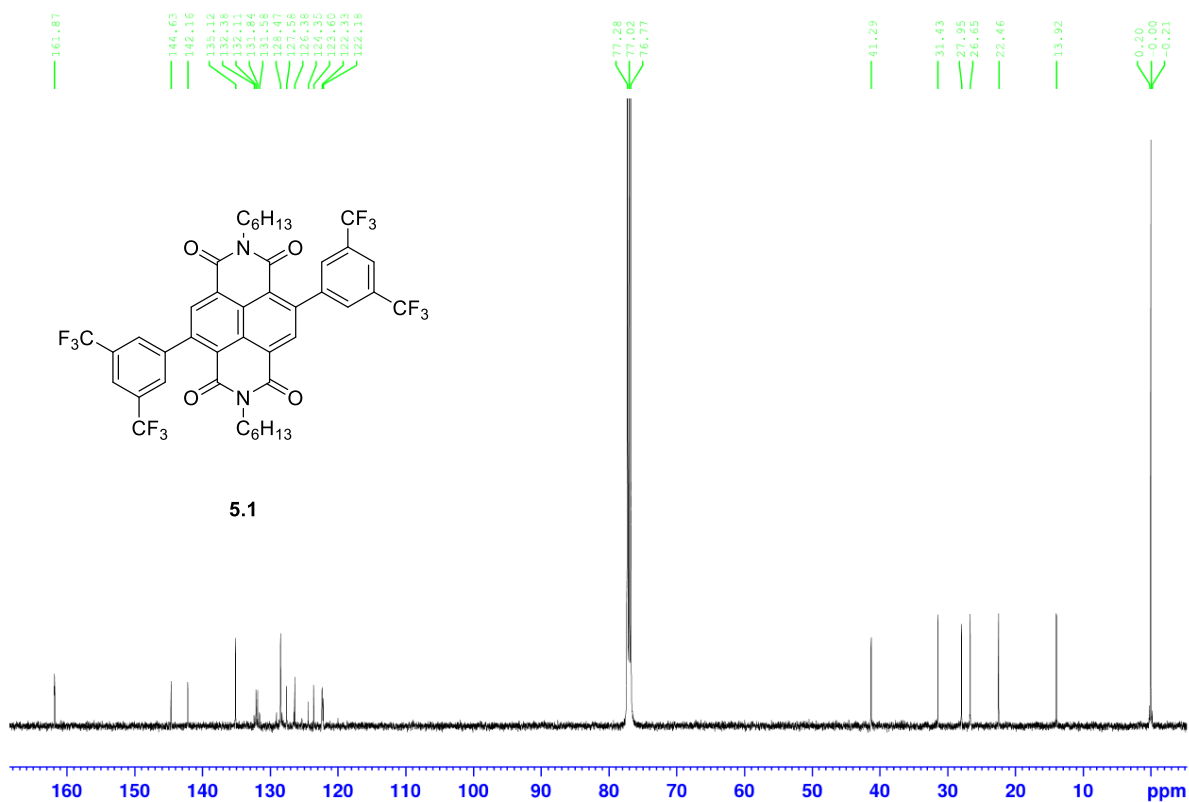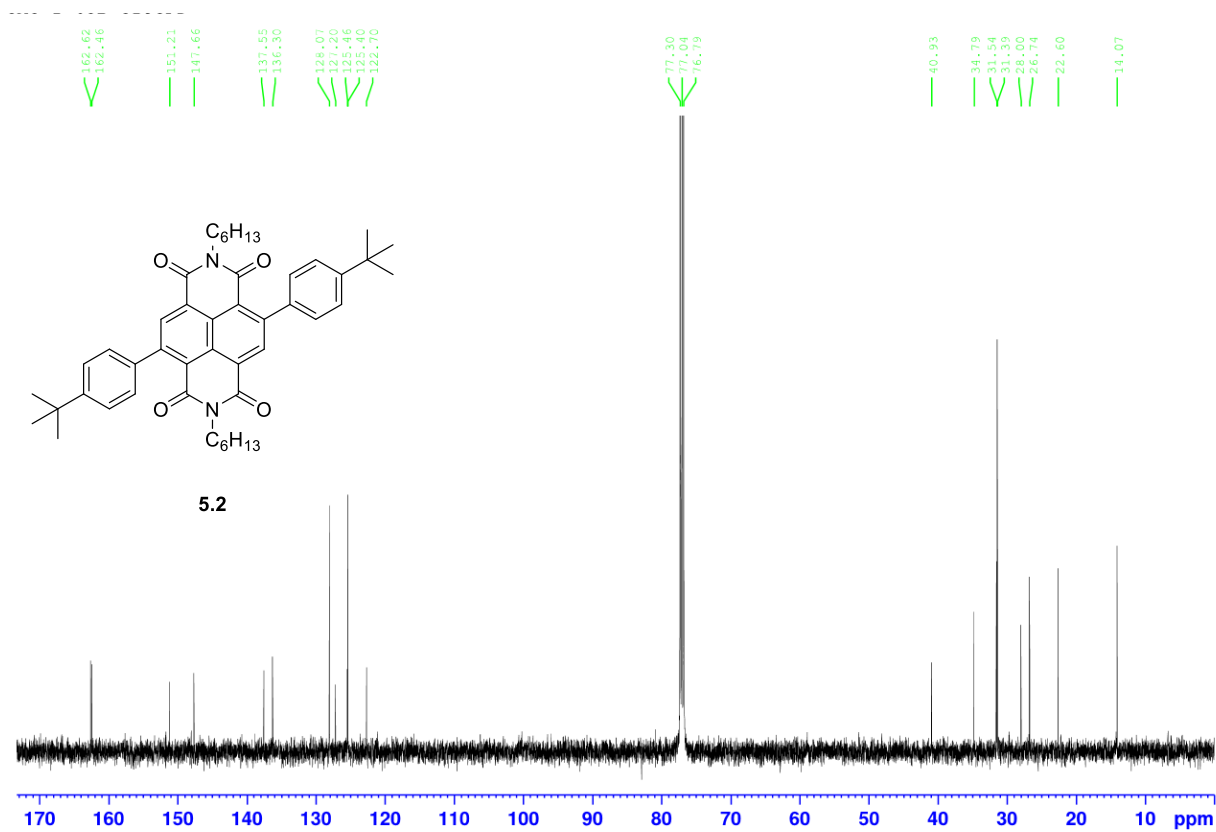
Figure 6.34. ^{13}C NMR of **5.2** in CDCl$_3$ at 125MHz.
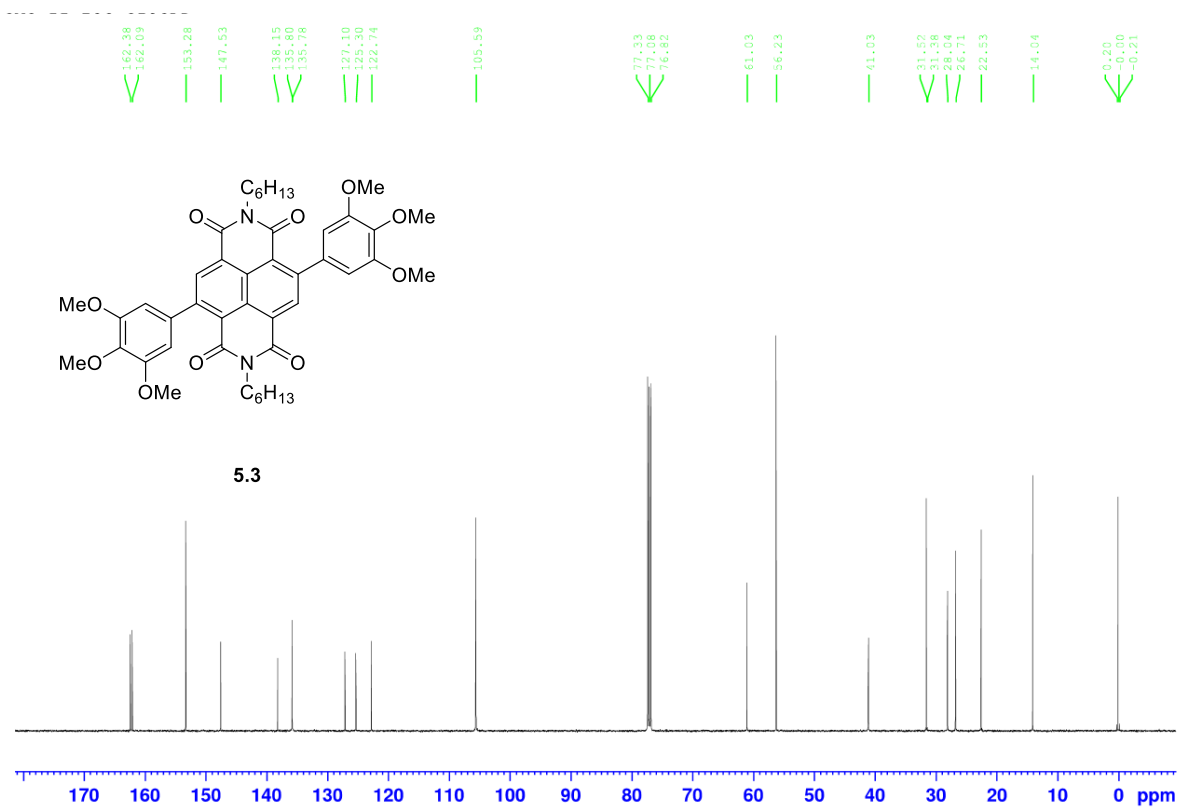
Figure 6.35. ^{13}C NMR of **5.3** in CDCl$_3$ at 125MHz.

APPENDIX C

ELEMENTAL ANALYSIS RESULTS

ATLANTIC MICROLAB, INC.

Sample No. CAC-I-53D

SUBMITTER

Company / School _____

6180 Atlantic Blvd. Suite M
Norcross, GA 30071

Dept _____ Chemistry

Address _____ American University of Beirut

www.atlanticmicrolab.com

City, St, Zip _____ Beirut 1107-2020, Lebanon

PROFESSOR/SUPERVISOR: Bilal Kaafarani

NAME _____ Bilal Kaafarani _____ DATE 8/16/18

PO# / CC#: _____

PHONE (961)-315-1451

Element	Theory	Found		Single ☑ Duplicate ☑
C	61.8300	61.94		Elements Present: C, H, F, N, O
H	4.4800	4.33		Analyze for: C, H, N
N	3.2800	3.27		Hygroscopic ☐ Explosive ☐ M.P. _____ B.P. _____
				To be dried: Yes ☑ No ☐ Temp. RT _____ Vac. _____ Time _____
				RUSH SERVICE ☐ Rush service guarantees analyses will be completed and results available by 5pm EST on the day the sample is received by 11am.
				Include Email Address or Fax # Below
				bilal.kaafarani@aub.edu.lb

Date Received _____ AUG 24 2018 _____ Date Completed _____ AUG 27 2018
Remarks:

Figure 6.36. Elemental analysis of compound **2.4**.

ATLANTIC MICROLAB, INC.

Sample No. CAC-II-33C

SUBMITTER

6180 Atlantic Blvd. Suite M
Norcross, GA 30071

www.atlanticmicrolab.com

PROFESSOR/SUPERVISOR: Bilal Kaafarani
PO# / CC#:

Company / School _____
Dept   Chemistry
Address   American University of Beirut
City, St, Zip   Beirut 1107-2020, Lebanon
NAME   Bilal Kaafarani   DATE 9/12/18
PHONE (961)-315-1451

Element	Theory	Found	
C	63.2900	63.54	
H	5.0900	5.12	
N	3.0800	3.03	

Single ☑   Duplicate ☑

Elements Present: C, H, F, N, O

Analyze for: C, H, N

Hygroscopic ☐   Explosive ☐
M.P. _____ B.P. _____

To be dried: Yes ☑   No ☐
Temp. RT _____ Vac. _____ Time _____

RUSH SERVICE ☐ Rush service guarantees analyses will be completed and results available by 5pm EST on the day the sample is received by 11am.

Include Email Address or Fax # Below

bilal.kaafarani@aub.edu.lb

Date Received   SEP 1 7 P.M.   Date Completed   SEP 18 2018
Remarks:

Figure 6.37. Elemental analysis of compound **2.5**.

ATLANTIC MICROLAB, INC.

Sample No. CAC-I-50B

SUBMITTER

Company / School _____

6180 Atlantic Blvd. Suite M
Norcross, GA 30071

Dept ___Chemistry___

Address ___American University of Beirut___

City, St, Zip ___Beirut 1107-2020, Lebanon___

www.atlanticmicrolab.com

PROFESSOR/SUPERVISOR: Bilal Kaafarani

PO# / CC#: _____

NAME ___Bilal Kaafarani___ DATE ___2/8/18___

PHONE (961)-315-1451

Element	Theory	Found		Single ☑ Duplicate ☐
C	82.9500	82.66		Elements Present: C, H, N, O
H	8.4100	8.56		Analyze for: C, H, N
N	4.0300	3.88		Hygroscopic ☐ Explosive ☐ M.P. _____ B.P. _____
				To be dried: Yes ☑ No ☐ Temp. RT Vac. _____ Time _____
				RUSH SERVICE ☐ Rush service guarantees analyses will be completed and results available by 5pm EST on the day the sample is received by 11am.
				Include Email Address or Fax # Below
				bilal.kaafarani@aub.edu.lb

Date Received FEB 13 2018 Date Completed FEB 14 2018

Remarks:

Figure 6.38. Elemental analysis of compound **2.6**.

ATLANTIC MICROLAB, INC.

Sample No. CAC-I-95C

SUBMITTER

| 6180 Atlantic Blvd. Suite M |
| Norcross, GA 30071 |

www.atlanticmicrolab.com

PROFESSOR/SUPERVISOR: Bilal Kaafarani

PO# / CC#: _____

Company / School _____
Dept: Chemistry
Address: American University of Beirut
City, St, Zip: Beirut 1107-2020, Lebanon
NAME: Bilal Kaafarani _____ DATE 7/4/18
PHONE (961)-315-1451

Element	Theory	Found		Single ☑ Duplicate ☐
C	83.1500	83.23		Elements Present: C, H, N, O
H	8.8600	9.01		Analyze for: C, H, N
N	3.7300	3.60		Hygroscopic ☐ Explosive ☐ M.P. _____ B.P. _____
				To be dried: Yes ☑ No ☐ Temp. RT Vac. ____ Time ____
				RUSH SERVICE ☐ Rush service guarantees analyses will be completed and results available by 5pm EST on the day the sample is received by 11am.
				Include Email Address or Fax # Below
				bilal.kaafarani@aub.edu.lb

Date Received ____ JUL 10 2018 ____ Date Completed ____ JUL 13 2018 ____

Remarks:

Figure 6.39. Elemental analysis of compound **2.7**.

ATLANTIC MICROLAB, INC.

Sample No. CAC-I-99C

SUBMITTER

6180 Atlantic Blvd. Suite M
Norcross, GA 30071

www.atlanticmicrolab.com

PROFESSOR/SUPERVISOR: Bilal Kaafarani
PO# / CC#:

Company / School
Dept   Chemistry
Address   American University of Beirut
City, St, Zip   Beirut 1107-2020, Lebanon
NAME   Bilal Kaafarani   DATE   7/4/18
PHONE (961)-315-1451

Element	Theory	Found		Single ☑ Duplicate ☐
C	72.4200	72.71		Elements Present: C, H, N, O
H	7.1300	7.41		Analyze for: C, H, N
N	3.6700	3.49		Hygroscopic ☐ Explosive ☐ M.P. _____ B.P. _____
				To be dried: Yes ☑ No ☐ Temp. RT ____Vac. ____Time ____
				RUSH SERVICE ☐ Rush service guarantees analyses will be completed and results available by 5pm EST on the day the sample is received by 11am.
				Include Email Address or Fax # Below
				bilal.kaafarani@aub.edu.lb

Date Received _____ JUL 10 2018 _____   Date Completed _____ JUL 11 2018 _____
Remarks:

Figure 6.40. Elemental analysis of compound **2.8**.

ATLANTIC MICROLAB, INC.

Sample No. CAC-I-97E

SUBMITTER

Company / School _____

| 6180 Atlantic Blvd. Suite M |
| Norcross, GA 30071 |

Dept ___ Chemistry

Address ___ American University of Beirut

City, St, Zip ___ Beirut 1107-2020, Lebanon

www.atlanticmicrolab.com

PROFESSOR/SUPERVISOR: Bilal Kaafarani

PO# / CC#: _____

NAME ___ Bilal Kaafarani ___ DATE 8/16/18

PHONE (961)-315-1451

Element	Theory	Found	
C	73.3200	73.28	
H	7.6300	7.68	
N	3.4200	3.45	

Single ☑   Duplicate ☐

Elements Present: C, H, N, O

Analyze for: C, H, N

Hygroscopic ☐   Explosive ☐
M.P. _____ B.P. _____

To be dried: Yes ☑   No ☐
Temp. RT _____ Vac. _____ Time _____

RUSH SERVICE ☐ Rush service guarantees analyses will be completed and results available by 5pm EST on the day the sample is received by 11am.

Include Email Address or Fax # Below

bilal.kaafarani@aub.edu.lb

Date Received ___ AUG 24 2018 ___ Date Completed ___ AUG 27 2018

Remarks:

Figure 6.41. Elemental analysis of compound **2.9**.

ATLANTIC MICROLAB, INC.

Sample No. CAC-I-69B

SUBMITTER

6180 Atlantic Blvd. Suite M
Norcross, GA 30071

www.atlanticmicrolab.com

PROFESSOR/SUPERVISOR: Bilal Kaafarani

PO# / CC#: _____

Company / School _____

Dept: Chemistry

Address: American University of Beirut

City, St, Zip: Beirut 1107-2020, Lebanon

NAME: Bilal Kaafarani — DATE: 2/8/18

PHONE (961)-315-1451

Element	Theory	Found	
C	78.9700	79.18	
H	8.7000	8.89	
N	5.7600	5.51	

Single ☑   Duplicate ☐

Elements Present: C, H, N, O

Analyze for: C, H, N

Hygroscopic ☐   Explosive ☐
M.P. _____   B.P. _____

To be dried: Yes ☑   No ☐
Temp. RT _____ Vac. _____ Time _____

RUSH SERVICE ☐ Rush service guarantees analyses will be completed and results available by 5pm EST on the day the sample is received by 11am.

Include Email Address or Fax # Below

bilal.kaafarani@aub.edu.lb

Date Received FEB 13 2018   Date Completed FEB 14 2018

Remarks:

Figure 6.42. Elemental analysis of compound **2.17**.

\

ATLANTIC MICROLAB, INC.

Sample No. CAC-II-18D

SUBMITTER

Company / School _____

6180 Atlantic Blvd. Suite M
Norcross, GA 30071

Dept _____Chemistry_____

Address _American University of Beirut_____

www.atlanticmicrolab.com

City, St, Zip _Beirut 1107-2020, Lebanon____

PROFESSOR/SUPERVISOR: Bilal Kaafarani

NAME _Bilal Kaafarani_____ DATE 8/16/18

PO# / CC#: _____

PHONE (961)-315-1451

Element	Theory	Found	
C	78.9700	78.93	
H	6.6300	6.55	
N	4.3900	4.37	

Single ☑ Duplicate ☑

Elements Present: C, H, N, O

Analyze for: C, H, N

Hygroscopic ☐ Explosive ☐
M.P. _____ B.P. _____

To be dried: Yes ☑ No ☐
Temp. RT____ Vac. _____ Time ____

RUSH SERVICE ☐ Rush service guarantees analyses will be completed and results available by 5pm EST on the day the sample is received by 11am.

Include Email Address or Fax # Below

bilal.kaafarani@aub.edu.lb

Date Received ___AUG 24 2018___ Date Completed ___AUG 27 2018___

Remarks:

Figure 6.43. Elemental analysis of compound **4.7**.

ATLANTIC MICROLAB, INC.

Sample No. CAC-II-17C

6180 Atlantic Blvd. Suite M
Norcross, GA 30071

www.atlanticmicrolab.com

PROFESSOR/SUPERVISOR: Bilal Kaafarani

PO# / CC#:

SUBMITTER

Company / School _____

Dept _____ Chemistry

Address _____ American University of Beirut

City, St, Zip _____ Beirut 1107-2020, Lebanon

NAME _____ Bilal Kaafarani _____ DATE 8/16/18

PHONE (961)-315-1451

Element	Theory	Found	
C	79.5100	79.36	
H	7.2500	7.41	
N	4.0300	4.04	

Single ☑   Duplicate ☑

Elements Present: C, H, N, O

Analyze for: C, H, N

Hygroscopic ☐   Explosive ☐
M.P. _____ B.P. _____

To be dried: Yes ☑ No ☐
Temp. RT _____ Vac. _____ Time _____

RUSH SERVICE ☐ Rush service guarantees analyses will be completed and results available by 5pm EST on the day the sample is received by 11am.

Include Email Address or Fax # Below

bilal.kaafarani@aub.edu.lb

Date Received **AUG 24 2018**   Date Completed **AUG 27 2018**

Remarks:

Figure 6.44. Elemental analysis of compound **4.8**.

ATLANTIC MICROLAB, INC.

SUBMITTER

Sample No. CAC-II-14C

6180 Atlantic Blvd. Suite M
Norcross, GA 30071

www.atlanticmicrolab.com

PROFESSOR/SUPERVISOR: Bilal Kaafarani

PO# / CC#: _____

Company / School _____

Dept _____ Chemistry

Address _____ American University of Beirut

City, St, Zip _____ Beirut 1107-2020, Lebanon

NAME Bilal Kaafarani _____ DATE 8/16/18

PHONE (961)-315-1451

Element	Theory	Found	
C	58.7500	58.91	
H	3.9900	3.88	
N	3.2600	3.30	

Single ☑   Duplicate ☑

Elements Present: C, H, F, N, O

Analyze for: C, H, N

Hygroscopic ☐   Explosive ☐
M.P. _____ B.P. _____

To be dried: Yes ☑   No ☐
Temp. RT _____ Vac. _____ Time _____

RUSH SERVICE ☐ Rush service guarantees analyses will be completed and results available by 5pm EST on the day the sample is received by 11am.

Include Email Address or Fax # Below

bilal.kaafarani@aub.edu.lb

Date Received **AUG 24 2018** _____ Date Completed **AUG 27 2018**

Remarks:

Figure 6.45. Elemental analysis of compound **5.1**.

ATLANTIC MICROLAB, INC.

SUBMITTER

Sample No. CAC-I-65B

6180 Atlantic Blvd. Suite M
Norcross, GA 30071

www.atlanticmicrolab.com

PROFESSOR/SUPERVISOR: Bilal Kaafarani

PO# / CC#:

Company / School _____

Dept _____Chemistry_____

Address _American University of Beirut_

City, St, Zip _Beirut 1107-2020, Lebanon_

NAME _Bilal Kaafarani_ DATE _2/8/18_

PHONE _(961)-315-1451_

Element	Theory	Found	
C	79.0500	79.03	
H	7.7900	8.01	
N	4.0100	3.91	

Single ☑   Duplicate ☐

Elements Present: C, H, N, O

Analyze for: C, H, N

Hygroscopic ☐   Explosive ☐
M.P. _____ B.P. _____

To be dried: Yes ☑ No ☐
Temp. RT _____ Vac. _____ Time _____

RUSH SERVICE ☐ Rush service guarantees analyses will be completed and results available by 5pm EST on the day the sample is received by 11am.

Include Email Address or Fax # Below

bilal.kaafarani@aub.edu.lb

Date Received FEB 13 2018   Date Completed FEB 14 2018

Remarks:

Figure 6.46. Elemental analysis of compound **5.2**.

ATLANTIC MICROLAB, INC.

Sample No. CAC-II-25C

SUBMITTER

6180 Atlantic Blvd. Suite M
Norcross, GA 30071

www.atlanticmicrolab.com

PROFESSOR/SUPERVISOR: Bilal Kaafarani
PO# / CC#: _____

Company / School _____
Dept   Chemistry
Address American University of Beirut
City, St, Zip Beirut 1107-2020, Lebanon
NAME Bilal Kaafarani   DATE 9/12/18
PHONE (961)-315-1451

Element	Theory	Found			
C	68.9100	68.88		Single ☑ Duplicate ☑	
				Elements Present: C, H, N, O	
H	6.5700	6.51		Analyze for: C, H, N	
N	3.6500	3.62		Hygroscopic ☐ Explosive ☐ M.P. _____ B.P. _____	
				To be dried: Yes ☑ No ☐ Temp. RT ____ Vac. ____ Time ____	
				RUSH SERVICE ☐ Rush service guarantees analyses will be completed and results available by 5pm EST on the day the sample is received by 11am.	
				Include Email Address or Fax # Below	
				bilal.kaafarani@aub.edu.lb	

Date Received **SEP 1 7 P.M.**   Date Completed **SEP 18 2018**

Remarks:

Figure 6.47. Elemental analysis of compound **5.3**.

REFERENCES

(1)   Forrest, S. R.; Thompson, M. E. *Chemical Reviews* **2007**, *107*, 923.

(2)   Forrest, S. R. *Nature* **2004**, *428*, 911.

(3)   Sekitani, T.; Someya, T. *Advanced Materials* **2010**, *22*, 2228.

(4)   Dou, L.; Liu, Y.; Hong, Z.; Li, G.; Yang, Y. *Chemical reviews* **2015**, *115*, 12633.

(5)   Müllen, K.; Scherf, U. *Organic light emitting devices: synthesis, properties and applications*; John Wiley & Sons, 2006.

(6)   Kippelen, B.; Brédas, J.-L. *Energy & Environmental Science* **2009**, *2*, 251.

(7)   Horowitz, G. *Advanced materials* **1998**, *10*, 365.

(8)   Bernards, D. A.; Owens, R. M.; Malliaras, G. G. **2008**.

(9)   Mustroph, H.; Stollenwerk, M.; Bressau, V. *Angewandte Chemie International Edition* **2006**, *45*, 2016.

(10)   Fahrenbach, A. C.; Warren, S. C.; Incorvati, J. T.; Avestro, A. J.; Barnes, J. C.; Stoddart, J. F.; Grzybowski, B. A. *Advanced Materials* **2013**, *25*, 331.

(11)   Brédas, J.-L.; Calbert, J. P.; da Silva Filho, D.; Cornil, J. *Proceedings of the National Academy of Sciences* **2002**, *99*, 5804.

(12)   Facchetti, A. *Nature materials* **2013**, *12*, 598.

(13)   Pope, M.; Swenberg, C. E. *Electronic processes in organic crystals and polymers*; Oxford University Press New York, 1999; Vol. 2.

(14)   Roncali, J.; Leriche, P.; Cravino, A. *Advanced materials* **2007**, *19*, 2045.

(15)   Sun, Y.; Welch, G. C.; Leong, W. L.; Takacs, C. J.; Bazan, G. C.; Heeger, A. J. *Nature materials* **2012**, *11*, 44.

(16)   Li, S.; Zhang, Z.; Shi, M.; Li, C.-Z.; Chen, H. *Physical Chemistry Chemical Physics* **2017**, *19*, 3440.

(17)   Zhou, J.; Zuo, Y.; Wan, X.; Long, G.; Zhang, Q.; Ni, W.; Liu, Y.; Li, Z.; He, G.; Li, C. *Journal of the American Chemical Society* **2013**, *135*, 8484.

(18)   Kaafarani, B. R.; Lucas, L. A.; Wex, B.; Jabbour, G. E. *Tetrahedron letters* **2007**, *48*, 5995.

(19)   Shirota, Y.; Kageyama, H. *Chemical reviews* **2007**, *107*, 953.

(20)   Fichou, D. *Journal of Materials Chemistry* **2000**, *10*, 571.

(21)   Kaafarani, B. R. *Chemistry of Materials* **2010**, *23*, 378.

(22)   Kumar, S. *Chemical Society Reviews* **2006**, *35*, 83.

(23)   Ponomarenko, S. A.; Kirchmeyer, S.; Elschner, A.; Huisman, B. H.; Karbach, A.; Drechsler, D. *Advanced Functional Materials* **2003**, *13*, 591.

(24)   Li, W.; Roelofs, W. C.; Wienk, M. M.; Janssen, R. A. *Journal of the American Chemical Society* **2012**, *134*, 13787.

(25)   Cui, W.; Wudl, F. *Macromolecules* **2013**, *46*, 7232.

(26)   Yang, J.; Xiao, B.; Tajima, K.; Nakano, M.; Takimiya, K.; Tang, A.; Zhou, E. *Macromolecules* **2017**, *50*, 3179.

(27)   Earmme, T.; Hwang, Y.-J.; Murari, N. M.; Subramaniyan, S.; Jenekhe, S. A. *Journal of the American Chemical Society* **2013**, *135*, 14960.

(28)   Wang, E.; Mammo, W.; Andersson, M. R. *Advanced Materials* **2014**, *26*, 1801.

(29)   Dasari, R. R.; Dindar, A.; Lo, C. K.; Wang, C.-Y.; Quinton, C.; Singh, S.; Barlow, S.; Fuentes-Hernandez, C.; Reynolds, J. R.; Kippelen, B. *Physical Chemistry Chemical Physics* **2014**, *16*, 19345.

(30)   Wuerthner, F.; Ahmed, S.; Thalacker, C.; Debaerdemaeker, T. *Chemistry-A European Journal* **2002**, *8*, 4742.

(31)   Sakai, N.; Mareda, J.; Vauthey, E.; Matile, S. *Chemical Communications* **2010**, *46*, 4225.

(32)   Bhosale, S. V.; Bhosale, S. V.; Bhargava, S. K. *Organic & biomolecular chemistry* **2012**, *10*, 6455.

(33)   Bhosale, S. V.; Jani, C. H.; Langford, S. J. *Chemical Society Reviews* **2008**, *37*, 331.

(34)   Gao, X.; Di, C.-a.; Hu, Y.; Yang, X.; Fan, H.; Zhang, F.; Liu, Y.; Li, H.; Zhu, D. *Journal of the American Chemical Society* **2010**, *132*, 3697.

(35)   Durban, M. M.; Kazarinoff, P. D.; Luscombe, C. K. *Macromolecules* **2010**, *43*, 6348.

(36)   Mishra, A.; Bäuerle, P. *Angewandte Chemie International Edition* **2012**, *51*, 2020.

(37)   Günes, S.; Neugebauer, H.; Sariciftci, N. S. *Chemical reviews* **2007**, *107*, 1324.

(38)   Sirringhaus, H. *Advanced materials* **2014**, *26*, 1319.

(39)   Li, H.; Shi, W.; Song, J.; Jang, H.-J.; Dailey, J.; Yu, J.; Katz, H. E. *Chemical reviews* **2018**, *119*, 3.

(40)   Wang, N.; Yang, A.; Fu, Y.; Li, Y.; Yan, F. *Accounts of chemical research* **2019**.

(41)   Gelinck, G.; Heremans, P.; Nomoto, K.; Anthopoulos, T. D. *Advanced materials* **2010**, *22*, 3778.

(42)   Lilienfeld, J. E. *US patent* **1930**, *1*, 175.

(43)   Millman, J. *Electronic Devices and Circuits [by] Jacob Millman [and] Christos C. Halkias*; McGraw-Hill, 1967.

(44)   Di, C.-A.; Liu, Y.; Yu, G.; Zhu, D. *Accounts of chemical research* **2009**, *42*, 1573.

(45)   Sze, S. M.; Ng, K. K. *Physics of semiconductor devices*; John wiley & sons, 2006.

(46)   Sokolov, A. N.; Roberts, M. E.; Bao, Z. *Materials today* **2009**, *12*, 12.

(47)   Di, C. a.; Zhang, F.; Zhu, D. *Advanced Materials* **2013**, *25*, 313.

(48)   Allard, S.; Forster, M.; Souharce, B.; Thiem, H.; Scherf, U. *Angewandte Chemie International Edition* **2008**, *47*, 4070.

(49)   Coulson, D.; Satek, L.; Grim, S. *Inorganic Syntheses: Reagents for Transition Metal Complex and Organometallic Syntheses* **1990**, *28*, 107.

(50)   Meredith, P.; Bettinger, C.; Irimia-Vladu, M.; Mostert, A.; Schwenn, P. *Reports on Progress in Physics* **2013**, *76*, 034501.

(51)   Głowacki, E. D.; Voss, G.; Sariciftci, N. S. *Advanced Materials* **2013**, *25*, 6783.

(52)   Clark, R. J.; Cooksey, C. J.; Daniels, M. A.; Withnall, R. *Endeavour* **1993**, *17*, 191.

(53)   Maugard, T.; Enaud, E.; Choisy, P.; Legoy, M. D. *Phytochemistry* **2001**, *58*, 897.

(54)   Papageorgiou, C.; Borer, X. *Helvetica chimica acta* **1988**, *71*, 1079.

(55)   Bogdanov, A. V.; Musin, L. I.; Mironov, V. F. *ARKIVOC: Online Journal of Organic Chemistry* **2015**, *2015*.

(56)   Vine, K.; Matesic, L.; Locke, J.; Ranson, M.; Skropeta, D. *Anti-Cancer Agents in Medicinal Chemistry (Formerly Current Medicinal Chemistry-Anti-Cancer Agents)* **2009**, *9*, 397.

(57)   Wee, X. K.; Yeo, W. K.; Zhang, B.; Tan, V. B.; Lim, K. M.; Tay, T. E.; Go, M.-L. *Bioorganic & medicinal chemistry* **2009**, *17*, 7562.

(58)   Lee, C.-C.; Lin, C.-P.; Lee, Y.-L.; Wang, G.-C.; Cheng, Y.-C.; Liu, H. E. *Leukemia & lymphoma* **2010**, *51*, 897.

(59)   Xiao, Z.; Wang, Y.; Lu, L.; Li, Z.; Peng, Z.; Han, Z.; Hao, Y. *Leukemia research* **2006**, *30*, 54.

(60)   Mei, J.; Graham, K. R.; Stalder, R.; Reynolds, J. R. *Organic letters* **2010**, *12*, 660.

(61)   Ren, Y.; Hiszpanski, A. M.; Whittaker-Brooks, L.; Loo, Y.-L. *ACS applied materials & interfaces* **2014**, *6*, 14533.

(62)   Estrada, L. A.; Stalder, R.; Abboud, K. A.; Risko, C.; Brédas, J.-L.; Reynolds, J. R. *Macromolecules* **2013**, *46*, 8832.

(63)   Elsawy, W.; Kang, H.; Yu, K.; Elbarbary, A.; Lee, K.; Lee, J. S. *Journal of Polymer Science Part A: Polymer Chemistry* **2014**, *52*, 2926.

(64)   Elsawy, W.; Lee, C.-L.; Cho, S.; Oh, S.-H.; Moon, S.-H.; Elbarbary, A.; Lee, J.-S. *Physical Chemistry Chemical Physics* **2013**, *15*, 15193.

(65)   Haines, P. J. *Thermal methods of analysis: principles, applications and problems*; Springer Science & Business Media, 2012.

(66)   Coats, A.; Redfern, J. *Analyst* **1963**, *88*, 906.

(67)   Ma, W.; Yang, C.; Gong, X.; Lee, K.; Heeger, A. J. *Advanced Functional Materials* **2005**, *15*, 1617.

(68)   Pungor, E.; Horvai, G. *A practical guide to instrumental analysis*; CRC press, 1994.

(69)   Jensen, F. *Introduction to computational chemistry*; John wiley & sons, 2017.

(70)   Lewars, E. *Introduction to the theory and applications of molecular and quantum mechanics* **2003**, 318.

(71)   Lin, J.-H.; Perryman, A. L.; Schames, J. R.; McCammon, J. A. *Journal of the American Chemical Society* **2002**, *124*, 5632.

(72)   Dwyer, M. A.; Looger, L. L.; Hellinga, H. W. *Science* **2004**, *304*, 1967.

(73)   Dronskowski, R. *Computational chemistry of solid state materials: A guide for materials scientists, chemists, physicists and others*; John Wiley & Sons, 2008.

(74)   Clark, T. *A handbook of computational chemistry: A practical guide to chemical structure and energy calculations*; Wiley-Interscience, 1985.

(75)   Hehre, W. J. *A guide to molecular mechanics and quantum chemical calculations*; Wavefunction Irvine, CA, 2003; Vol. 2.

(76)   Gilson, M. K.; Zhou, H.-X. *Annual review of biophysics and biomolecular structure* **2007**, *36*.

(77)   DiVincenzo, D. P. *Science* **1995**, *270*, 255.

(78)   Nielsen, M. A.; Chuang, I.; AAPT: 2002.

(79)   Nelson, E. *Physical review* **1966**, *150*, 1079.

(80)   Szabo, A.; Ostlund, N. S. *Modern quantum chemistry: introduction to advanced electronic structure theory*; Courier Corporation, 2012.

(81)   Labanowski, J. K.; Andzelm, J. W. *Density functional methods in chemistry*; Springer Science & Business Media, 2012.

(82)   Orio, M.; Pantazis, D. A.; Neese, F. *Photosynthesis research* **2009**, *102*, 443.

(83)   Heyrovský, J.; Kůta, J. *Principles of polarography*; Elsevier, 2013.

(84)   Kounaves, S. P.; Prentice Hall, Upper Saddle River, NJ, USA: 1997, p 709.

(85)   Kissinger, P. T.; Heineman, W. R. *Journal of Chemical Education* **1983**, *60*, 702.

(86)   Lewandowski, J.; Malchesky, P. S.; Google Patents: 1990.

(87)   Lovrić, M.; Osteryoung, J. *Electrochimica Acta* **1982**, *27*, 963.

(88)   Brumleve, T. R.; O'Dea, J. J.; Osteryoung, R. A.; Osteryoung, J. *Analytical Chemistry* **1981**, *53*, 702.

(89)   Osteryoung, J. G.; Osteryoung, R. A. *Analytical Chemistry* **1985**, *57*, 101.

(90)   Popere, B. C.; Della Pelle, A. M.; Thayumanavan, A. P. S. *Phys Chem Chem Phys* **2012**, *14*, 4043.

(91)   Holliday, S.; Donaghey, J. E.; McCulloch, I. *Chem. Mater.* **2014**, *26*, 647.

(92)   Wang, E.; Mammo, W.; Andersson, M. R. *Adv. Mater.* **2014**, *26*, 1801.

(93)   Gsaenger, M.; Bialas, D.; Huang, L.; Stolte, M.; Wuerthner, F. *Adv. Mater.* **2016**, *28*, 3615.

(94)   Glowacki, E. D.; Voss, G.; Sariciftci, N. S. *Adv. Mater.* **2013**, *25*, 6783.

(95)   Perpete, E. A.; Preat, J.; Andre, J. M.; Jacquemin, D. *J. Phys. Chem. A* **2006**, *110*, 5629.

(96)   Jacquemin, D.; Perpete, E. A.; Scuseria, G. E.; Ciofini, I.; Adamo, C. *J. Chem. Theory Comput.* **2008**, *4*, 123.

(97)   Jacquemin, D.; Wathelet, V.; Perpete, E. A.; Adamo, C. *J. Chem. Theory Comput.* **2009**, *5*, 2420.

(98)   Jacquemin, D.; Preat, J.; Wathelet, V.; Perpete, E. A. *J. Chem. Phys.* **2006**, *124*, 074104(1.

(99)   Adamo, C.; Scuseria, G. E.; Barone, V. *J. Chem. Phys.* **1999**, *111*, 2889.

(100)   Jacquemin, D.; Preat, J.; Wathelet, V.; Fontaine, M.; Perpete, E. A. *J. Am. Chem. Soc.* **2006**, *128*, 2072.

(101)   Ashizawa, M.; Masuda, N.; Higashino, T.; Kadoya, T.; Kawamoto, T.; Matsumoto, H.; Mori, T. *Organic Electronics* **2016**, *35*, 95.

(102)   Dasari, R. R.; Dindar, A.; Lo, C. K.; Wang, C.-Y.; Quinton, C.; Singh, S.; Barlow, S.; Fuentes-Hernandez, C.; Reynolds, J. R.; Kippelen, B.; Marder, S. R. *Phys. Chem. Chem. Phys.* **2014**, *16*, 19345.

(103)   Hasegawa, T.; Ashizawa, M.; Matsumoto, H. *RSC Advances* **2015**, *5*, 61035.

(104)   Park, Y. J.; Seo, J. H.; Elsawy, W.; Walker, B.; Cho, S.; Lee, J.-S. *Journal of Materials Chemistry C: Materials for Optical and Electronic Devices* **2015**, *3*, 5951.

(105)   Patil, H.; Gupta, A.; Bhosale Sheshanath, V.; Chang, J.; Wu, J.; Gupta, A.; Bilic, A.; Sonar, P. *Molecules* **2015**, *20*, 17362.

(106)   Shao, J.; Zhang, X.; Tian, H.; Geng, Y.; Wang, F. *Journal of Materials Chemistry C: Materials for Optical and Electronic Devices* **2015**, *3*, 7567.

(107)   Tomassetti, M.; Ouhib, F.; Cardinaletti, I.; Verstappen, P.; Salleo, A.; Jerome, C.; Manca, J.; Maes, W.; Detrembleur, C. *RSC Advances* **2015**, *5*, 85460.

(108)   Wang, X.; Zhao, Z.; Ai, N.; Pei, J.; Liu, Y.; Wan, X. *Eur. J. Org. Chem.* **2016**, *2016*, 2603.

(109)   Wu, T.; Yu, C.; Guo, Y.; Liu, H.; Yu, G.; Fang, Y.; Liu, Y. *J. Phys. Chem. C* **2012**, *116*, 22655.

(110)   Yoo, D.; Hasegawa, T.; Ashizawa, M.; Kawamoto, T.; Masunaga, H.; Hikima, T.; Matsumoto, H.; Mori, T. *Journal of Materials Chemistry C: Materials for Optical and Electronic Devices* **2017**, *5*, 2509.

(111)   Yue, W.; He, T.; Stolte, M.; Gsaenger, M.; Wuerthner, F. *Chem. Commun.* **2014**, *50*, 545.

(112)   Voronina, Y. K.; Krivolapov, D. B.; Bogdanov, A. V.; Mironov, V. F.; Litvinov, I. A. *J. Struct. Chem.* **2012**, *53*, 413.

(113)   Estrada, L. A.; Stalder, R.; Abboud, K. A.; Risko, C.; Brédas, J.-L.; Reynolds, J. R. *Macromolecules* **2013**, *46*, 8832.

(114)   Frisch, M. J.; Trucks, G. W.; Schlegel, H. B.; Scuseria, G. E.; Robb, M. A.; Cheeseman, J. R.; Scalmani, G.; Barone, V.; Mennucci, B.; Petersson, G. A.; Nakatsuji, H.; Caricato, M.; Li, X.; Hratchian, H. P.; Izmaylov, A. F.; Bloino, J.; Zheng, G.; Sonnenberg, J. L.; Hada, M.; Ehara, M.; Toyota, K.; Fukuda, R.; Hasegawa, J.; Ishida, M.; Nakajima, T.; Honda, Y.; Kitao, O.; Nakai, H.; Vreven, T.; Montgomery Jr., J. A.; Peralta, J. E.; Ogliaro, F.; Bearpark, M. J.; Heyd, J.; Brothers, E. N.; Kudin, K. N.; Staroverov, V. N.; Kobayashi, R.; Normand, J.; Raghavachari, K.; Rendell, A. P.; Burant, J. C.; Iyengar, S. S.; Tomasi, J.; Cossi, M.; Rega, N.; Millam, N. J.; Klene, M.; Knox, J. E.; Cross, J. B.; Bakken, V.; Adamo, C.; Jaramillo, J.; Gomperts, R.; Stratmann, R. E.; Yazyev, O.; Austin, A. J.; Cammi, R.; Pomelli, C.; Ochterski, J. W.; Martin, R. L.; Morokuma, K.; Zakrzewski, V. G.; Voth, G. A.; Salvador, P.; Dannenberg, J. J.; Dapprich, S.; Daniels, A. D.; Farkas, Ö.; Foresman, J. B.; Ortiz, J. V.; Cioslowski, J.; Fox, D. J.; Gaussian, Inc.: Wallingford, CT, USA, 2009.

(115)   Becke, A. D. *J. Chem. Phys.* **1993**, *98*, 5648.

(116)   Lee, C. T.; Yang, W. T.; Parr, R. G. *Phys. Rev. B* **1988**, *37*, 785.

(117)   Miehlich, B.; Savin, A.; Stoll, H.; Preuss, H. *Chem. Phys. Lett.* **1989**, *157*, 200.

(118)   Hehre, W. J.; Ditchfield, R.; Pople, J. A. *J. Chem. Phys.* **1972**, *56*, 2257.

(119)   Mclean, A. D.; Chandler, G. S. *J. Chem. Phys.* **1980**, *72*, 5639.

(120)   Krishnan, R.; Binkley, J. S.; Seeger, R.; Pople, J. A. *J. Chem. Phys.* **1980**, *72*, 650.

(121)   Turro, N. J.; Ramamurthy, V.; Scaiano, J. C. *Principles of molecular photochemistry: an introduction*; University Science Books: Sausalito, Calif, 2009.

(122)   Feng, X.; Ding, X.; Jiang, D. *Chemical Society Reviews* **2012**, *41*, 6010.

(123)   Ding, S.-Y.; Wang, W. *Chemical Society Reviews* **2013**, *42*, 548.

(124)   Cote, A. P.; Benin, A. I.; Ockwig, N. W.; O'keeffe, M.; Matzger, A. J.; Yaghi, O. M. *science* **2005**, *310*, 1166.

(125)   El-Kaderi, H. M.; Hunt, J. R.; Mendoza-Cortés, J. L.; Côté, A. P.; Taylor, R. E.; O'keeffe, M.; Yaghi, O. M. *Science* **2007**, *316*, 268.

(126)   Doonan, C. J.; Tranchemontagne, D. J.; Glover, T. G.; Hunt, J. R.; Yaghi, O. M. *Nature chemistry* **2010**, *2*, 235.

(127)   Ding, S.-Y.; Gao, J.; Wang, Q.; Zhang, Y.; Song, W.-G.; Su, C.-Y.; Wang, W. *Journal of the American Chemical Society* **2011**, *133*, 19816.

(128)   Wan, S.; Guo, J.; Kim, J.; Ihee, H.; Jiang, D. *Angewandte Chemie* **2008**, *120*, 8958.

(129)   Furukawa, H.; Yaghi, O. M. *Journal of the American Chemical Society* **2009**, *131*, 8875.

(130)   Li, Y.; Yang, R. T. *AIChE Journal* **2008**, *54*, 269.

(131)   Lanni, L. M.; Tilford, R. W.; Bharathy, M.; Lavigne, J. J. *Journal of the American chemical society* **2011**, *133*, 13975.

(132)   Chan-Thaw, C. E.; Villa, A.; Katekomol, P.; Su, D.; Thomas, A.; Prati, L. *Nano letters* **2010**, *10*, 537.

(133)   Uribe-Romo, F. J.; Doonan, C. J.; Furukawa, H.; Oisaki, K.; Yaghi, O. M. *Journal of the American Chemical Society* **2011**, *133*, 11478.

(134)   Uribe-Romo, F. J.; Hunt, J. R.; Furukawa, H.; Klock, C.; O'Keeffe, M.; Yaghi, O. M. *Journal of the American Chemical Society* **2009**, *131*, 4570.

(135)   Segura, J. L.; Mancheno, M. J.; Zamora, F. *Chemical Society Reviews* **2016**, *45*, 5635.

(136)   Matsumoto, M.; Dasari, R. R.; Ji, W.; Feriante, C. H.; Parker, T. C.; Marder, S. R.; Dichtel, W. R. *Journal of the American Chemical Society* **2017**, *139*, 4999.

(137)   Bessinger, D.; Ascherl, L.; Auras, F.; Bein, T. *Journal of the American Chemical Society* **2017**, *139*, 12035.

(138)   Figueira-Duarte, T. M.; Mullen, K. *Chemical reviews* **2011**, *111*, 7260.

(139)   Zhan, X.; Facchetti, A.; Barlow, S.; Marks, T. J.; Ratner, M. A.; Wasielewski, M. R.; Marder, S. R. *Advanced Materials* **2011**, *23*, 268.

(140)   Avlasevich, Y.; Li, C.; Müllen, K. *Journal of Materials Chemistry* **2010**, *20*, 3814.

(141)   Holtrup, F. O.; RJ Müller, G.; Quante, H.; De Feyter, S.; De Schryver, F. C.; Müllen, K. *Chemistry–A European Journal* **1997**, *3*, 219.

(142)   Huang, C.; Barlow, S.; Marder, S. R. *The Journal of organic chemistry* **2011**, *76*, 2386.

(143)   Al Kobaisi, M.; Bhosale, S. V.; Latham, K.; Raynor, A. M.; Bhosale, S. V. *Chemical reviews* **2016**, *116*, 11685.

(144)   Vollmann, H.; Becker, H.; Corell, M.; Streeck, H. *Justus Liebigs Annalen der Chemie* **1937**, *531*, 1.

(145)   Erten, Ş.; Posokhov, Y.; Alp, S.; İçli, S. *Dyes and pigments* **2005**, *64*, 171.

(146)   Zhong, C. J.; Kwan, W. S. V.; Miller, L. L. *Chemistry of materials* **1992**, *4*, 1423.

(147)   Black, S. P.; Wood, D. M.; Schwarz, F. B.; Ronson, T. K.; Holstein, J. J.; Stefankiewicz, A. R.; Schalley, C. A.; Sanders, J. K.; Nitschke, J. R. *Chemical science* **2016**, *7*, 2614.

(148)   Ponnuswamy, N.; Pantos, G. D.; Smulders, M. M.; Sanders, J. K. *Journal of the American Chemical Society* **2011**, *134*, 566.

(149)   Bhosale, S. V.; Jani, C. H.; Lalander, C. H.; Langford, S. J.; Nerush, I.; Shapter, J. G.; Villamaina, D.; Vauthey, E. *Chemical Communications* **2011**, *47*, 8226.

(150)   Katz, H.; Lovinger, A.; Johnson, J.; Kloc, C.; Siegrist, T.; Li, W.; Lin, Y.-Y.; Dodabalapur, A. *Nature* **2000**, *404*, 478.

(151)   Anthony, J. E.; Facchetti, A.; Heeney, M.; Marder, S. R.; Zhan, X. *Advanced Materials* **2010**, *22*, 3876.

(152)   Vadehra, G. S.; Maloney, R. P.; Garcia-Garibay, M. A.; Dunn, B. *Chemistry of Materials* **2014**, *26*, 7151.

(153)   Anant, P.; Lucas, N. T.; Ball, J. M.; Anthopoulos, T. D.; Jacob, J. *Synthetic Metals* **2010**, *160*, 1987.

(154)   Bhosale, S. V.; Kalyankar, M. B.; Bhosale, S. V.; Langford, S. J.; Reid, E. F.; Hogan, C. F. *New Journal of Chemistry* **2009**, *33*, 2409.

(155)   Kishore, R. S.; Kel, O.; Banerji, N.; Emery, D.; Bollot, G.; Mareda, J.; Gomez-Casado, A.; Jonkheijm, P.; Huskens, J.; Maroni, P. *Journal of the American Chemical Society* **2009**, *131*, 11106.

(156)   Bhosale, R.; Míšek, J.; Sakai, N.; Matile, S. *Chemical Society Reviews* **2010**, *39*, 138.

(157)   Krishna, G. R.; Devarapalli, R.; Lal, G.; Reddy, C. M. *Journal of the American Chemical Society* **2016**, *138*, 13561.

(158)   Vydrov, O. A.; Scuseria, G. E. *The Journal of chemical physics* **2006**, *125*, 234109.

(159)   Vydrov, O. A.; Heyd, J.; Krukau, A. V.; Scuseria, G. E. *The Journal of chemical physics* **2006**, *125*, 074106.

(160)   Vydrov, O. A.; Scuseria, G. E.; Perdew, J. P. *The Journal of chemical physics* **2007**, *126*, 154109.

(161)   Kendall, R. A.; Dunning Jr, T. H.; Harrison, R. J. *The Journal of chemical physics* **1992**, *96*, 6796.

(162)   Yuan, Z.; Ma, Y.; Geßner, T.; Li, M.; Chen, L.; Eustachi, M.; Weitz, R. T.; Li, C.; Müllen, K. *Organic letters* **2016**, *18*, 456.

(163)   Gaussian09, R. A. *Inc., Wallingford CT* **2009**, *121*, 150.

(164)   Becke, A. D. *The Journal of chemical physics* **1993**, *98*, 5648.

(165)   Ditchfield, R.; Hehre, W. J.; Pople, J. A. *The Journal of Chemical Physics* **1971**, *54*, 724.

(166)   Stein, T.; Eisenberg, H.; Kronik, L.; Baer, R. *Physical review letters* **2010**, *105*, 266802.

(167)   Stein, T.; Kronik, L.; Baer, R. *Journal of the American Chemical Society* **2009**, *131*, 2818.

(168)   Stein, T.; Kronik, L.; Baer, R. *The Journal of chemical physics* **2009**, *131*, 244119.